The American Mineralogist

Journal of the Mineralogical Society of America

Vol. 40 SEPTEMBER–OCTOBER, 1955 Nos. 9 and 10

Contents

Variation of composition and physical properties of tourmaline with its position in the pegmatite ..... M. H. Staatz, K. J. Murata, and J. J. Glass 789
Identification of metamict minerals by *x*-ray diffraction ..... Joseph Berman 805
Neomesselite and beta-roselite: Two new members of the fairfieldite group .. .. Clifford Frondel 828
Thermal analysis study of the natrolite group ..... C. J. Peng 834
Wulfenite symmetry as shown on crystals from Jugoslavia ..... Cornelius S. Hurlbut, Jr. 857
A crystal chemical study of montroseite and paramontroseite ..... Howard T. Evans, Jr., and Mary E. Mrose 861
A precision *x*-ray powder camera ..... Clifford Frondel 876
The structural scheme of sepiolite ..... Bartholomew Nagy and W. F. Bradley 885
Crystallography of monocalcium and dicalcium phosphates ..... James P. Smith, James R. Lehr, and Walter E. Brown 893
Bulfonteinite from Crestmore, California ..... Joseph Murdoch 900
Murdochite, a new copper lead oxide mineral ..... Joseph J. Fahey 905
The crystal structure of murdochite ..... C. L. Christ and Joan R. Clark 907
Notes and news: Studies of uranium minerals (XXI): Synthetic hydrogen-autunite ..... Virginia Ross 917
Manganese content of garnets from the Franciscan schists ..... A. Pabst 919
Laumontite and leonhardite cement in Miocene sandstone from a well in San Joaquin valley, California ..... M. E. Kaley and R. F. Hanson 923
Unit cell dimensions of uranite ..... Eleanor R. Berman 925
Removal of mineral grains from thin sections ..... Stewart R. Wallace 927
A simple collector for concentrating a mineral phase for analysis ..... V. D. Frechette 931
Mineralogical Society (London) 933
Book reviews 935
New mineral names 941

Published bi-monthly by the Society

Mineralogical Society of America

ASSOCIATED WITH THE GEOLOGICAL SOCIETY OF AMERICA

The enlarged issues of this journal for 1955 are made possible by a grant from the Penrose Fund of the Geological Society of America.

The American Mineralogist—Journal of the Mineralogical Society of America

A journal containing articles on mineralogy, crystallography, petrography, and allied sciences, is issued every two months. Contributions are invited from everyone.
Office of Publication, Mineralogical Laboratory, Ann Arbor, Michigan.

The general conduct of the journal is in the hands of the editor, **Walter F. Hunt,** Ann Arbor, Michigan, to whom all manuscripts should be submitted. To assist the editor the council of the Mineralogical Society has appointed **Lewis S. Ramsdell,** Ann Arbor, Michigan, assistant editor, and the following board of associate editors:

William F. Bradley, Illinois State Geological Survey, Urbana, Illinois.
Ian Campbell, California Institute of Technology, Pasadena 4, California.
Brian H. Mason, American Museum of Natural History, New York, N. Y.
Elburt F. Osborn, Pennsylvania State University, University Park, Pennsylvania.
Adolf Pabst, University of California, Berkeley 4, California.
Francis J. Turner, University of California, Berkeley 4, California.

It will expedite publication if two copies of each manuscript are submitted to the editor.

Contributors of leading articles are given without charge 100 reprints (without covers) of their article. If additional reprints are desired these can be purchased at the following rates:

Pages	*1–4*	*5–8*	*9–12*	*13–16*	*17–20*	*21–24*	*25–28*	*29–32*	*Covers*
Copies									
25	$3.50	$5.00	$ 8.00	$ 9.50	$11.00	$13.00	$15.00	$16.00	$4.90
50	3.80	5.55	8.80	10.40	12.10	14.20	16.40	17.50	5.50
75	4.10	6.10	9.60	11.30	13.20	15.40	17.80	19.00	6.10
100	4.40	6.65	10.40	12.20	14.30	16.60	19.20	20.50	6.70
Addl. C's	1.20	2.20	3.20	3.60	4.40	4.80	5.60	6.00	2.40

Cover composition $1.55.

Sent to all members and fellows of the Mineralogical Society of America. Membership dues $4.00 annually, fellowship dues $5.00 annually. Subscriptions for libraries, colleges, institutions, companies and similar organizations $6.00 annually.

Entered as second class matter at the post office at Menasha, Wis., under Act of March 3, 1879. Acceptance for mailing at the special rate of postage provided for in section 1103, Act of Oct. 3, 1917, paragraph 4 section 429 P. L. & R. authorized March 13, 1922.

Notice of change of address, orders, and remittances should be sent to Dr. Earl Ingerson, U. S. Geological Survey, Washington 25, D. C.

Printed by the George Banta Publishing Company, Menasha, Wisconsin
Printed in the United States of America

THE AMERICAN MINERALOGIST

JOURNAL OF THE MINERALOGICAL SOCIETY OF AMERICA

Vol. 40 SEPTEMBER-OCTOBER, 1955 Nos. 9 and 10

VARIATION OF COMPOSITION AND PHYSICAL PROPERTIES OF TOURMALINE WITH ITS POSITION IN THE PEGMATITE*

M. H. STAATZ, K. J. MURATA, AND JEWELL J. GLASS, *U. S. Geological Survey, Washington 25, D. C.*

ABSTRACT

Tourmaline crystals of the bizonal, lepidolite-bearing Brown Derby pegmatites no. 2 and no. 3 of Gunnison County, Colo., show a consistent variation in color, refractive index, and composition with position in the pegmatite. Starting with the outer wall of the pegmatite and going inward toward the core, the colors of the tourmaline crystals are black, dark green, blue, light green, and pink. The omega index decreases from 1.655 to 1.635 in the same direction.

The concentration of K, Rb, Cs, Pb, Be, and Li in tourmaline increases toward the pegmatite core. Fe, Mg, Ti, Na, Co, Ni, Cr, and V decrease in concentration toward the core; the last four are restricted to the crystals of the outermost part of the pegmatite. The main variation in tourmaline composition is a substitution of lithium for iron. Elements that remain more or less constant are Ga, Sr, Sc, Zr, Nb, Sn, Cu, Bi, and Zn. The concentrations of Mn, Y, and La show an interesting maximum at an intermediate position between the pegmatite wall and core.

Most of the spatial variations in composition of the tourmaline crystals may be explained on the basis of a gradual change in the composition of a single pegmatite fluid crystallizing in a closed system. Competition among different ions for sites in the crystal structure of tourmaline is invoked to explain the maxima in the variation trends. The variation trends of sodium and calcium, which are out of harmony with the variation trends in the composition of the pegmatite fluid, are apparently controlled by the charge requirements connected with isomorphous substitutions in the tourmaline structure.

INTRODUCTION

Tourmaline is well known for its wide variation in chemical composition and physical properties. Its atomic structure allows extensive substitution of ions of octahedral coordination such as Fe″, Mg, Li, and Al, and also those of somewhat larger coordination such as Na and Ca (Donnay and Buerger, 1950). The mineral also occurs in a wide variety

* Publication authorized by the Director, U. S. Geological Survey. This report concerns work done partly on behalf of the U. S. Atomic Energy Commission, and is published with the permission of the Commission.

of rocks, which shows that it can crystallize in quite different chemical environments, incorporating within itself whatever appropriate ions are available.

That the color and composition of tourmaline are grossly related to the kind of rock in which it occurs has been recognized for a long time—the common black variety, rich in iron, is found in granites, granite pegmatites, and schists; the brown magnesian variety occurs characteristically in dolomites and granular limestones; and the varicolored lithian variety is restricted to granite pegmatites. The present study deals with variation in composition and physical properties of tourmaline within zones of granite pegmatites. Our interest in this problem was first aroused by the systematic variation in the mineral's color from the outside to the center of certain pegmatites of the Quartz Creek pegmatite district, Gunnison County, Colo., during field work on behalf of the Division of Raw Materials of the U. S. Atomic Energy Commission.

Many authors, including Scharizer (1889) and Landes (1928), have emphasized the fact that in lithium pegmatites black tourmaline occurs in the outer part and the other variously colored varieties, in the inner part. Jenks (1935) studied the manner in which tourmaline varied in its optical properties with position in the lithium pegmatites of Portland, Conn. He published a very striking diagram showing progressive decrease of refractive indices from maximum values in crystals of the wall zone to minimum values in those of the pegmatite core. Unfortunately, he did not make any chemical analysis of these well-located samples. On the other hand, practically all of the chemical and spectrographic analyses of tourmaline in geologic literature are accompanied by information of only the most general kind as to the occurrence of the specimens.

We are concerned with precise locations of tourmaline crystals within the pegmatite because we wish not only to work out the spatial variation in composition of the mineral, but also to explore the thesis that this variation in part reflects changes in composition of the pegmatite mother liquor throughout the depositional history. Holland and Kulp (1949) discussed the general problem from a theoretical standpoint and have pointed out the lack of suitable data to check the theoretical conclusions. Preliminary studies of variation in composition of beryl and plagioclase with position in the pegmatite have been published by others (Page et al., 1953). Tourmaline seems to be especially suitable for such a study because it permits extensive isomorphous substitutions, involving many different elements. A list of elements compiled from analyses of tourmaline reported by Shainin,[1] de Azcona (1947), Carobbi and Pieruccini (1947), Warner (1935), and the authors includes 36 elements.

[1] Shainin, V. E., Unpublished analyses of tourmaline from the Newry-Rumford area, Maine.

Field Relationships

The Quartz Creek pegmatite district has an area of about 30 square miles and contains 1803 mapped pegmatites (Staatz, and Trites, 1954). Only 48 of the pegmatites contain tourmaline, and most of these show only a few crystals. The relative scarcity of the mineral in the district stands in sharp contrast to its widespread occurrence in pegmatites of other districts. Some units in the lepidolite-bearing pegmatites of the district, however, contain as much as 3 per cent tourmaline by volume.

In the field, the most striking variation of the mineral is in its color, so field relationships will be described in terms of the color of the specimens. The tourmaline is black, dark green, blue, light green, and pink. The dark-green, blue, light-green, and pink varieties are found only in the lepidolite-bearing pegmatites; the black variety occurs in both lepidolite-bearing and nonlepidolite-bearing pegmatites. Of the 48 tourmaline-bearing pegmatites, 38 contain only the black variety.

In many places in the nonlepidolite-bearing pegmatites, black tourmaline occurs in small pods of coarse-grained quartz or quartz-perthite pegmatite in an otherwise homogeneous pegmatite. Black tourmaline has been found adjacent to quartz, perthite, albite (ordinary and cleavelandite varieties), muscovite, beryl, garnet, biotite, monazite, columbite-tantalite, and gahnite, but not adjacent to lepidolite and topaz. In lepidolite-bearing pegmatites, black tourmaline is found only in the outer zones that are completely free of lepidolite, where it is commonly restricted to the extreme hanging-wall or footwall part.

Dark-green tourmaline is found usually in the zone adjacent to the lepidolite-bearing zone. Medium-green to yellowish-green tourmaline is found either in zones containing lepidolite or adjacent zones and is common in outer parts of lepidolite-bearing units and the inner parts of the adjacent unit. This variety of tourmaline is never in contact with lepidolite but occurs in the cleavelandite-quartz parts of the zone. Only pale-green and pink tourmaline crystals occur adjacent to lepidolite in lepidolite-bearing units. These two varieties frequently occur together, for example, samples 12 and 13 of Table 2; the pink variety is more abundant.

In zoned pegmatites of the Quartz Creek district having an albite-quartz wall zone and a cleavelandite-quartz-lepidolite core, the tourmaline on the hanging wall is black, becomes dark green inward and gradually lightens through shades of green to light green in the center with the lepidolite, and then darkens again as one crosses the core towards the footwall side. A dark-blue variety of tourmaline occurs as massive wavy bands in lepidolite-bearing pegmatites, where it is found in part with the medium-green and in part with the dark-green tourmaline. It was never

found in close association with lepidolite. There is often a thin band of small reddish-brown garnets in the center of the blue tourmaline bands.

Collection of Samples

The relationship between color and location of tourmaline in different pegmatite units was noted along the entire length of several pegmatites. It is best seen in the back of two cuts 5 feet long (Fig. 1) in the Brown Derby no. 2 and Brown Derby no. 3 dikes. These two pegmatites are remarkably similar in composition and consist of an albite-quartz wall zone surrounding a cleavelandite-quartz-lepidolite core. The mineralogy of these two dikes, as exposed in the two cuts, with estimated volume

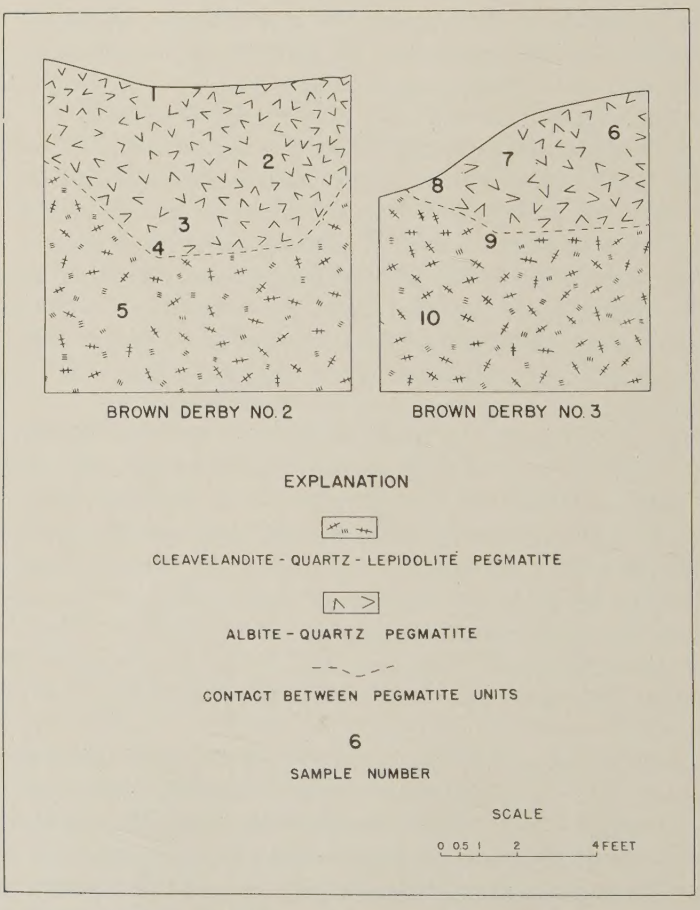

Fig. 1. Backs of vertical cuts in Brown Derby no. 2 and no. 3 pegmatites, showing location of the tourmaline samples.

percentages of the various minerals is presented in Table 1.

The mineralogy of the dikes as a whole is similar to that of the two cuts but shows some variation, chiefly in the presence of 1 to 2 per cent biotite in the wall zone of both dikes and lesser amounts of lepidolite in

TABLE 1. ESTIMATED VOLUME (IN PER CENT) OF MINERALS FOUND IN PEGMATITES

Mineral	Brown Derby No. 2		Brown Derby No. 3	
	Wall zone (avg. grain size $\frac{1}{4}$ in.)	Core (avg. grain size $1\frac{1}{2}$ in.)	Wall zone (avg. grain size $\frac{1}{8}$–$\frac{1}{4}$ in.)	Core (avg. grain size 2 in.)
Cleavelandite	—	54	—	70
Albite	64	—	59	—
Quartz	30	25	35	25
Lepidolite	—	20	—	4
Muscovite	4	1	5	<1
Tourmaline	2	<1	1	<1
Columbite-tantalite	—	—	—	<1 (trace)
Beryl	—	—	—	<1 (trace)
Topaz	—	<1	—	—
Garnet	<1	—	<1	—

the core of the Brown Derby no. 2. Lepidolite is chiefly concentrated in the central part of the cores with only a rare aggregate close to the core-wall zone contact.

A suite of five tourmaline crystals was collected from the back of each of the two cuts (Fig. 1). These cuts each show a part of the hanging-wall edge of the pegmatite, the whole thickness of the wall zone on the hanging-wall side, and most of the core. The cuts are not deep enough to show the footwall side of the pegmatite and only in the cut in the Brown Derby no. 2 is any of the footwall wall zone exposed.

TECHNIQUES OF STUDY

The ten tourmaline specimens were carefully collected and separated in the field from other pegmatite minerals. Though megascopically appearing fairly clean, when examined under the microscope they were found to contain various impurities. Each sample was then carefully crushed, hand picked, and separated from as many impurities as possible with heavy solutions. Except for inclusions, such as bubbles of liquids, and microscopic crystalline intergrowths, the final samples were reasonably pure. Pure grains were selected for optical determinations. The optical data, including notations about recognizable impurities, are to be found

TABLE 2. OPTICAL PROPERTIES OF TOURMALINE CRYSTALS FROM SUCCESSIVE POSITIONS IN TWO PEGMATITES

Specimen No.	*Pegmatite*	*Color*	N_ϵ	N_ω	*Birefringence*	*Pleochroism*	*Microscopic inclusions*
1	Brown Derby No. 2	Black	1.626	1.653	.027	Gray to black	Crystals & liquid
2	Brown Derby No. 2	Dk. greenish brown	1.629	1.655	.026	Cs.* to greenish brown	Qtz. & liquid
3	Brown Derby No. 2	Dk. bluish green	1.624	1.650	.026	Cs. to bluish or greenish	Liquid & "dust"†
4	Brown Derby No. 2	Blue	1.624	1.644	.020	Cs. to blue	Qtz.
5	Brown Derby No. 2	Pink	1.618	1.635	.017	None	Cs. mica
6	Brown Derby No. 3	Dark olive	1.629	1.650	.021	Pale green to olive	Qtz.
7	Brown Derby No. 3	Yellowish green	1.623	1.644	.021	Cs. to yellowish green	Qtz. & "dust"
8	Brown Derby No. 3	Grayish blue	1.623	1.645	.022	Cs. to gray blue	Qtz. & "dust"
9	Brown Derby No. 3	Light green	1.622	1.644	.022	Cs. to gray blue	Qtz. & "dust"
10	Brown Derby No. 3	Pink	1.619	1.635	.016	None	Qtz.
				Supplementary data			
11	Opportunity No. 4	Pink	—	1.637			
12	Brown Derby No. 1	Pink	—	1.643			
13	Brown Derby No. 1	Pale green	—	1.643			
14–24	Other pegmatites of district	Black	—	1.652–1.664‡			

* Cs. is symbol for colorless.

† Dust refers to minute opaque inclusions and occasionally to liquid or bubble inclusions.

‡ The two lowest values of N_ω among these black tourmaline crystals 1.652 and 1.655, were shown by specimens from lepidolite-bearing pegmatites.

in Table 2. Supplementary data based on tourmaline from other pegmatites of the district are given in the lower part of the table.

Spectrographic analyses (Table 3) were made of the purified sample by means of the *d-c* arc method (Gordon and Murata, 1952). In order to take advantage of the analytical curves already established for a large number of elements in a standard groundmass of 6 parts of quartz and 4 parts of microcline, each sample of tourmaline was mixed with an equal weight of pure quartz powder. This resulted in a mixture that corresponded approximately in composition to the standard groundmass with respect to silica, alumina, and the alkalies. All elements were determined in the range of 2230 to 4730Å excepting Li, K, Rb, and Cs, which were determined in the range of 6350 to 8850Å by means of Eastman *I-L* plates, and the samples and special alkali standards in quartz were buffered with 10 per cent Na_2CO_3.

We were fortunate in obtaining chemically analyzed tourmalines that enabled us to confirm the validity of our analytical curves for two of the most important elements, namely lithium and iron. We are indebted to W. W. Brannock and Leonard Shapiro for special chemical analyses for lithium and iron in this connection, and also to Janet Fletcher for some of the spectrographic determinations of lithium. The precision attained for the various elements was about ± 5 per cent of the mean.

The results of spectrographic analysis are presented in Table 3, in which the elements are grouped according to the type of substitutional position they are believed to occupy in the tourmaline structure. All the elements found have been assigned to tourmaline because no correlation could be established between the microscopic impurities observed and the analytical results. For example, the presence or absence of "dust" impurities, reported in Table 2, could not be correlated with the fluctuations of any of the elements. Although a small amount of mica was seen intergrown with sample 5 of the Brown Derby no. 2 pegmatite, potassium in this sample is lower than in the corresponding sample 10 of the no. 3 pegmatite, which contained no mica. Furthermore, if we are satisfied that potassium is an integral part of these two tourmalines, we can then quite readily reach the same conclusion for the other large ions, Pb, Rb, Cs, and Ba, which are also enriched in these tourmalines.

Variation of Refractive Indices

The variation in the refractive indices of the tourmaline samples will be discussed only in terms of N_ω, because N_ϵ changes sympathetically with it, and the birefringence varies only moderately over the range of indices represented. The lowest value for N_ω of 1.635, for both samples 5 and 10, is among the lowest to be found in the literature for lithium

TABLE 3. SPECTROGRAPHIC ANALYSES OF TOURMALINE CRYSTALS FROM SUCCESSIVE POSITIONS IN TWO PEGMATITES

Specimen No.	*Color*	*Large ions*										*Ions of octahedral coordination*				
		Na	Ca	K	Pb	Rb	Cs	Ba	Sr	Y	La	Fe	Li	Mn	Mg	Sc
1	Black	1.1	.59	.07	.004	—	—	—	.03	—	—	6.6	.20	.29>1.0		.001
2	Dk. greenish brown	1.1	.26	.09	.006	.002	—	.001	.004	—	—	5.3	.27	.17	.13	.0005
3	Dk. bluish green	1.4	.36	.04	.006	—	—	—	.003	—	—	4.6	.39	.60	.04	.0005
4	Blue	1.2	.31	.06	.007	.0007	—	—	.003	.08	.03	3.2	.47	.79	.02	.0008
5	Pink	.8	.64	.49	.030	.042	.005	.001	.003	—	—	.07	.61	.22	.01	—
6	Dark olive	1.4	.23	.09	.006	.006	—	—	.007	—	—	6.3	.36	.19	.15	—
7	Yellowish green	1.5	.34	.04	.004	—	—	—	.007	.02	—	4.8	.47	.62	.14	.001
8	Grayish blue	1.5	.27	.06	.005	.0008	—	—	.004	.10	—	4.8	.47	.97	.02	.0005
9	Light green	1.6	.57	.05	.010	—	—	—	.007	—	—	4.2	.60	.88	.01	—
10	Pink	0.8	.74	.70	.058	.032	.002	.002	.003	—	—	.05	.97	.14	.03	—

		Ions of octahedral coordination (continued)												*Ion of tetrahedral coordination*
		Co	Ni	Cr	V	Ti	Ga	Zr	Nb	Sn	Cu	Bi	Zn	Be
1	Black	.003	.002	.001	.01	.24	.014	.007	—	.007	.0005	—	.09	.0006
2	Dk. greenish brown	—	—	—	—	.22	.009	.006	.022	.006	.0017	—	.10	.0006
3	Dk. bluish green	—	—	—	—	.05	.012	—	.030	.006	.0005	.004	.20	.0004
4	Blue	—	—	—	—	.01	.008	.018	.022	.005	.0005	—	.04	.0003
5	Pink	—	—	—	—	—	.011	—	—	.007	.0007	—	—	.010
6	Dark olive	—	—	—	—	.20	.010	—	.017	—	.0004	.007	.12	.0003
7	Yellowish green	—	—	—	—	.01	.011	.006	—	.02	—	.005	.10	.0006
8	Grayish blue	—	—	—	—	.02	.010	.005	—	.009	.0006	—	.06	.0003
9	Light green	—	—	—	—	.06	.015	—	—	.007	—	—	.16	.0008
10	Pink	—	—	—	—	—	.010	—	—	.005	.0007	—	—	.0063

Elements not found: Ag, Mo, W, As, Sb, Cd, In, Ge, Tl, Th, U, Au, Pt, P, Ta.

tourmaline. The highest value of 1.655 is, however, much lower than 1.682 found by Ward (1931) for a nonpegmatitic tourmaline containing 16 per cent Fe. An unanalyzed black tourmaline with N_ω of 1.698 is reported by Larsen and Berman (1934).

Many authors, including Schaller (1913), Kunitz (1926), and Winchell (1932), have discussed the relationship between refractive indices and composition of tourmaline. Maximum indices are found in iron tourmaline, and the value falls as the iron content falls and the composition approaches either that of magnesium tourmaline or that of ithium tourmaline.

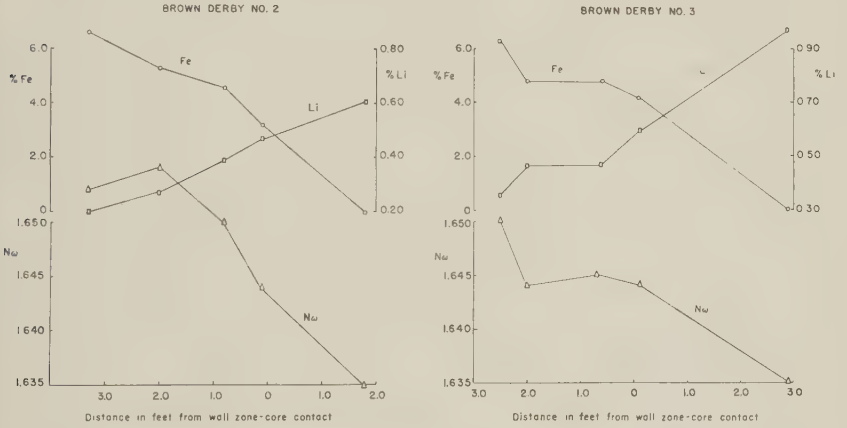

FIG. 2. Relationship between the position of a tourmaline crystal in a pegmatite dike and the crystal's iron content, lithium content, and upper index of refraction (N_ω). Center of pegmatite is to the right.

Figure 2 shows that the relative variations in N_ω of our samples is closely related to the percentage of iron. Sample 1, which is an exception, is the only one that contains appreciable magnesium, which would lower the refractive index. It is also to be noted that for any given percentage of iron the index depends on the lithium content of the samples. The iron content of tourmaline for each pegmatite ranges from 0.05 to 6 per cent, but the values of N_ω run lower in samples from Brown Derby no. 3 because of the higher lithium content.

VARIATION IN CHEMICAL COMPOSITION

Space relationships for the different tourmaline crystals within the two pegmatites are shown by plotting their actual separation in the pegmatite along the abscissa in Figs. 2 and 4. The positions of the various samples were measured in feet from the nearest point on the contact

between the wall zone and the core. The outer contact of the pegmatite, which is a more prominent change, was not used because it was not exposed continuously along the back of the cuts. For both pegmatites the outermost tourmaline has been plotted to the left, and the innermost one to the right-hand side of the graph. This is desirable because we shall be

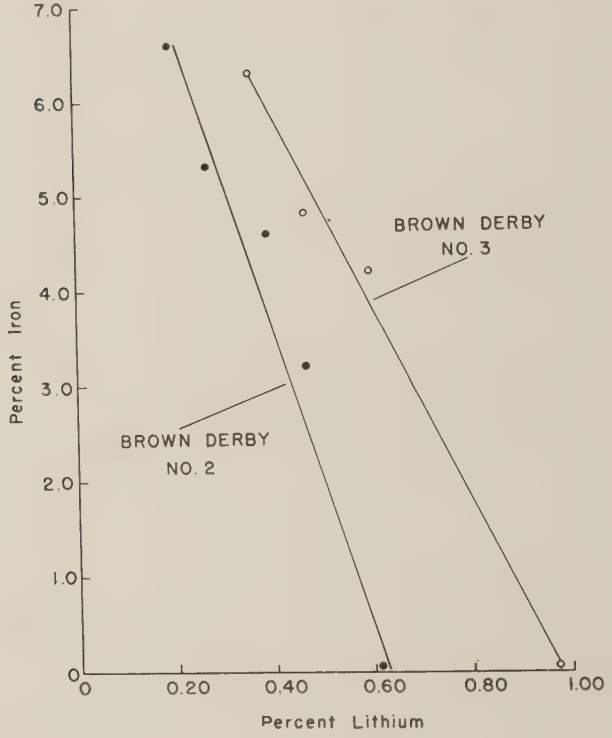

FIG. 3. Relationship between iron and lithium in tourmalines from Brown Derby no. 2 and no. 3 pegmatites.

constantly referring to variation in the tourmaline in the direction across the pegmatite dike from the wall zone inward.

With the single exception of sample no. 1 the tourmaline crystals contain only negligible amounts of magnesium. Therefore, the major variation in the composition of the samples is a transition from iron tourmaline to lithium tourmaline. This gives rise to the inverse relationship between Fe and Li that is plotted in Fig. 3. Although the weight percentages of Li are not high, the element looms large in terms of atomic ratios because of its low atomic weight. It must be also remembered that the substitution of Li for Fe″ in the octahedral positions of tourmaline involves simultaneous addition of aluminum, a major element for which

we did not make an analysis. The substitution may be of the type $LiAl \rightleftharpoons Fe''Fe''$, so that a small amount of Li, with the aid of Al, will take the place of a much larger amount of Fe''. Schaller (1913) has shown that the maximum concentrations of aluminum are found in lithium tourmalines low in iron and magnesium.

The several types of variation shown by different ions of tourmaline are presented in Fig. 4, in which points along the abscissa are plotted in the same way as in Fig. 2. Eleven of the 28 elements found in the spectrographic analyses have been plotted; those omitted were either found in only a few specimens or showed little variation. A number of the ions show similar trends, so these will be discussed together.

Four general types of variations are noted: (1) an increase in the percentage of the element in the tourmaline toward the center of the pegmatite, (2) a decrease in the percentage, (3) little variation in the percentage, and (4) a sharp increase and then a decrease in the percentage of the element.

The amounts of lithium, potassium, calcium, lead, and beryllium in the tourmaline increase toward the center of the pegmatite. In addition, rubidium and cesium, which were found in only a few specimens, showed their greatest concentration in the pink tourmaline from the central part of the core. The beryllium, lead and potassium curves are fairly level until the tourmaline in the central part of the core is reached; then they rise abruptly. The most gradual rise occurs with the element lithium. The increase of lithium, potassium, rubidium, and cesium of the tourmaline in the central part of the pegmatite seems to be a direct result of the higher concentration of these elements found there, as indicated by the associated minerals (Table 1). Beryl, the only mineral that contains major amounts of beryllium, is restricted to the core. Lepidolite, which is concentrated in the central part of the core, contains approximately 8 per cent potassium, 2 per cent lithium, 1 per cent rubidium, and 0.1 per cent cesium (Stevens, 1938). The increase in calcium toward the center of the pegmatite, however, is in opposition to the decrease in calcium shown by the albite of these pegmatites. One sample of albite and one sample of cleavelandite were taken from the wall zone and core, repectively, from the Brown Derby no. 2 and no. 3 pegmatites. The composition of each sample with respect to alkalies and alkaline earths is given in Table 4.

Because albite is the only major mineral capable of accommodating calcium in each unit of the two pegmatites, a general decrease in the total calcium content is indicated towards the center of the pegmatite. Among the other minerals present in the core, lepidolite is known to contain only traces of calcium (Stevens, 1938) and hence does not act as a significant repository for this element. The depletion of strontium that

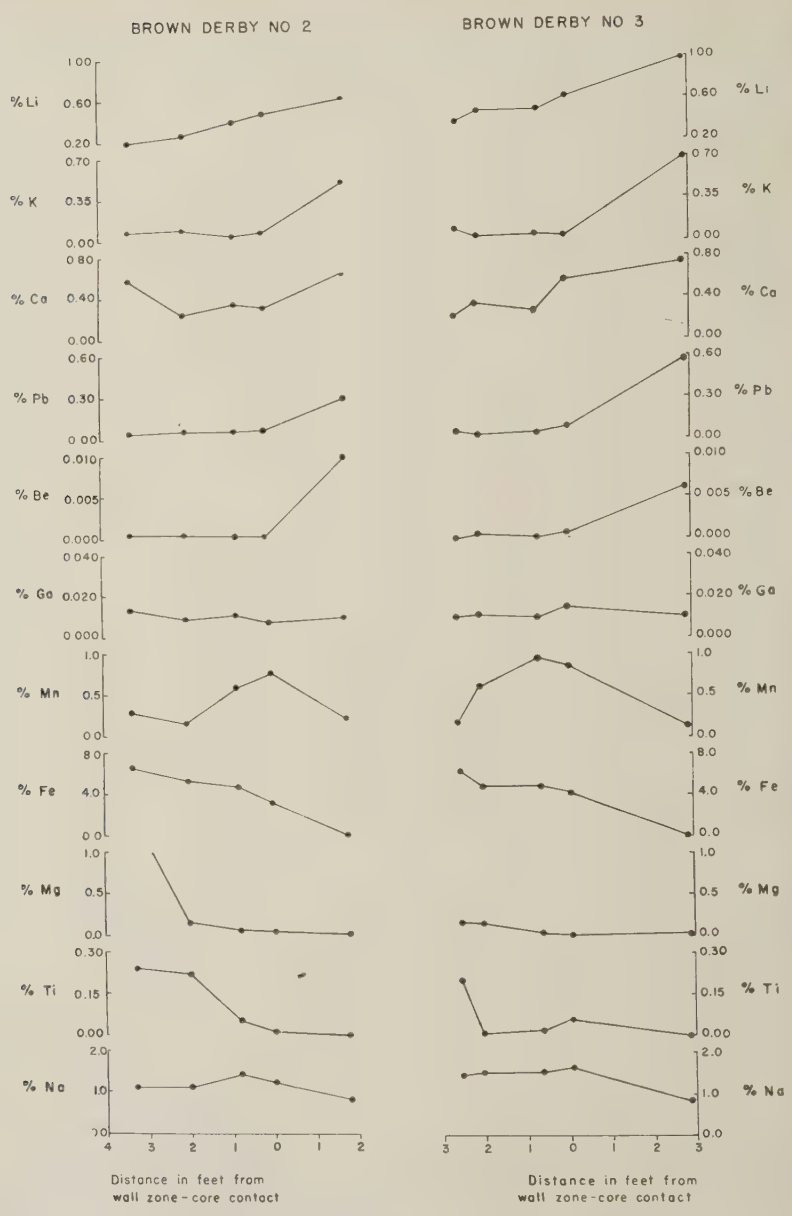

FIG. 4. Relationship between the position of a tourmaline crystal in a pegmatite dike and the crystal's content of various metallic elements. Center of pegmatite is to the right.

is indicated in Table 4 also supports the idea of a decrease in calcium towards the core. The contrary trend of enrichment of calcium in tourmaline crystals in the direction of the core must therefore be due to some peculiar requirement of the tourmaline structure, such as the use of calcium in place of sodium to balance charges arising from substitutions in the structure.

Lead seems to be found chiefly in the tourmaline. Lead was looked for but not found in either the equigranular and platy (cleavelandite) forms of albite or in the lepidolite from both pegmatites.

A general decrease in the amount of iron, titanium, magnesium, and sodium occurs toward the center with the elements cobalt, nickel, chromium, and vanadium occurring in only one specimen adjacent to the outer

Table 4. Partial Analyses of Albite in Brown Derby No. 2 and No. 3 Pegmatites

	Brown Derby No. 2		Brown Derby No. 3	
	Wall zone	Core	Wall zone	Core
Na[1]	7.84	8.34	7.98	8.50
Ca[2]	.15	.10	.21	.13
Sr[2]	.005	0	.003	0
K[1]	.10	.13	.11	.11
Li[2]	.001	.002	.001	.003

[1] Flame photometer determinations by S. M. Berthold.

[2] Spectrographic determinations by K. J. Murata. Zero in unit column means that the concentration of the element was below the limit of spectrographic sensitivity. Barium, rubidium, and cesium were also undetected.

wall of the pegmatite. The sodium content of the tourmaline is fairly constant but is lower in the pink tourmaline of the core. This relationship is the opposite of the calcium in the tourmaline, which increased in the core. It is also the opposite of the sodium content in the albite, which increases with a decrease in calcium, indicating a general increase of sodium in the central part of the pegmatite. The decrease of sodium in tourmaline is due to the incorporation of substantial amounts of potassium and calcium, the entry of potassium being governed by its abundance and of calcium by probable charge requirements as previously discussed. Titanium in amounts of 0.20 per cent or greater was found in three specimens, which ranged from black to dark greenish brown, and which contained the highest amounts of iron. In specimens closer to the center of the pegmatite, the titanium content dropped rapidly to less than a fourth of this value and then its concentration toward the center was low and erratic.

Several elements, found in small amounts, occur with minor and ap-

parently no consistent variation. A good example is gallium, which is illustrated in Fig. 4. The variation of this element is small and does not appear related to the type of tourmaline or to the surrounding minerals. Elements with similar behavior include strontium, scandium, zirconium, niobium, tin, copper, bismuth, and zinc. Only minor amounts of these elements appear to be retained in the tourmaline structure; thus, though their presence in the pegmatite fluid may be noted by their presence in tourmaline, a large increase in the amount of these elements would probably not bring a corresponding increase of these elements in the tourmaline. These elements, with the exception of niobium, are not the chief constituents of any mineral in these two pegmatites. The minor amounts of these elements present in the pegmatite fluid substitute into whatever mineral that will accommodate them.

Three elements, manganese, yttrium, and lanthanum increase and then decrease in the tourmaline on going from the outside toward the center of the pegmatites. Maximum concentration is found in the blue tourmaline of both pegmatites. The blue tourmaline commonly surrounds small brown spessartite-almandite crystals. Garnet, the chief manganese mineral, is found in the wall zone and outer part of the core. No garnet occurs in the central part of the pegmatite adjacent to the pink tourmaline with the low manganese content. The reason for the probable increase in manganese content of the tourmaline in the inner part of the wall zone, which is not paralleled by the manganese content of the pegmatite as a whole, as indicated by the garnet, will be discussed later.

Three major factors control the amount of an ion that is incorporated into tourmaline or any other mineral: (1) the structure of the mineral, which determines the ease of incorporation of an ion of a certain size; (2) the presence or absence of other ions which would compete with that ion for a position in the mineral's structure; and (3) the concentration of the ion in the pegmatitic fluid. If an ion fits into a particular position in the tourmaline structure and the pegmatitic fluid contains no other ions that fit better in the same position, then an increase or decrease of this original ion in the pegmatitic fluid will be reflected by an increase or decrease in its content in the tourmaline. An ion, whose concentration does not increase in the pegmatitic fluid, may actually show a higher concentration in the tourmaline, if some other ion which fits better in the same position in the tourmaline decreases in concentration. An example may be manganese, whose concentration rises in tourmaline from the outside toward the inner part of the wall zone as the concentration of iron decreases. The concentration of manganese in the outer part of the wall zone, however, is as high as that in the inner part, as indicated by numerous garnet crystals. The decrease of manganese in the tourmaline at the inner edge of the wall zone and core probably represents an actual decrease in manganese concentration in the pegmatite, as is suggested by

the less common occurrence of garnet crystals, the central part of the core being entirely free of them.

The major transition from the outside to the center of the pegmatite is from iron to lithium, which occurs gradually with the lessening of iron. Iron appears to fit better into the tourmaline structure than does lithium, and iron-rich tourmaline crystals are common in pegmatites or parts of pegmatites containing biotite and magnetite. Light-pink and light-green tourmaline crystals are found only where iron-rich minerals are absent. Iron is responsible for the density of color; the lightest tourmaline, irrespective of the color, carries the smallest amount of iron. After the iron content has increased to approximately 6.5 per cent the tourmaline becomes black in hand specimen and greater amounts of iron or varying amounts of other elements do not visibly affect its color. Thus, among the lighter shades of tourmaline in pegmatite, the color density may be used for approximating the iron content, or inversely the lithium content.

Chromium, vanadium, and titanium have ionic radii of 0.64 Å, 0.65 Å, and 0.69 Å, respectively, and thus can easily substitute for ferric iron (ionic radius of 0.67 Å) in the tourmaline structure. Nickel has the same ionic radius as magnesium (0.78 Å) and may enter into the tourmaline structure with equal ease. Cobalt with an ionic radius of 0.82 Å may substitute for ferrous iron (0.83 Å), as can both nickel and magnesium. Some of these elements (Cr, V, Ni, and Co) occurred in only the black tourmaline that was collected adjacent to the outside wall of the pegmatite (specimen no. 1). The small amount of these elements present may well be used up by the first tourmaline formed. Goldschmidt (1937) formulated a rule on the crystal chemistry of ionic crystals which states, "If two ions have almost the same radius the smaller one has the tighter bond." In the case of crystallization from a melt the smaller ion will be concentrated in early crystals of an isomorphous series. Thus, as Cr^3 and V^3 have slightly smaller ionic radii than Fe^3, and as Ni^2 and Co^2 have a slightly smaller ionic radii than Fe^2, chromium, nickel, cobalt, and vanadium will be favored to substitute in the early crystals in place of iron.

The abrupt rise in the lead, rubidium, and cesium content in the pink tourmaline crystals from the central part of the pegmatites may be due to two causes: (1) increase in concentration of the elements in the fluid, and (2) decrease in the fluid of ions that fitted into the tourmaline structure more easily.

The tourmaline from the outside of the pegmatite to the core shows a gradual change in composition of such major components as iron and lithium. Some of the minor elements also parallel the change of these elements. The increase of some elements in tourmaline is commonly the same as occurs in other minerals that surround the tourmaline. The change noted in the Brown Derby no. 2 and no. 3 pegmatites is a gradual one that is most simply explained by means of a single process in which

the pegmatite fluid changes in composition during crystallization. In other words the tourmaline was formed from one fluid whose chief method of change was of decreasing some elements by crystallizing out minerals rich in these elements and increasing the elements left in solution. Hydrothermal replacement, with its influx of new fluids, would produce erratic variations in the concentration of such elements as lithium and iron from the outside wall to the core. This is not what is found, and it is believed that the two pegmatites were formed in a closed system by gradual crystallization from the wall inward.

References

Azcona, J. M. L., de (1947), Is there lead of radioactive origin in tourmaline?: *Rept. Comm. Measurement of Geol. Time*, Washington, 1943–1946, p. 61.

Carobbi, Guido, and Pieruccini, Renzo (1947), Spectrographic analysis of tourmalines from the Island of Elba with correlation of color and composition: *Am. Mineral.*, **32,** 121–130.

Donnay, Gabrielle, and Buerger, M. J. (1950), Determination of the crystal structure of tourmaline: *Acta Crystallographica*, **3,** 379–388.

Goldschmidt, V. M. (1937), Principles of distribution of chemical elements in minerals and rocks: *Chem. Soc. London Jour.*, pt. **1,** 655–673.

Gordon, Mackenzie, and Murata, K. J. (1952), Minor elements in Arkansas bauxite: *Econ. Geol.*, **47,** 169–179.

Holland, H. D., and Kulp, J. L. (1949), Distribution of accessory elements in pegmatites: *Am. Mineral.*, **34,** 35–60.

Jenks, W. F. (1935), Pegmatites at Collins Hill, Portland, Connecticut: *Am. Jour. Sci.*, 5th ser., **30,** 177–197.

Kunitz, W. (1926), Chemisch-optische Untersuchungen an der Turmalin- und Glimmergruppe: *Zeits. Krist*, **64,** 521–523.

Landes, K. K. (1928), Sequence of mineralization in the Keystone, South Dakota, pegmatites: *Am. Mineral.*, **13,** 510–530 and 537–558.

Larsen, E. S., and Berman, Harry (1934), Microscopic determinations of the nonopaque minerals: *U. S. Geol. Survey, Bull.* **848,** 247.

Page, L. R., and others (1953), Pegmatite investigations 1942–1945 Black Hills, South Dakota: *U. S. Geol. Survey Prof. Paper* **247.**

Schaller, W. T. (1913), Beitrag zur Kenntniss der Turmalingruppe: *Zeits. Krist.*, **51,** 321–343.

Scharizer, Rudolph (1889), Ueber die chemische Constitution und ueber die Farbe der Turmalin von Schuttenhofen: *Zeit. Krist.*, **15,** 337–365.

Staatz, M. H., and Trites, A. F. (1954), Geology of the Quartz Creek pegmatite district, Gunnison County, Colorado: *U. S. Geol. Survey, Prof. Paper* **265.**

Stevens, R. E. (1938), New analyses of lepidolites and their interpretation: *Am. Mineral.*, **23,** 607–627.

Ward, G. W. (1931), Chemical and optical study of the black tourmalines: *Am. Mineral.*, **16,** 145–190.

Warner, T. W., Jr. (1935), Spectrographic analyses of tourmalines with correlation of color and composition: *Am. Mineral.*, **20,** 531–536.

Winchell, A. N. (1932), Ferrotremolite, oxyhornblende, and tourmaline: *Am. Mineral.*, **17,** 472–477.

Manuscript received Aug. 4, 1954.

IDENTIFICATION OF METAMICT MINERALS BY *X*-RAY DIFFRACTION

JOSEPH BERMAN, *U. S. Department of the Interior, Bureau of Mines, College Park, Md.*

ABSTRACT

The physical properties of the metamict minerals are discussed and tabulated. Because of their isotropy and the variability of the index of refraction of these minerals, the petrographic microscope has limited value for their identification. Ordinarily, *x*-ray diffraction yields little additional information. Heating of certain specimens, however, induces some crystallinity in many of these "amorphous" minerals. A technique was developed for treating the metamict minerals to facilitate their systematic study for purposes of identification. Data are given for metamict zircon, thorite and uranothorite, euxenite, brannerite, fergusonite, samarskite, davidite, and allanite.*

It is also observed that some of the "more stable" related minerals that ordinarily occur in the crystalline state are structurally changed when subjected to temperatures at which many of the metamict minerals crystallize. This may indicate that the crystallized (by heating) metamict material is not reconstituted to the original crystal structure.

INTRODUCTION

Although the minerals that occur in the metamict condition have aroused increasing interest in recent years, little information has been published on methods of identification of the various minerals of this type. It is recognized that several naturally occurring substances having external crystallographic form nevertheless lack internal order and in many cases are amorphous to *x*-rays. The word "metamict" has been applied to these noncrystalline pseudomorphs of material presumed to have been crystalline originally. This term has been widely used, but it has been only recently that a detailed discussion of the subject has been published by Pabst (47). Brooker and Nuffield (10, 11) discuss the term as it has been applied to uraninite. These two readily available recent articles give a rather complete history and description of the word metamict, and nothing further on its origin and use will be included herein.

PHYSICAL PROPERTIES OF METAMICT MINERALS

The following list of physical properties of the metamict minerals is presented because it should be a useful guide to understanding of the difficulties and limitations of the problem of identification and classification.

* Tables are presented comparing in detail the *x*-ray diffraction patterns of these and related minerals after various heat treatments. An extensive bibliography of the general subject of metamictization is included.

1. *Optically isotropic and lacking in Debye-Scherrer X-ray diffraction* (2, 3, 4, others).

This is generally true. There are minerals, such as some allanites, however, that have a definite birefringence but give no x-ray diffraction pattern. Specimens are found in different stages of isotropism from relatively well crystallized to completely "amorphous"; some show heterogeneity in the same specimen. It is important to note that isotropism alone is no criterion as to the metamict condition of minerals that crystallize in the cubic system.

2. *Brittle with a conchoidal fracture and no cleavage.* Many of these noncrystalline "minerals" are clear, fresh appearing, and glassy. Some, however, appear altered and weathered in both the hand specimen and under the microscope. Many samples are filled with close fractures.

3. *Density increases when ignited.* This is usually true, but the difficulty of measurements on fractured or powdered material has probably led to some apparent contradictions. Consequently, this is not a particularly reliable criterion.

4. *Become incandescent on heating* (18, 36, 47, others). This phenomenon is included here, although it has been possible to crystallize all the metamict minerals studied by the author at temperatures appreciably below that required for glowing. In many instances this pyrognomic effect is not observed at any temperature.

5. *Crystallization by ignition below fusion or sintering temperature* (2, 6, 47, others). Crystallization may be very complex. With the possible exception of some zircons, no case of reconstitution of a single crystal has been observed. Some authors, however, have reported the re-formation of single crystals.

6. *Contain radioactive element* (20, 21, others). The radioactivity may be very low as in some allanites, gadolinites, and zircons; or it may be very high, as in thorites, brannerites, euxenites, etc. It is, however, apparently present in every instance in the metamict mineral. Not all radioactive minerals become metamict, as note thorianite, which is always found well crystallized.

This paper is not concerned with the causes and processes of metamictization, but only with the methods of identification of the metamict minerals. However, the author is firmly convinced that radiation from elements within predisposed minerals causes the metamict condition. Those references in the bibliography that are marked with an asterisk contain material on this phase of the metamict problem. The articles

by J. C. Slater (54) and F. Seitz (53) are particularly informative as to the effects of radiation.

Methods of Identification

Because of their isotropy and the variability of the index of refraction of metamict minerals the petrographic microscope has very limited value for their identification (17, others). Likewise, because of the complete disorder and consequent noncrystallinity of many of these naturally occurring compounds, x-ray diffraction yields little additional information (6, 47, 58, others). However, early in the study of these minerals mineralogists found that heating of certain specimens would give some crystallinity to many of these "amorphous" minerals (25, 46).

To make a systematic study of these heating effects, the following technique was developed (5).

1. All samples were handpicked with the aid of a microscope to remove contaminants.

2. Each sample was studied with the petrographic microscope to ascertain its general optical characteristics. Detailed optics were not determined because of the great variations occurring in similar specimens or sometimes in different parts of the same specimen.

3. Each sample was carefully split into several fractions to assure that the different tests would be run on identical materials.

4. One fraction was used for a semiquantitative spectrochemical analysis.

5. Other fractions were heat-treated as follows:
   (*a*) Crushed material was heated in an open crucible over a Meker burner for approximately 5 minutes.
   (*b*) Different portions of each specimen of crushed material were heated to different controlled temperatures in air for definite periods of time in an electric furnace.
   (*c*) Duplicate portions of the crushed material were heated to the same controlled temperatures in an inert atmosphere.

Difficulty was encountered in maintaining an inert atmosphere because it was found that both tank nitrogen and helium contained enough impurities to allow oxidation of the sample. Oxygen-bearing impurities were eliminated by passing the gas through a drying tube and then through a plug of heated steel wool before it reached the specimen being treated. This method had been suggested by F. A. Bannister and J. E. T. Horne (3).

Data Observed

It has been found that the only reliable method that can be used for the identification of the metamict minerals is the use of x-ray diffraction pat-

terns of heat-treated samples. Therefore, Tables 1 through 7, which contain pertinent and reproducible x-ray powder patterns of these minerals, are included. Where the author's results correspond to those previously published, the proper reference is noted and the data are not repeated here.

Since only semi-quantitative spectrochemical analyses were used as a check on the samples studied, the x-ray data may be open to some questions. However, the x-ray patterns tabulated herein are only those that have been reproduced on other samples from the same and other localities. No criterion was set up as to the number of different samples studied, but no table is included that has not been reproduced from at least five localities. For example, nearly identical fergusonite patterns have been produced by at least ten samples from different deposits.

The powder patterns of heat treated originally metamict zircon, thorite, and fergusonite can be indexed using the lattice parameters reported in the literature. However, attempts to index heat treated euxenite, davidite, brannerite, and samarskite were unsuccessful. Arnott (2) obtained similar (to those listed here) x-ray powder patterns of euxenite and states " . . . it was found that all but a few very weak lines could be satisfactorily indexed." Our data show some of these extraneous lines (which are invariably present) were too strong to be ignored. Efforts to relate these patterns to other ABO_4 or AB_2O_6 compounds (9) were likewise unsuccessful.

A. *Zircon:* (7, 15, 30, 35, 56, 61, others) (x-ray data in Table 1).

Specimens examined varied from completely "fresh," with sharp powder diffraction patterns in the small interplanar region as well as in the large interplanar region, through specimens with slight disorder (line broadening and poor diffraction in the small interplanar region), to those samples which appeared completely metamict and gave no powder diffraction pattern. Observations with the petrographic microscope disclosed that the fresh zircon had consistent optics that agreed well with those in the literature. In those specimens that are somewhat metamict, both the index of refraction and the birefringence decreased; complete isotropy was reached in the totally metamict specimens. Many zircons were studied, including the specimens labeled with the varietal names alvite, cyrtolite, and hagatalite. Heat treatment of these specimens generally resulted in well crystallized microcrystalline tetragonal zircon. However, there were exceptions and more detailed data on zircon have been included in another paper (35).

B. *Thorites and Uranothorites:* (8, 45, 46, others) (x-ray data in Table 2)

These minerals occur in nature in all stages of metamictization from

comparatively well crystallized to completely metamict material. *X*-ray diffraction data corroborated the petrographic data that all available thorites showed some degree of change to the metamict state.

The comparatively unchanged thorites give a powder pattern of the tetragonal zircon type. One of these samples studied has a unit cell that can be indexed with tetragonal lattice parameters of $a_0 = 7.15 \pm .01$ Å, $c_0 = 6.29 \pm .01$ Å. This material, heated to 1300° ± 20° C. in an inert atmosphere, gives an excellent pattern with $a_0 = 7.11 \pm .01$ and $c_0 = 6.32 \pm .01$ Å. The latter figures agree well with those reported by Pabst (46) for an unaltered uranothorite.

Pabst (45, 47) has discussed the dimorphism of thorium silicate and has presented data on the heat treatment of some thorites. The experiments carried out in our laboratories give data in general agreement with his, but some significant differences probably result mainly from variations in method of treatment of the original sample and possibly from the condition of the mineral before heat treatment.

These investigations disclosed the following results: when completely metamict thorites were heated to ca 800° C. for one minute or longer, face-centered cubic thorium oxide crystallized. The powder patterns of the heated samples always showed broad, diffuse lines resulting from either small particle size or internal disorder. When these same or similar samples were heated to higher temperatures (ca 1100° C.) in air for longer periods, tetragonal thorite or monoclinic huttonite was formed in addition to the thorium oxide. Spectrochemical analysis did not disclose any significant compositional difference in the specimens that crystallize differently when heat treated. Upon increase in temperature of heat treatment to ca 1350° C. in air, the original completely metamict material always became the monoclinic variety of thorium silicate plus some crystalline thorium oxide (present in all specimens ignited). When these samples were heated in a completely inert atmosphere at temperatures up to ca 1250° C., the monoclinic dimorph of thorium silicate was formed in some and the tetragonal variety in others. However, if the temperature in the inert atmosphere is raised above ca 1350° C., the tetragonal variety of thorium silicate plus some thorium oxide crystallizes and remains until the temperature of dissociation into thorium oxide and amorphous silica is reached at a temperature probably between 1600° C. and 1700° C.

Although the *x*-ray powder patterns of heated originally metamict thorium silicate differ in accordance with the method of heat treatment, our data indicate that this material can be definitely identified when heated under controlled conditions. However, evidence is as yet inconclusive as to whether the original mineral was huttonite or thorite.

C. *Euxenite:* (2, 14) (*x*-ray data in Table 3)

All euxenites examined and all that have been reported in the literature have been completely metamict. When powdered euxenites were heated in a crucible over a Meker burner, considerable variations in the resulting powder patterns occurred in material with almost identical composition, However, it was found that, when the same original material was heated at temperatures between ca 400° C. and 800° C. for extended periods (6+ hours), reproducible *x*-ray patterns could be made. Heating to ca 1200° C. in air for a short period (5+ minutes) produced sharp powder patterns that are likewise specific for euxenite but differ from those of the same samples heated at the lower temperatures. Ignition at this high temperature in an inert atmosphere produced still another structure. However, all three diffraction patterns are specific for the metamict mineral euxenite.

D. *Brannerite:* (48)

The brannerites examined were either completely metamict or produced only very weak and diffuse *x*-ray patterns that were useless for accurate identification. All metamict brannerites that were heated crystallized below ca 1000° C., and most of them became crystalline at temperatures somewhat less than 750°C. in only a few minutes. There is no discernible difference in the crystallization of the brannerites when they are ignited in an inert atmosphere.

E. *Fergusonite:* (4, 6) (*x*-ray data in Table 4)

Crystalline fergusonite has been reported from only one locality (60). This occurrence is of doubtful authenticity, and in all other described localities the mineral is found in the metamict state.

Fergusonite begins to crystallize at ca 400° C. and, if heated between this temperature and ca 800° C. for some time, will form a structure that can be indexed with a tetragonal unit cell ($a_0 = 5.18$, $c_0 = 5.48 \pm .02$ Å—Table 3). Because of originally poor diffraction patterns it was at first believed to have an orthorhombic cell (7). However, more precise measurements indicate that the tetragonal cell noted above is the correct one. If the temperature is raised above ca 800° C., fergusonite crystallizes with a structure identical to that formed when equimolecular proportions of Y_2O_3 and Nb_2O_5 are sintered or fused together. Barth (4) has indexed the pattern of this high-temperature modification on the basis of a tetragonal unit cell and states that it is the original fergusonite structure. The author believes, however, that more detailed work on both the high-temperature and low-temperature dimorphs described above is necessary

before a definite decision can be reached as to the original fergusonite structure.

It is of interest to note that if the a_0 of ignited fergusonite (ca 7.75 Å—Barth) is divided by the square root of 2 the result is nearly identical to what has here been indexed as the c_0 of this smaller tetragonal unit cell (5.48 Å). This suggests some structural relation between the two polymorphs of fergusonite.

F. *Samarskite:* (42) (*x*-ray data in Table 4)

All samarskite specimens examined were found to be metamict. Upon ignition the samples crystallized in a manner that depended largely on the method and temperature of ignition. Samarskite heated to ca 1000° C. in air gives consistently reproducible patterns for identification purposes.* When heated to approximately 1200° C. the specimens began to fuse, and the resultant powder patterns were poor and unreliable.

G. *Davidite*

The few samples studied were metamict. They crystallized readily when heated in air over a Meker burner or at higher controlled temperatures (to ca 1200° C.) to one structural type regardless of the temperature. The specimens examined give the same *x*-ray pattern as the Tete mineral described by Bannister and Horne (3).

H. *Allanite:* (*x*-ray data in Table 5)

Although allanite does occur fairly well crystallized, it very often is found in the metamict state. Some specimens may appear to be crystalline optically, having birefringence and giving an interference figure. However, this same material may give no diffraction pattern. Usually the specimens that do give a pattern have weak and diffuse peaks in the large 2θ region, indicating at least partial disorder.

When this mineral occurs in the metamict state it usually can be crystallized by heating to red heat in air or in an inert atmosphere. The resultant *x*-ray powder pattern is similar to that given by nonmetamict material. Although all nonmetamict allanites gave similar patterns, many showed significant differences in *d*-distances. Likewise, when crystalline allanite was ignited, the lattice parameters did not remain constant. Allanites fuse or decompose at relatively low temperatures so that, in order to get reliable *x*-ray patterns, the material must not be heated over ca 850° C.

* It is noted that the samarskite pattern in Table 4 does not correspond to that published by Murdock. However, because this pattern has been consistently reproduced for numerous samples of National Museum and other material labeled samarskite, it is believed this pattern is representative of that metamict mineral.

Discussion

Data have been presented to aid in identifying some of the metamict minerals. This information is necessarily incomplete and may require subsequent revisions. It is believed, however, that enough new information has been obtained to serve as an aid to any future systematic work in this field.

In any study on these materials one must bear in mind that many of these metamict minerals have such complete internal disorder that they no longer fit the definition usually applied to the term "mineral," and that many have had certain constituents either added or subtracted since they were originally deposited. Hence, the term "recrystallization" is not strictly applicable in most instances, and "crystallization" would be more appropriate.

When metamict minerals are heated to comparatively low temperatures, structural changes take place at a slow rate. This sluggish crystallization becomes much more rapid with increase in temperature. Whereas crystallization of fergusonite may take place in less than 5 mintues at 800° C., the identical crystallization at 500° C. may take 24 hours. It has been observed that changes due to ignition are not confined to the metamict minerals. Data on the columbite-tantalite group (Table 6) and a barium-containing pyrochlore (Table 7) are included to show what happens to "nonmetamict" related minerals when subjected to elevated temperatures.

It is generally accepted (17, 23, 31 others) that the metamict condition is brought about by radiation from radioactive material included in the crystal, or from radioactive elements contained in the structure of the crystal. It is, however, a possibility that some of the massive varieties of metamict minerals may never have formed as crystalline material. Likewise, many of these minerals may have been stable only at the physical-chemical conditions at the time of formation; subsequent changes in these conditions, together with the included radioactivity, may have led to a rapid destruction of the metastable structures. This would explain why some of these minerals have never been found in a crystalline condition.

Data presented so far indicate that many metamict minerals may not recrystallize to the structure which they had when originally formed in nature. Hence, "reconstitution" data should be used with caution because such data in many instances may have no relation to the original structure of the mineral.

More work on the synthesis of those minerals that become metamict and artificial metamictization of these synthesized minerals would supply much valuable information on this problem.

Acknowledgments

This work was begun while the author was with the U. S. Geological Survey, as part of the program being conducted on behalf of the U. S. Atomic Energy Commission. The methods and procedures were developed in the Survey's laboratories.

All of the final data presented in the tables were compiled from work conducted by the author as a member of the Bureau of Mines, U. S. Department of the Interior, at the Laboratories of the College Park, Md., station.

The author is especially indebted to George Switzer, U. S. National Museum, Washington, D. C., and to Clifford Frondel, Harvard University, for supplying many of the samples of metamict minerals.

Table 1. *X*-Ray Diffraction Data

Zircon* from Lincoln County, Calif. Not metamict		Cyrtolite(Hybla, Ont.) Not heated		Cyrtolite† (Hybla, Ont.) heated to ca 950° C. in air	
d(Å)[2]	*I.*[1]	*d*(Å)	*I.*	*d*(Å)	*I.*
4.43	70	4.48VB	60	4.43	50
3.30	100	3.34VB	100	3.31	100
				2.97 ZrO_2	40
2.65	10			2.65	5
2.52	60	2.54VB	30	2.52	60
		Traces ↓			
2.33	20			2.34B	10
2.22	15			2.22VB	5
2.06	40			2.07B	20
1.908	15			1.91B	15
				1.83B, 1.82B } ZrO_2	10
1.751	20			1.754B	10
1.712	70			1.714	30
1.651	60			1.656	10
				1.555B ZrO_2	10
1.547	5			1.548B	5

B = Broad peak, VB = Very broad.

* Tetragonal cell. $a_0 = 6.60 \pm .01$[2], $c_0 = 5.98 \pm .01$.

† Tetragonal cell. $a_0 = 6.62 \pm .03$, $c_0 = 5.98 \pm .03$.

[1] Intensities in all of the Tables are relative based on 100 for the strongest line.

[2] In this and all of the following tables lattice spacings and unit cell dimensions are in Ångstrom units. CuK_α, wavelength of 1.5405 Å, is used to calculate the *d* values. The data have been obtained by a Norelco wide range goniometer using a silicon standard and having a 3° take-off. The goniometer was run at $\frac{1}{4}$° per minute.

TABLE 1—(*continued*)

Zircon* from Lincoln County, Calif. Not metamict		Cyrtolite (Hybla, Ont.) Not heated		Cyrtolite† (Hybla, Ont.) heated to ca 950° C. in air	
d(Å)[2]	*I.*[1]	*d*(Å)	*I.*	*d*(Å)	*I.*
1.494	1			1.50B	5
1.476	25			1.483B	10
1.381	20			1.385B	5
1.362	7			1.365B	5
1.290	7			1.289VB	1
1.259	5			1.259VB	3
1.249	5				
1.246	3				
				1.191B	5
1.188	20			1.186B	1
1.167	5				
1.109	5			1.109VB	1
1.101	23				
1.068	3				
1.059	15			1.054VB	5
1.051	5				
1.048	5				
1.045	5				
1.042	3				
1.002	2				
0.9751	2			0.976VVB	1
.9719	3			Broad	
.9538	3			Traces	
.9321	5				
.9200	2				
.9160	3				
.8999	3				
.8975	3			.897VVB	1
.8919	10				
.8867	5				
.8829	2				
.8562	5			.857VVB	3
.8530	2				
.8398	2				
.8331	10				
.8256	5				
.8118	5				
.8011	7				
.7901B	7				
.7811	10				

TABLE 2

Thorite*-partly metamict from Nigeria		Thorite† heated to ca 1050° C. in air Same material from Nigeria		Uranothorite‡ (Mostly metamict) heated to ca 1300° C. in air. Locality unknown	
d(Å)	*I.*	*d*(Å)	*I.*	*d*(Å)	*I.*
				5.25	20
				4.71	10
4.68	100	4.69	80	4.65	50
				4.18	90
				4.03	40
3.55	100	3.53	100	3.56	10
				3.49	40
		3.34(SiO_2)	5	3.27	60
		3.18(ThO_2)	20	3.13B(U, ThO_2)	2
				3.07	100
				2.96	30
				2.88	10
2.84	20	2.83	20	2.86	70
2.82		2.82			
				2.70B(U, ThO_2)	2
2.65B	60	2.66	60	2.67	5
				2.63	20
		2.51	20	2.51	2
2.50B	15			2.46	20
				2.42	15
				2.38	5
				2.34	5
2.22B	20	2.21	20	2.17	20
				2.16	20
				2.14	25
				2.10	20
2.00B	20	2.005	10		
		1.94B(U, ThO_2?)	1	1.940(U, ThO_2?)	25
				1.914	10
				1.891	15
1.88B	20	1.877B	10	1.870	20
		1.865B			
				1.847	15
		1.823	30		
1.825B	30				

B = Broad peak.

* Tetragonal cell. $a_0 = 7.10 \pm .02$, $c_0 = 6.32 \pm .02$.

† Tetragonal cell. $a_0 = 7.05 \pm .02$, $c_0 = 6.32 \pm .02$.

‡ Monoclinic cell. Using Pabst's value for $\beta = 104°55'(45)$ this pattern gives: $a_0 = 6.74 \pm .02$, $b_0 = 6.95 \pm .02$, $c_0 = 6.60 \pm .02$.

TABLE 2—(*continued*)

Thorite*-partly metamict from Nigeria		Thorite† heated to ca 1050° C. in air. Same material from Nigeria		Uranothorite‡ (Mostly) metamict) heated to ca 1300° C. in air. Locality unknown	
d(Å)	*I.*	*d*(Å)	*I.*	*d*(Å)	*I.*
				1.793	10
				1.770	15
		1.760B			
				1.754B	2
				1.740	15
				1.720	20
				1.679	5
		1.660B	10		
				1.633B	10
				1.589B	10
		1.580B	10		
				1.568B	2
				1.540B	10
		1.480B	10	Traces	
		1.437 1.433	10		
				1.369B	10
		1.330B	10	1.330B	10
				1.323B	10
				1.292 1.289	10
				1.283B	2
		1.270B	2	1.273B	5
		1.170B	2	Traces	
		1.120B	2		
				1.078B	5
		1.060B	2	1.060B	10
		1.02B	2	1.030B	5
				.9678B	5
				.9563B	10
				.8629B	5
				.8166B	5
				.8075B	5
				.8070B	5
				.7894B	5

TABLE 3

Euxenite (No. BM 26)* heated to ca 1200° C. in air		Euxenite (No. BM 26) heated to ca 430° C. in air		Euxenite (No. BM 26) heated to 1250° C. in helium	
d(Å)	*I.*	*d*(Å)	*I.*	*d*(Å)	*I.*
7.28	15	5.47	20		
Weak		4.62	7		
broad peaks		4.46	7		
3.66	40	4.41	20	3.67	1
3.37	20	4.25	10		
3.28	10	3.96	10	3.30	40
				3.13	60
2.99	100	3.76	5	2.99B	1
2.95	40	3.70	7	2.96	100
2.78	25	3.34B	10	2.75	30
2.63	10	3.07	30	2.65	20
2.60	30	2.98	70		
2.55	20	2.91	100		
2.52	5	2.77	20	2.53	40
2.45+ } 2.45− }	15	2.59B	20		
		2.43	5		
2.43	20	2.23	20		
2.31	17	2.21	10	2.34	10
2.21	13	2.11B	5	2.23	10
2.19	13	2.03B	7	2.17	10
2.12	20	1.980	20		
2.08	3	1.950	10	Faint	
2.04	5	Weak		Traces	
1.979	10	Peaks		1.98	1
1.941 } 1.939 }	13	1.855	20		
		1.820B	10		
1.897	25	1.732B	5	1.91	50
1.880B	3	1.681	15	1.87	30
1.830	30	1.676	15	1.84B	1
1.806	20	1.638B	5	1.81	60
1.774	25	1.576	15	1.77B	2
1.731	25	1.563B	5		
1.727	27	1.505VB	10		
1.704	3	Weak		1.71	40
1.683	3	Peaks			
				1.655	30
				1.651	20
1.643	25	1.195B	10		
1.625	5	1.185B	3		
1.614B	10	1.166B	5		
1.590	11	1.150B	3		
1.565	15	1.148B	3	1.572B	20
1.540	15	1.141B	2	1.544	60
1.505	10	1.128B	3	1.511B	10

B = Broad peak, VB = Very broad.

* Sample from Risö, Norway; very similar patterns are given by euxenites from Kragerö, Norway; Lyndoch, Ontario; Perth, Ontario; Swaziland, South Africa; Spruce Pine, N. C.; Iveland, Norway, Hiterö, Norway; and other unknown localities.

TABLE 3—(*continued*)

Euxenite (No. BM 26)* heated to ca 1200° C. in air		Euxenite (No. BM 26) heated to ca 430° C. in air		Euxenite (No. BM 26) heated to 1250° C. in helium	
d(Å)	*I.*	*d*(Å)	*I.*	*d*(Å)	*I.*
1.496	15	1.095B	3		
1.492	25	1.069B	3		
1.488		1.061B	3		
1.476	5	1.054	3	1.478	20
1.474		Weak peaks			
1.462	7				
1.441	10	.943B	3		
1.437	10	.886B	3		
				1.385	20
				1.369	10
Weak peaks					
1.344	5				
1.336	5				
				1.326B	3
1.296	10				
1.278	3			1.280B	3
1.277					
				1.262B	3
1.246	3			1.243B	1
1.224B	3			1.224B	10
1.209B	3				
				1.195B	10
1.187B	5				
1.173B	5			1.174B	5
1.160	7				
1.157				1.158B	3
1.143B	3			1.142B	3
1.119B	3			1.114B	10
1.102B	3				
1.082B	3			1.086B	2
1.058B	3			1.060B	3
1.056B	3			1.053B	3
1.043B	3			1.046B	20
1.039B	2				
1.034B	3				
1.0235B	3				
1.0205B	3				
1.0170B	3				
.9991B	2				
.9966B	2				
.9892B	2				
.9832B	3			.9842B	10
.9630B	3				
.9430B	2				
.9155B	5				
.9104B	2				
				.9058B	10
				.8958B	2
.8626B	2			.8652B	10
.8592B	2				

TABLE 4

Fergusonite* (No. LM-1)[2] heated to ca 1200° C. in air		Fergusonite (No. LM-1)[1] heated to ca 700° C. in air		Samarskite† heated to ca 1050° C. in air[3]	
d(Å)	*I.*	*d*(Å)	*I.*	*d*(Å)	*I.*
5.47	3	3.04	100		
4.58	3	2.74	30		
4.02	3	2.59VB	30	4.03	20
		1.88B	40	3.59	20
3.29	3	1.63	10	3.23B	30
3.12	100	1.57 B	5	3.13	40
3.01	20	1.56	2		
2.96	90	1.22B	2	2.98	100
				2.92	90
				2.81B	5
2.74	40			2.75	10
2.64	20			2.64B	5
2.59B	2			2.59	5
2.53B	10			2.52B	20
2.52	10				
				2.45	10
2.22	3			2.33	5
2.16	5			2.17B	5
				2.07B	2
2.01	5			2.05B	3
1.901	50			1.909	20
				1.890B	10
				1.863	20
1.855	30				
				1.830	20
1.754B	10				
				1.739	10
				1.709	20
				1.689	20
				1.654	5
1.646	10			1.650	
1.643B	10				

B = Broad peak, VB = Very broad.

* Sample supplied by Louis Moyd from Madawaska, Ontario. Nearly identical patterns are given by fergusonite from: Ahikambara, Madagascar; Llano Co., Texas; Amherst Co., Va. (2 localities); Arendal, Norway; Hiterö, Norway; Mitchell Co., N. C.; and other unknown localities.

† Locality unknown. Nearly identical patterns are given by samarskite from: Wheatland, Wyo.; Glastonbury, Conn.; Molinda, Ga.; Mitchell Co., N. C. and other localities.

[1] Tetragonal cell. $a_0 = 5.18 \pm .02$, $c_0 = 5.48 \pm .02$.

[2] Tetragonal cell. Unit cell as indexed by Barth. $a_0 = 7.74$, $c_0 = 11.34$.

[3] Could not be indexed.

TABLE 4—(*continued*)

Fergusonite* (No. LM-1)[2] heated to ca 1200° C. in air		Fergusonite (No. LM-1)[1] heated to ca 700° C. in air		Samarskite† heated to ca 1050° C. in air[3]	
d(Å)	*I.*	*d*(Å)	*I.*	*d*(Å)	*I.*
1.627B	15			1.630VB	5
1.620	15				
1.569	10			1.573B	10
1.563B	15			1.561	30
1.559	10				
1.508B	5			1.515B	10
1.504	5				
1.500B	5			1.500B	5
1.478B	3			1.478B	3
				1.462B	5
				1.437B	10
				1.425B	5
1.369	3				
1.321B	2				
1.288B	1				
1.263B	1				
1.245B	1				
1.236B	2				
				1.221B	1
1.213VB	3				
1.189	3			1.188B	1
1.146VB	3				
1.107B	3				
1.088B	2				
1.082B	3				
1.079B	3				
1.053B	1			1.056VB	1
1.048B	2				
1.046B	3				
1.041B	2				
1.036B	2				
1.025B	1				
1.001B	3				
0.9856B	1				
0.9168B	2				
0.9112B	2				
Traces					

TABLE 5

Allanite-mostly metamict (No. H. M. 86077)		Allanite-not metamict (supplied by Brian Mason)		Metamict allanite* (No. H. M. 86077) heated to ca 800° C. in air ½ hr.		Metamict allanite (No. H. M. 86077) heated to ca 850° C. for 14 hr.	
d(Å)	*I.*	*d*(Å)	*I.*	*d*(Å)	*I.*	*d*(Å)	*I.*
		9.20	20			9.30	30
		8.05	20				
		7.96	20				
		5.09	10	5.09	10	5.07	30
		5.01	10				
		4.87	5			4.84	10
		4.69	20	4.65	30	4.67	10
						4.62	50
						4.43B	2
						4.10B	2
						4.00	20
		3.78	10	3.79B	2	3.81B	10
		3.59	10	3.59B	1	3.60B	1
3.52VB	50	3.52	40	3.51	80	3.50	80
						3.34	30
		3.30	10	3.28B	2	3.27	20
		3.23	20	3.22B	2	3.20	10
				2.95B	100	2.96	100
2.93VB	100	2.92	90				
		2.91	100				
		2.86	50	2.84B	40		
		2.82	10			2.83	30
						2.79B	2
						2.74	30
2.69VB	30	2.68	40	2.68B	60	2.67	80
2.62VB	10	2.62	40	2.61B	50	2.60	40
		2.51	20			2.54	30
		2.50B	10			2.48B	2
						2.43	30
						2.40B	2
		2.33B	10			2.33B	10
						2.24B	10
		2.20	10			2.20B	10
		2.18B	20	2.16B	2	2.16B	30
		2.15	10			2.13B	30
		2.14	10				
		2.10B	2				
		2.05B	2			2.06B	10

B = Broad peak, VB = Very broad.

* Similar patterns given by samples from Arendal, Norway (orthite); Johannesburg, So. Africa, and numerous other unlisted localities.

TABLE 5—(*continued*)

Allanite-mostly metamict (No. H. M. 86077)		Allanite-not metamict (supplied by Brian Mason)		Metamict allanite* (No. H. M. 86077) heated to ca 800° C. in air ½ hr.		Metamict allanite (No. H. M. 86077) heated to ca 850° C. for 14 hr.	
d(Å)	*I.*	*d*(Å)	*I.*	*d*(Å)	*I.*	*d*(Å)	*I.*
		1.91B	2				
		1.89B	20			1.90B	20
		1.78B	2				
		1.67B	10				
		1.65B	10			1.65B	30
		1.64B	20			1.63B	60
		1.56B	20				
						1.47VB	10
						1.42B	20
		1.12B	2				

TABLE 6

Columbite #1[1]*		Columbite #1† heated to ca 1250° C. in air		Columbite-Tantalite[2]‡ (No. Ta 14)-high tantalum	
d(Å)	*I.*	*d*(Å)	*I.*	*d*(Å)	*I.*
7.15	1	7.15	20	7.15	5
		5.33	10	5.33	3
		5.15	10		
		4.78	10		
		3.74[z]	20		
3.65	40	3.67	50	3.67	60
		3.60[z]	30		
		3.57	25	3.58	5
		3.03	10		
2.97	100	2.97	100	2.98	100
		2.93[z]	50		
2.87	20	2.87	10	2.87	10
		2.86	10		
		2.83	5		
		2.82[z]	5		
		2.78	10		
		2.77	5		
2.55	10	2.54	10	2.55	7
		2.53	5		

[z] = $FeNb_2O_6$.

B = Broad Peak.

* Orthorhombic cell. $a_0 = 5.10 \pm .01$, $b_0 = 14\ 24 \pm .01$, $c_0 = 5.73 \pm .01$.

[1] Mitchell Co., N. C.

[2] Black Hills, South Dakota.

† More than one compound.

‡ Orthorhombic cell. $a_0 = 5.10 \pm .01$, $b_0 = 14.24 \pm .01$, $c_0 = 5.73 \pm .01$.

TABLE 6—(*continued*)

Columbite #1[1]*		Columbite #1† heated to ca 1250° C. in air		Columbite-Tantalite[2]‡ (No. Ta 14)-high tantalum	
d(Å)	*I.*	*d*(Å)	*I.*	*d*(Å)	*I.*
2.50	20	2.50	25	2.50	20
		2.47	10		
		2.43	5		
2.38B	2	2.39	10	2.38B	7
		2.34	5		
		2.24	3	2.25	3
2.21	15	2.21	10	2.22	7
		2.18	10		
2.09	10	2.09	10	2.09	7
		2.06	10		
		2.05	10		
		2.00	10		
1.91	20	1.907	10	1.91	7
1.83B	10	1.834	15	1.836	7
		1.805	5		
1.77B	10	1.780	20	1.777	15
		1.773	30		
1.74B	20	1.740B	20	1.745	20
		1.737	40		
1.72B	30	1.726	40	1.727	30
		1.698	20		
		1.580	10		
		1.573	10		
		1.562	10		
1.542B	20	1.532	20	1.542	10
		1.487	10	1.490	7
1.464B	30	1.467	20	1.466	15
		1.456	20	1.459	20
		1.440	20		
1.380B	10	Traces		1.384	3
Traces ↓		1.244	10	1.248	2
		1.224	10	1.225	3
				1.223	
		1.198	20	1.196	7
		1.179	10		
				1.140	3
		1.136	5		
		1.121	5		
		1.103	10	1.103	5
				1.092B	2
		1.080B	5	1.079B	2
				1.067B	1
				1.048B	2
		1.032B	5	1.036B	2
		1.020B	5	1.024B	3
		Traces		.997B	3
				.925B	2
				.883B	2
				.840B	2

TABLE 7

Barium-bearing pyrochlore*		Sample heated to ca 900° C. in air	
d(Å)	I.	d(Å)	I.
		7.14	5
6.08	80		
		5.97	20
		5.34B	2
		3.87	80
		3.59B	1
3.18	40	3.19	10
		3.13	100
3.04	100	3.01	60
		2.77	20
2.64	30		
		2.59	10
2.42	10	2.44	50
		2.39	10
		Traces	
2.03	10	2.00B	2
		1.940B	10
1.86	30	1.860B	1
		1.838B	10
		1.808B	10
1.78	10		
		1.763B	5
		1.642B	20
1.61B	2		
		1.609	2
		1.602	
1.590	30		
		1.568B	10
1.541B	1		
1.521B	10		
		1.499B	1
1.478B	5		
		1.456B	5
		Traces	
1.374B	1		
		1.326B	
1.319B	1	1.320B	2
1.210B	10		
1.180B	5	1.182B	5
1.158B	2		

B = Broad peak, VB = Very broad.

* Sample from Alaska; exact locality unknown.

$a_0 = 11.53 \pm .02$.

TABLE 7—(*continued*)

Barium-bearing pyrochlore*		Sample heated to ca 900° C. in air	
d(Å)	*I.*	*d*(Å)	*I.*
1.076B	5		
1.016	10		
Traces			
.893VB	10		
.881VB	5		
.836VB	2		

REFERENCES

*1. ALLEN, A. O., AND GHORMLEY, J. A. (1947), Decomposition of solid barium nitrate by fast electrons: *Jour. Chem. Phys.*, **15,** 208–209.

2. ARNOTT, RONALD J. (1950), *X*-ray diffraction data on some radioactive oxide minerals: *Am. Mineral.*, **35,** 386–400.

3. BANNISTER, F. A., AND HORNE, J. E. T. (1950), A radioactive mineral from Mozambique related to davidite: *Mineral. Mag.*, **29,** 101–112.

*4. BARTH, TOM F. W. (1926), The structure of synthetic, metamict, and recrystallized fergusonite—The structure of Risörite: *Norsk. geol. Tidskr.*, **9,** 23–39.

5. BERMAN, JOSEPH (1951 Abstr.), Studies of metamict minerals. (I): Methods and procedures: *Geol. Soc. Am., Bull.* **62,** 1422–1423.

6. ——— (1952 Abstr.), Studies of metamict minerals (II): Re-examination of fergusonite: *Geol. Soc. Am., Bull.* **63,** 1235.

7. BOROVSKII, I. B., AND BLOKHIN, M. A. (1931), Roentgen study of metamictic state of zircon: *Contr. of Lomonosov Inst., Ac. of Sci.*, **7,** 197–207.

8. BONATTI, S., AND GALLITELLI, P. (issued 1951; dated 1950), Sulla Torite di Nettuno (Roma): *Att. soc. tosc., Mem.*, **57,** (*A*) 3–4.

9. BRANDT, KARIN (1943), *X*-ray studies on ABO_4 compounds of rutile type and AB_2O_6 compounds of columbite type: *Arkiv. För Kemi, Mineralogi Och Geologi, Band* **17 A,** No. 15, 1–8.

10. BROOKER, E. J., AND NUFFIELD, E. W. (1951 Abstr.), Studies of radioactive compounds: IV—Pitchblende from Lake Athabasca: *Geol. Soc. Am., Bull.* **62,** 1425–1426.

*11. ——— (1952), Studies of radioactive compounds: IV—Pitchblende from Lake Athabaska, Canada; *Am. Mineral.*, **37,** 363–385.

*12. BUERGER, M. J. (1948), The role of temperature in mineralogy: *Am. Mineral.*, **33,** 101–121.

*13. ——— (1951), Crystallographic Aspects of Phase Transformations: Common Solids, Div. of Phy. Sci. Nat. Research Council, Symposium at Cornell U. (Aug. 1948) on Phase transformations in solids—John Wiley and Sons, Inc., 183–211.

14. CHUDOBA, K. F., AND LANGE, H. (1949), Rekristallisationsversuche an autoisotropisiertem Gadolinit, Samarskit und Euxenite: *Neues Jb. Min.*, Monatshefte, **A,** 30–45.

15. CHUDOBA, K., AND V. STACKELBERG, M. (1936), Dichte und Struktur des Zirkons: *Zeit. Krist.*, **95,** 230–246.

16. DAMOUR, M. A. (1864), Note sur la densité des zircons: *Compt. Rend.*, **58,** 154–159.

*17. Dana, J. D., and E. S. (1944), The System of Mineralogy, ed. 7, vol. 1, by C. Palache, H. Berman, and C. Frondel, John Wiley and Sons, Inc., N. Y.
18. Des Cloizeaux, A., and Damour, A. (1806), Examen des proprietes optiques et pyrogenetiques des mineraux connus sous les noms de gadolinites, allanites, orthites, euxenite, tyrite, yttrotantalite et fergusonite: *Ann. chim. phys.* (3), **59,** 357–379.
19. Dihlström, Klas (1938), Über den Bau des wahren Antimontetroxyds und des damit isomorphen Stibiotantalits, $SbTaO_4$: *Zeit. anorganische und allgemeine Chemie,* Band **239,** 57–64.
20. Ellsworth, H. V. (1925), Radioactive minerals as geological age indicators: *Am. J. Sc.,* **209,** 127–144.
21. ——— (1932), Rare element minerals of Canada: *Geol. Surv. Canada, Econ. Geol. Series II.*
22. Evans, R. D., and Goodman, C. (1941), Radioactivity of rocks: *Geol. Soc. Am., Bull.* **52,** 459–490.
*23. Faessler, A. (1942), Untersuchungen zum Problem des metamikten Zustandes: *Zeit. Krist.,* **104,** 81–113.
24. George, D. R. (1951), Thorite from California: *Am. Mineral.,* **36,** 129–132.
*25. Goldschmidt, V. M. (1924), Über die Umwandlung krystallisierter Mineralien in den metamikten Zustand (isotropisierung): *Norsk. Ak., Skr.,* **L.** 1. No. 5, Geochemische Verteilungsgesetze der Elemente. III. (Anhang), 51–58.
26. Hamberg, Axel (1914), Die radioktiven Substanzen und die geologische Forschung: *Geol. För. Förh.,* **36,** 31–96.
27. Hess, F. L., and Wells, R. C. (1930), Samarskite from Petaca, New Mexico: *Am. J. Sc.,* **19,** 18–26.
*28. Holland, Heinrich D., and Kulp, Laurence J. (1950), Geologic age from metamict minerals: *Science,* **3,** 312.
29. Hurley, Patrick M. (1951), Alpha ionization damage as a cause of low helium ratios: *Technical Report, Office of Naval Research, Contract No. N5ori-07829.*
30. ———, and Fairbairn, H. W. (1952), Alpha-Radiation damage in zircon: *Jour. Appl. Phys.,* **23,** No. 12, 1408.
*31. ——— (1953), Radiation damage in zircon: A possible age method, *Geol. Soc. Am., Bull.* **64,** 659–673.
*32. Hutton, C. Osborne (1950), Studies of heavy detrital minerals: *Geol. Soc. Am., Bull.* **61,** 635–716.
*33. Kostyleva, E. E. (1951), On metamictic disintegration of the zircon group of minerals—Problems of mineralogy, geochemistry and petrography, *Ac. Sc. U.S.S.R.,* 27–35 (in Russian).
*34. Kulp, J. L., Volchok, H. L., and Holland, H. D. (1952), Age from metamict minerals, *Am. Mineral.,* **37,** 709–718.
35. Larsen, E. S., Jr., Waring, C. L., and Berman, J. (1953), Zoned zircon from Oklahoma: *Am. Mineral.,* **38,** 1118–1125.
36. Liebisch, Th. (1910), Über die Rückbildung des kristallisierten Zustandes aus dem amorphen Zustande beim Erhitzen pyrognomischer Mineralien: *Ak. Berlin Ber.,* **I,** 350–364.
37. Machatschki, F. (1929), Über die Formel des Risörites und Fergusonites: *Zeit. Krist.* **72,** 291–300.
*38. ——— (1941), Zur Frage der Stabilität des Zirkongitters: *Zbl. Min.,* **A,** 38–40.
*39. Morehead, F. F., and Daniels, F. (1952), Storage of radiation energy in crystalline lithium fluoride and metamict minerals, *Jour. Phys. Chem.,* **46,** 546–548.

40. Morgan, J. H., and Auer, Marianna L. (1941), Optical, spectroscopic and radioactivity studies of zircon: *Am. J. Sc.*, **239**, 305–311.
41. Mügge, O. (1922), Über isotrop gewordene Kristalle: *Cbl. Min.*, 721–739 and 753–765.
42. Murdoch, Joseph (1951), Notes on some California minerals: *Am. Mineral.*, **36**, 358–359.
43. Orcel, Jean (1953), Analyse thermique differentielle de quelques minéraux métamictes: *Compt. Rend.*, **236**, 1052–1054.
44. Orcel, Jean et Lévy, Claude (1953), Analyse thermique de la betafite, mineral métamicte: *Compt. Rend.*, **236**, 1, 1177–1179.
45. Pabst, A., and Hutton, C. Osborne (1951), Huttonite, a new monoclinic thorium silicate; with an account of its occurrence, analysis and properties: *Am. Mineral.*, **36**, 60–69.
46. Pabst, A. (1951), *X*-ray examination of uranothorite: *Am. Mineral.*, **36**, 557–562; abstract in *Geol. Soc. Am., Bull.* **61**, 1492 (1950)
*47. ——— (1952), The metamict state: *Am. Mineral.*, **37**, 137–157.
48. ——— (1954), Brannerite from California: *Am. Mineral.*, **39**, 109–117.
*49. Pellas, P. (1951), Mineralogie—sur la destruction spontanée des réseaux cristallins de minéraux radioactivs: *Compt. Rend.*, **232**, 1369–1371.
*50. ——— (1953), Sur l'establissement de l'état métamicte dans gadolinite. Bilan énergétique de la recristallization: *Compt. Rend.*, **236**, 619–621.
51. Peterson, Walfr. (1890), Studier öfver gadolinit: *Geol. För. Förh.*, **12**, 275–347.
52. Prior, G. T. (1894), On fergusonite from Ceylon: *Mineral. Mag.*, **10**, 234–237.
*53. Seitz, F. (1949), On the disordering of solids by action of fast massive particles: *Proc. Faraday Soc.*, 271–282.
*54. Slater, J. C. (1951), The effects of radiation on materials: *Jour. Appl. Phys.*, **22**, 237–256.
55. v. Stackelberg, M., and Chudoba, K. (1937), Dichte und Struktur des Zirkons, II: *Zeit. Krist.*, **97**, 252–262.
56. v. Stackelberg, M., and Rottenbach, E. (1940), Dichte und Struktur des Zirkons, III and IV: *Zeit. Krist.*, **97**, 173–182 and 207–208.
*57. Stech, B. (1952), Structural change produced in crystals by alpha particle bombardment: *Zeit. Naturforsch.* **7a**, Feb. 175–185.
58. Vegard, L. (1916), Results of crystal analysis: *Phil. Mag.* (6), **32**, 65–96.
59. ——— (1927), Results of crystal analysis: *Phil. Mag.* (7), **4**, 11.
60. Vogt, Th. (1911), Vorläufige Mitteilung über Yttrofluorite, eine . . . : (On nonmetamictic fergusonite): *Centralblatt für Min., Geologie und Paläontologie*, **12**, 373.
61. Wyckoff, Ralph W. G., and Hendricks, Sterling B. (1927), Die Kristallstruktur von Zirkon und die Kriterien für spezielle Lagen in tetragonalen Raumgruppen: *Zeit. Krist.*, **66**, 73–102.
62. Zhirov, K. K. (1952), Conversion of zircon into the metamict state: *Doklady Akad. Nauk., U.S.S.R.*, **85**, 889–891 (in Russian).

Manuscript received Oct. 30, 1954.

NEOMESSELITE AND BETA-ROSELITE: TWO NEW MEMBERS OF THE FAIRFIELDITE GROUP*

CLIFFORD FRONDEL, *Harvard University, Cambridge, Massachusetts.*

ABSTRACT

Neomesselite, (Ca, Fe, Mn)$_3$(PO$_4$)$_2$·2H$_2$O, is the disordered, iron-rich analogue of fairfieldite, Ca$_2$(Mn, Fe)(PO$_4$)$_2$·2H$_2$O. Found as a hydrothermal mineral in pegmatite at Palermo, North Groton, New Hampshire. Triclinic, as greenish white to white fibrous and fine-granular aggregates. Optically biaxial positive, with nX = 1.653, nY = 1.659, nZ = 1.676, 2V = 25°, specific gravity 3.16 for material with Ca:Fe:Mn:Mg = 12.3:8.6:1.6:1; also nX = 1.644, nY = 1.649, nZ = 1.663, 2V small, for material with Ca:Fe:Mn:Mg = 26.8:8.4:5.4:1.

Beta-roselite, Ca$_2$Co(AsO$_4$)$_2$·2H$_2$O, is a triclinic polymorph of roselite isostructural with fairfieldite. Found as dark rose-red granular aggregates at Schneeberg, Saxony. Biaxial negative, with nX = 1.723 (pink), nY = 1.737 (pale pink), nZ = 1.756 (nearly colorless), 2V = 80°–90°, $r < v$. Specific gravity 3.71, hardness 3½–4, perfect cleavage {010}.

NEOMESSELITE, (Ca, Fe, Mn)$_3$(PO$_4$)$_2$·2H$_2$O

The name messelite was applied by Muthmann in 1889 to a mineral with the composition Ca$_2$Fe(PO$_4$)$_2$·2½H$_2$O found at Messel in Hesse, Germany. Messelite was re-examined in 1940 by Wolfe. He concludes from x-ray, optical and chemical study that the mineral actually is anapaite, Ca$_2$Fe(PO$_4$)$_2$·4H$_2$O, partly altered to collinsite and discredits it as a species. The circumstance has now come about that an unaltered mineral has been found whose chemical composition is essentially that attributed to the original messelite. This mineral, for which the name neomesselite is proposed, has the composition (Ca, Fe, Mn)$_3$(PO$_4$)$_2$·2H$_2$O and is isostructural with fairfieldite. Anapaite (messelite) is a crystallographically distinct higher hydrate that is isostructural with parahopeite. The position of neomesselite and of an allied new mineral, beta-roselite, described beyond, among minerals of the formula-type A$_2$B(XO$_4$)$_2$·2H$_2$O is given in Table 1.

Neomesselite occurs as a late hydrothermal mineral in the Palermo pegmatite at North Groton, New Hampshire, in two ways: (1) as granular, cleavable masses with a pale greenish white to greenish gray color associated principally with granular siderite, plagioclase and quartz. Other associated minerals, present sparingly, include goyazite, whitlockite, herderite, platy crystals and lamellar masses of amblygonite, radial-fibrous aggregates of brown eosphorite, brazilianite, and grains of sphalerite. (2) As platy-fibrous, almost pure white masses either deposited upon and molded around euhedral crystals of ludlamite in veinlets cutting

* Contribution from the Department of Mineralogy and Petrography, Harvard University, No. 355.

triphylite, or embedded in veinlets or patches of granular material composed largely of siderite, quartz and plagioclase with minor amounts of platy amblygonite, ludlamite, whitlockite and sphalerite. This type of neomesselite has been mentioned under the name fairfieldite by Wolfe (1949) in his paper on ludlamite from Palermo. While two modes of occurrence of the neomesselite can be distinguished, both are of essentially the same period of formation and are products of the re-working of triphylite crystals formed during the magmatic stage of crystallization by late-stage hydrothermal solutions.

Neomesselite has a single, nearly perfect cleavage on {001}. The color varies from almost pure white to pale greenish white and greenish gray. Luster vitreous. Hardness $3\frac{1}{2}$; specific gravity of the granular material

TABLE 1. MINERALS OF THE $A_2B(XO_4)_2 \cdot 2H_2O$ FORMULA-TYPE

Fairfieldite Group (Triclinic)		Roselite Group (Monoclinic)	
Fairfieldite	$Ca_2(Mn, Fe)(PO_4)_2 \cdot 2H_2O$	Roselite	$Ca_2(Co, Mg)(AsO_4)_2 \cdot 2H_2O$
Neomesselite	$(Ca, Fe, Mn, Mg)_3(PO_4)_2 \cdot 2H_2O$	Brandtite	$Ca_2Mn(AsO_4)_2 \cdot 2H_2O$
Collinsite	$Ca_2(Mg, Fe)(PO_4)_2 \cdot 2H_2O$		
Beta-roselite	$Ca_2(Co, Mg)(AsO_4)_2 \cdot 2H_2O$		

3.16. Distinct, measurable crystals have not been found. In open cavities the mineral sometimes forms globular or sheaf-like arrangements of lamellae with a rudely radial arrangement. When broken these show curved and irregular cleavage surfaces. The surface of the globules is indistinctly crystalline. Under magnification, the crystals composing the aggregates are seen to be terminated either by a single plane inclined to the elongation or by a pair of steeply inclined planes whose common edge is inclined at an angle to the elongation. The appearance of these aggregates is very similar to that of the fairfieldite found in the New England pegmatites. The symmetry of neomesselite is indicated to be triclinic by the optical properties and by the close resemblance of its powder pattern to those of collinsite and fairfieldite.

Optically, neomesselite is biaxial positive. Flakes resting on the cleavage show the acute bisectrix X emerging just outside of the field of view. 2V varies from about 20° to 35°. Cleavage flakes show an extinction angle of 16° to 23° as measured from Z′ either to the elongation of occasional lath-like flakes, or to an indistinct lineation in the grains that in some instances are parallely arranged needle-like inclusions, and in others appear to be either a second cleavage or extremely narrow polysynthetic twin lamellae. Turned on edge, the cleavage flakes show inclined extinction up to about 22°. The indices of refraction, given in Table 2, and the

other optical constants vary somewhat with the ratio of the cations present.

Chemical analyses of the granular and fibrous types of neomessolite are cited in Table 2 in comparison with some reported analyses of fairfieldite. Analysis 1, of the greenish, granular material, conforms closely to the formula $(Ca, Fe, Mn, Mg)_3(PO_4)_2 \cdot 2.4H_2O$. The true water content probably is $2H_2O$. The several cations, present in the ratio Ca:Fe:Mn:Mg = 12.3:8.6:1.6:1. appear to be structurally equivalent, and in this the mineral departs from the general formula $A_2B(XO_4)_2 \cdot 2H_2O$, where A = Ca and B = Mg, Co, Fe″ or Mn″, found for the related minerals (Table 1). Analysis 2, of the white, fibrous material, affords a somewhat different ratio of the cations, with Ca:Fe:Mn:Mg = 26:8.4:5.4:1, and here also these appear to be structurally equivalent.

Neomessilite apparently forms a continuous isomorphous series with

Table 2. Chemical Analyses and Optical Data for Neomesslite and Fairfieldite

	1	2	3	4	5	6
CaO	23.19	28.00	30.76	30.85	30.02	29.77
MgO	1.36	0.77				
FeO	20.92	11.54	7.00	4.75	3.42	1.00
MnO	3.94	7.35	12.40	14.82	17.40	19.68
Fe_2O_3	0.83	nil				
P_2O_5	36.90		39.62	39.55	[37.69]	37.79
H_2O	11.30		9.67	9.70	9.81	9.94
Insol.	1.39		0.55	0.50	1.66	1.07
Total	99.83		100.30	100.58	[100.00]	99.25
G	3.16			3.016	3.07	
*n*X	1.653	1.644		1.640	1.636	1.633
*n*Y	1.659	1.649		1.650	1.644	1.641
*n*Z	1.676	1.663		1.660	1.654	1.562
2V	25°	small		86°	very large	—
Ext. angle	20°	23°		—	—	—

1. Neomesselite, Palermo, N. H. Greenish white, granular. L. C. Peck analysis, 1948.
2. Neomesselite. Palermo, N. H. White, platy-fibrous. H. J. Hallowell analysis, 1949.
3. Fairfieldite. Branchville, Conn. Penfield analysis in Brush and Dana, *Am. J. Sci.*, **17,** 359 (1879). Sum includes Na_2O 0.30.
4. Fairfieldite. Poland, Maine. Gonyer analysis in Berman and Gonyer, *Am. Mineral.*, **15,** 375 (1930). Sum includes Na_2O 0.41.
5. Fairfieldite. Branchville, Conn. Wells analysis in Brush and Dana, *Am. J. Sci.*, **39,** 212 (1890). It is not certain if the optical data, from Larsen, *U. S. Geol. Surv. Bull.* **679,** 74 (1921), refer to material of this particular composition.
6. Fairfieldite. Buckfield, Maine. Vassar analysis in Landes, *Am. Mineral.*, **10,** 386 (1925).

fairfieldite, as seen from the selected analyses cited in Table 2, and the name might then be restricted to that part of the series with fairfieldite with Fe > Mn. Before uniting these species in a series, however, it would be desirable to establish the structural relations of the two minerals. All of the reported analyses of fairfieldite conform to the formula $A_2B(XO_4)_2 \cdot 2H_2O$ while neomesselite apparently is the disordered equivalent $(A, B)_3(XO_4)_2 \cdot 2H_2O$. Fairfieldite itself needs further study, since a close comparison of *x*-ray powder photographs of this mineral from some of its reported localities show slight unexplained differences. The material from Newry, Maine, and Hagendorf, Bavaria, is virtually identical in pattern with that of the fibrous neomesselite from Palermo and is relatively close to that of collinsite, whereas the fairfieldite from Branchville, Connecticut, and Buckfield, Maine, have identical patterns which differ slightly from those of the other fairfieldites and from neomesselite. The *x*-ray powder spacing data for the fibrous neomesselite and the analyzed Buckfield fairfieldite are given in Table 3.

TABLE 3. *X*-RAY POWDER SPACING DATA FOR NEOMESSELITE, FAIRFIELDITE AND BETA-ROSELITE

Iron radiation, manganese filter, in Ångstroms

Neomesselite				Fairfieldite				Beta-Roselite			
I	*d*	*I*	*d*	*I*	*d*	*I*	*d*	*I*	*d*	*I*	*d*
5	9.00	3	2.48	2	7.06	5	2.30	2	6.40	4	1.719
3	7.01	3	2.45	9	6.40	3	2.24	1	5.66	3	1.701
10	6.34	2	2.41	6	5.08	2	2.21	3	5.12	1	1.606
5	5.07	3	2.35	5	4.53	4	2.17	1	4.68		
4	4.57	1	2.25	6	4.33	5	2.13	4	3.98		
4	4.51	3	2.23	1	3.96	6	2.10	6	3.59		
1	3.83	1	2.21	6	3.60	7	2.04	3	3.38		
4	3.74	4	2.13	3	3.48	1	1.986	4	3.22		
4	3.58	4	2.10	2	3.34	3	1.963	9	3.08		
3	3.49	1	2.05	10	3.23	3	1.934	10	2.75		
2	3.40	3	2.02	7	3.20	5	1.928	2	2.61		
2	3.34	1	1.989	8	3.03	1	1.902	1	2.52		
6	3.28	3	1.962	7	2.86	3	1.852	1	2.45		
10	3.17	1	1.923	5	2.84	4	1.828	1	2.33		
8	3.02	2	1.875	2	2.80	6	1.801	2	2.17		
3	2.95	4	1.839	6	2.69	3	1.744	1	2.13		
4	2.86	4	1.813	7	2.66	5	1.730	2	2.08		
6	2.79	7	1.788	7	2.63	5	1.722	1	2.02		
8	2.68	6	1.708	3	2.57	6	1.690	4	1.894		
4	2.62	6	1.689	4	2.52	2	1.672	1	1.875		
7	2.57	4	1.656	7	2.46	2	1.657	1	1.790		

Beta-Roselite, $Ca_2Co(AsO_4)_2 \cdot 2H_2O$

In connection with the study of neomesselite an examination was made of all of the available specimens of minerals belonging to the $A_2B(XO_4)_2 \cdot 2H_2O$ family. No new data were obtained except in the case of roselite. Nine specimens of this mineral, all from Schneeberg, Saxony, were available for study. These included the specimens earlier described by Peacock (1936) and by Wolfe (1940) in their studies of these species. Eight of these specimens conformed to the definitive description of roselite given by Peacock. One specimen, however, gave an x-ray powder pattern identical with that of collinsite, and similar to those of fairfieldite and neomesselite, but quite distinct from that of roselite proper. A chemical analysis established the composition as $Ca_2Co(AsO_4)_2 \cdot 2H_2O$, identical with that of roselite. The mineral thus is a member of the triclinic fairfieldite group and is dimorphous with roselite. The name beta-roselite is proposed for it.

Beta-roselite occurs as granular masses and distinct crystals were not found. The mineral is associated with pale pink cobaltian calcite and a few grains of dark rose-colored roselite in vein material consisting principally of quartz and pyrite. All of the minerals appear to be primary hydrothermal deposits.

Beta-roselite has a dark rose-red color and is indistinguishable in the hand specimen from the darker-colored types of roselite. There is one almost perfect cleavage, here taken as on {010}. No other cleavages were observed, although additional cleavages have been found on other members of the group. Hardness $3\frac{1}{2}$ to 4; specific gravity 3.71. Luster is weakly vitreous. Cleavage fragments are markedly composite on a fine scale. with irregularly curved surfaces much like neomesselite and fairfieldite, and this circumstance has precluded getting useful single-crystal x-ray photographs. The x-ray powder spacing data are given in Table 3. Beta-roselite may have been represented among the crystals of the several rather conflicting types of so-called roselite described by Schrauf (1874, 1873), and it may prove possible in the future to identify any such crystals if crystallographic data can be obtained on the present species.

Optically, beta-roselite is biaxial negative (−). Grains resting on the perfect {010} cleavage show the acute bisectrix X at a considerable angle thereto with Y′ and Z in the plane of {010}. An optic axis appears just outside the field of view. Turned on edge, so that the line of view is parallel to the cleavage, the flakes show inclined extinction up to about 40°. Small grains are colorless; larger grains are faintly pleochroic, nearly colorless to pink. The dispersion is rather strong, distinctly crossed, with $r < v$. The indices of refraction are given in Table 4 in comparison with those of roselite as cited by Peacock (1936). The chemical analysis of

TABLE 4. OPTICAL PROPERTIES OF BETA-ROSELITE AND ROSELITE

	Beta-roselite	Roselite (dark rose)	Roselite (pale rose)
nX (Na)	1.723± .003	1.725± .003	1.694± .003
nY	1.737± .003	1.728± .003	1.704± .003
nZ	1.756± .003	1.735± .003	1.719± .003
2V	80°–90°	60°	75°
Dispersion	$r<v$	$r<v$	$r<v$
Pleochroism			
X	pink	deep rose	pale rose
Y	pale pink	pale rose	paler rose
Z	nearly colorless	paler rose	palest rose

beta-roselite, cited in Table 5, affords the formula $Ca_2Co(AsO_4)_2 \cdot 2H_2O$. Small amounts of Mg, Ni and Fe″ substitute for Co. The analysis shows a slight excess of Ca over the 2:1 ratio required by the A and B positions.

TABLE 5. CHEMICAL ANALYSIS OF BETA-ROSELITE

	CaO	CoO	MgO	NiO	FeO	As_2O_5	P_2O_5	H_2O	Total
1	24.76	16.54				50.74		7.96	100.00
2	26.29	13.28	0.92	1.43	0.32	49.66	tr.	8.41	100.31

1. Theoretical weight percentages, $Ca_2Co(AsO_4)_2 \cdot 2H_2O$.
2. Beta-roselite. Schneeberg, Saxony. H. J. Hallowell analysis, July, 1949.

ACKNOWLEDGMENT

The writer wishes to acknowledge the aid of Miss Mary Mrose in the preparation of numerous x-ray powder photographs.

REFERENCES

MUTHMANN, W., Messelith, ein neues Mineral: *Zeit. Krist.*, **17**, 93 (1890).

PEACOCK, M. A., On roselite and the rule of highest pseudo-symmetry: *Am. Mineral.*, **21**, 589 (1936).

SCHRAUF, A., Monographie des Roselith: *Min. Mitth.*, 137 (1874); 291 (1873).

WOLFE, C. W., Classification of minerals of the type $A_3(XO_4)_2 \cdot nH_2O$: *Am. Mineral.*, **25**, 738 (1940).

WOLFE, C. W., Ludlamite from the Palermo mine, North Groton, N. H.: *Am. Mineral.*, **34**, 94 (1949).

Manuscript received Aug. 16, 1954.

THERMAL ANALYSIS STUDY OF THE NATROLITE GROUP

C. J. Peng*

Abstract

The three members of the natrolite group, natrolite, scolecite, and mesolite, from ten different localities have been examined by both static and differential thermal analysis methods. The thermal changes taking place in the specimens at reaction peak temperatures given by the *DTA* curves have been investigated by coordinated optical and *x*-ray diffraction methods. Despite their close similarity in composition and crystal structure, the three zeolites show different thermal behavior. Natrolite gives off its water rapidly in a single temperature range, whereas scolecite and mesolite lose their water in two and three stages respectively. It is thus inferred that there is only one type of water molecule in natrolite, while the water molecules in scolecite and mesolite consist, respectively, of two and three types with different bond strengths. This is supported on structural grounds. The range of stability also is different for the three zeolites. Natrolite will not break down completely until about 940° C., but scolecite collapses structurally at 560° C. and mesolite at a still lower temperature of 490° C. This is explained as a consequence of their different degrees of hydration.

Introduction

Much study has been made of the dehydration phenomenon of zeolites and their changes in physical properties that accompany the effect of decomposition. The method generally employed is to determine the loss of water at various elevated temperatures under equilibrium conditions with or without control of the water vapor pressure. Owing to certain technical differences and possible variations in the composition of the specimens studied, the results are not consistent and hence the interpretations of their thermal history vary.

The purpose of this report is to give the results of an investigation of the thermal behavior of the natrolite group by both static dehydration and differential thermal analysis methods. The natrolite group was selected because its members, natrolite, scolecite, and mesolite, have a relatively simple and definite composition and have been nearly completely studied structurally. An attempt has also been made to correlate the thermal effects with the structures of the zeolites.

Although the three zeolites are isostructural and show markedly similar physical properties, they do not undergo the same thermal changes. Further, the intensity of those thermal reactions due to dehydration and the temperatures at which they take place are different for the three because each contains different amounts of water and the water molecules may occupy different lattice positions. Thus, the thermal reaction data

* Department of Geology, Columbia University, New York, N. Y. Present address: University of Wisconsin, Madison, Wisconsin.

should be useful not only for the purpose of identification but also in the interpretation of the structure.

Acknowledgment

The research was undertaken at Columbia University at the suggestion of Prof. P. F. Kerr. The writer wishes to express his indebtedness to Prof. Kerr for his interest and advice throughout the study and critical reading of the paper. He is also grateful to Prof. J. L. Kulp and Prof. R. J. Holmes for their helpful suggestions and criticism. The encouragement and assistance given by Prof. Chas. H. Behre, Jr. during the course of the work are highly appreciated.

Materials

The specimens used for the study were obtained from the Egleston Mineralogical Collection of Columbia University and included the following:

(1) Natrolite, Giant's Causeway, Ireland. White, radiating needle-like crystals.
(2) Natrolite, West Paterson, N. J. White, radiating hairy needles.
(3) Natrolite, Brevig, Norway. White accicular crystals, partly admixed with chlorite.
(4) Natrolite, Auvergne, France. Groups of white, stout, translucent crystals with good prisms and pyramids.
(5) Scolecite, Poonah, India. White, slender, glassy needles in radiating groups.
(6) Scolecite, Bombay, India. Thick clusters of long white glassy crystals.
(7) Scolecite, Moore, Mercer County, N. J. White accicular crystals.
(8) Mesolite, Peter's Point, Nova Scotia. Divergent groups of white slender needles.
(9) Mesolite, Cape d'Or, Nova Scotia. A mass of radiating white, fibrous crystals densely matted together.
(10) Mesolite, Scotland. Groups of white fibrous crystals.

The three zeolites, natrolite ($Na_2Al_2Si_3O_{10} \cdot 2H_2O$), scolecite ($CaAl_2Si_3O_{10} \cdot 3H_2O$), and mesolite ($Ca_2Na_2Al_6Si_9O_{30} \cdot 8H_2O$), have practically a constant composition as first pointed out by Winchell (1925) and show only limited ionic substitutions of the types $Na_2 \rightarrow Ca$ and $Na \rightarrow K$ (Hey & Bannister, 1932, 1933, 1936). Chemical analyses of previously described specimens probably from the same localities as a number of the specimens here studied are given in the following table (Table 1). It is believed that they are representative of the chemical composition of the three zeolites since all the tested specimens have been thoroughly examined optically and by means of x-ray diffraction to ensure purity and identity.

Experimental Equipment and Procedure

Specimens were first examined with a binocular microscope and material was selected for further study. The standard immersion method was used to determine the optical constants. X-ray powder photographs of

all specimens were taken by means of a Philips x-ray unit to confirm the identity of the minerals. X-ray spectrometer measurements were made on some of the specimens. Copper—K radiation with nickel filter was used throughout.

Both static dehydration and differential thermal analysis methods were applied to the study of the thermal behavior of the zeolites. The procedure to obtain dehydration data is similar to that generally followed. Material was heated in a Freas electric oven for successive periods of

Table 1. Chemical Analyses of Natrolite, Scolecite and Mesolite

	Natrolite			Scolecite		Mesolite	
	1	2	3	4	5	6	7
SiO_2	47.22	47.88	47.60	45.16	46.10	46.01	46.26
Al_2O_3	27.21	26.12	27.40	25.90	26.32	26.66	26.48
Na_2O	15.86	15.63	15.36	0.16	0.12	4.66	4.98
K_2O	0.06	—	0.23	0.06	—	0.20	—
CaO	—	0.45	0.13	14.86	14.22	9.88	9.24
H_2O	9.70	9.80	9.47	13.66	13.60	12.69	13.04
Total	100.05	99.88	100.19	99.80	100.36	100.10	100.00

1. Kinbane (White Head), County Antrim (Giant's Causeway), Ireland. Analyst F. N. Ashcroft, *Mineral. Mag.*, **17,** 307 (1916).
2. Tour de Gevillat, Auvergne, France. Analyst F. Gonnard, *Bull. Soc. Franc. Mineral.*, **14,** 170 (1891).
3. Puy de Marmant, Puy-de-Dome, France. Analyst M. H. Hey, *Mineral. Mag.*, **23,** 246 (1932).
4. B. M. 33887, Syhadree Mts., Bombay, India. Analyst M. H. Hey, *Mineral. Mag.*, **24,** 228 (1936).
5. Poonah, Bombay, India. Analyst G. Tschermak, *Sitzungsber. Akad. Wiss. Wien, naturwiss. Kl., Abt. I*, **126,** 541 (1917).
6. Cape d'Or, Nova Scotia. Analyst E. W. Todd, *Univ. Toronto Studies, Geol. Ser. no.* **14,** 57 (1922).
7. Isle of Skye, Scotland. Analyst M. F. Heddle, *Mineral. Mag.*, **5,** 118 (1883).

20 hours at about 20° intervals up to 350° C. The temperature was measured with a thermometer inserted into the furnace through a hole on the top of the chamber. For higher temperatures, heating was carried out in a rheostat-controlled electric muffle for 3 hours at about 50° C. intervals; the temperature was measured with a Brown portable electric pyrometer with an accuracy of about 5°. After a desired temperature was reached, the sample was cooled to room temperature in a desiccator and then weighed. This was followed by reheating it at the same tempera-

ture for another 2 hours in order to check the weight previously obtained. Weight losses were practically the same before and after reheating and only in a few cases was further heating called for to reach a constant weight, indicating that heating over a period of 20 hours up to 350° C. and 3 hours at higher temperatures is sufficient to bring about equilibrium at a given temperature. The process was then repeated at higher temperatures. Each sample to be heated was ground to pass a 200-mesh sieve. No attempt was made to control the water vapor pressure in the furnace.

The differential thermal analysis method not only provides dehydration data, but also reveals those thermal reactions that are not accompanied by changes in weight, such as structural breakdown, recrystallization, phase transition, etc. The multiple *DTA* unit developed in the Mineralogical Laboratory of Columbia University (Kerr & Kulp, 1948) was used in the present study. The pulverized samples were packed uniformly in the specimen recesses which, $\frac{1}{8}$ in. in radius and $\frac{1}{2}$ in. deep for each, are spaced symmetrically with the alundum holes with respect to the vertical axis of the furnace. Heating was carried out without covering from room temperature up to about 1050° C. at the rate of $12\frac{1}{2}$° per minute. Two or three runs were made on each sample. The high sensitivity scale 2000 for the d.c. amplifier was used throughout, for which the amplification is about two. For identifying each thermal reaction, the specimen was first heated up to the peak reaction temperature and then examined by optical and x-ray powder methods.

The endothermic peaks on the *DTA* curves of the zeolites due to loss of water in general correlate well with the shoulders on their dehydration curves. But as a rule, they occur at higher temperatures than corresponding shoulders, although initial decomposition usually takes place at approximately the same temperature in both cases. The difference in temperature maximum between these two kinds of thermal curves observed in the present study is about 100° C. The reason for the reaction-temperature lag in the *DTA* curves lies in the dynamic character of the method by which the sample is heated at a constant rate, thus extending the reaction over a longer temperature range, while each water loss shown on a dehydration curve is determined at a constant temperature under equilibrium conditions.

With the zeolites some experimental difficulties were encountered and the most serious one concerned the *DTA* method. The three zeolites all fuse at about 1000° C. Since they adhere firmly to the sample holder after fusing, the thermocouple head was often found to be either dislocated or broken when a heated sample was taken out of the specimen hole for further study. This caused considerable trouble and discouraged the application of the technique to other zeolites.

Thermal Analyses

(*A*) *Dehydration Curves*

Two specimens of each member of the natrolite group were selected for the static thermal analysis in order to verify their dehydration course. Two groups of specimens were tested, one comprising (1) natrolite, Giant's Causeway, Ireland, (2) scolecite, Bombay, India, and (3) mesolite, Peter's Point, Nova Scotia; and the other group including (1) natrolite, Auvergne, France, (2) scolecite, Moore, N. J., and (3) mesolite, Cape d'Or, Nova Scotia. The specimens of each group were heated simultaneously, but the study of the first group was made in January while the second group in June of the same year. The dehydration curve of each of the zeolites is essentially constant, although the specimens of the first group generally showed a water-loss at a lower temperature than the corresponding ones of the second group (Fig. 1 and Table 2). The discrepancies are explained as being chiefly due to the usual lower humidity of the air in winter.

The dehydration curves of the three zeolites are markedly distinctive. Scolecite loses its water in two stages and mesolite in three as shown by the shoulders on their curves, while natrolite completes its dehydration in a single stage, represented by a smooth straight line. Further, each stage represents the loss of a definite number of water molecules in proportion to the total water content of the mineral. The last shoulder on the curves of both scolecite and mesolite does not level off sharply but slopes upward gently over a large temperature range. Such an extended and slow dehydration may result from an increasing firmness of binding of water molecules in the structure at higher temperatures so that their probability of escape from the tightest lattice positions may be decreased exponentially. But the considerably pronounced secondary break of the last shoulder on the scolecite curve at about 450° C., although not sharp enough, indicates a possibility that the two water molecules removed during the shoulder may differ slightly in structural capacity.

The general shape and water-temperature relationship of the curves of natrolite and scolecite are in good agreement with those of previous workers (Rinne, 1890; Walker & Parsons, 1922; Cavinato, 1927; Hey & Bannister, 1932, 1935). Milligan and Weiser (1937) reported that natrolite loses its water in two stages; but an examination of their curve reveals that it is very similar to their scolecite curve and hence suggests that their specimen might be actually scolecite.

Some of the published curves of mesolite show a nearly continuous dehydration (Zambonini, 1908; Pelacani, 1908; Hey & Bannister, 1933), but others bear a striking similarity to the writer's curve (Fig. 2). It is believed that the discrepancies are not a difference of matter but of de-

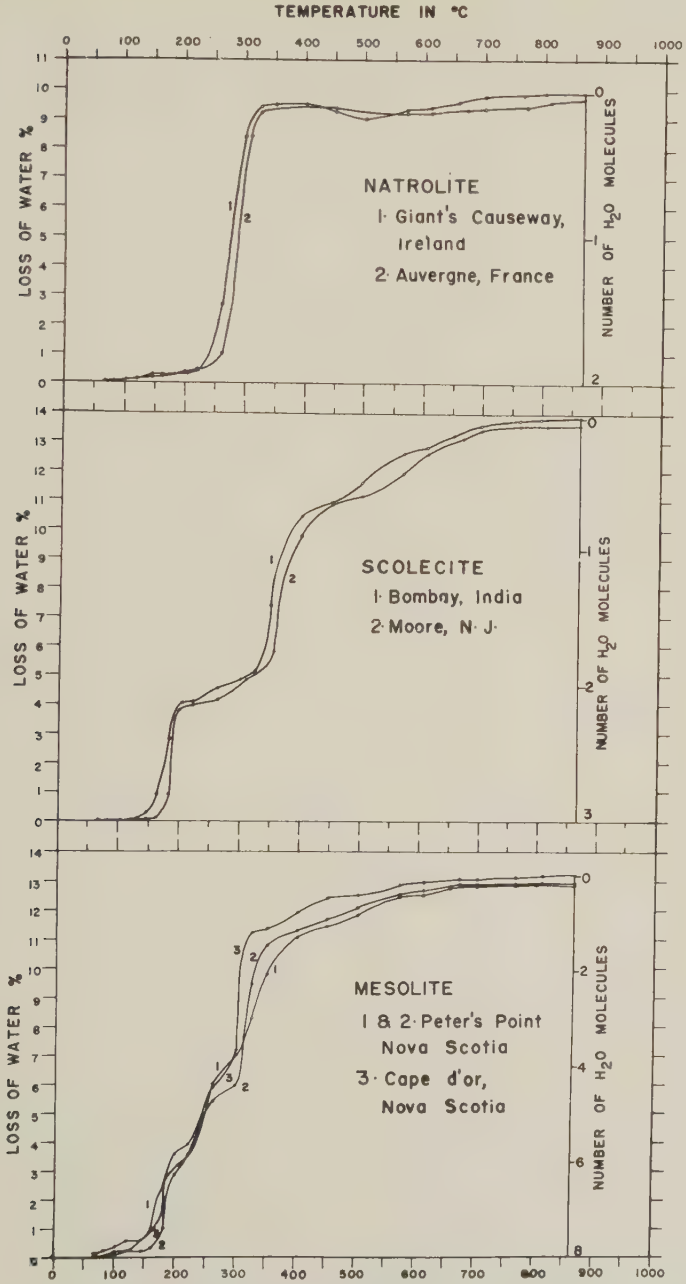

FIG. 1. Dehydration curves of natrolite, scolecite, and mesolite.

TABLE 2. DEHYDRATION DATA OF NATROLITE, SCOLECITE, AND MESOLITE

(Percentage of water lost up to temperature stated)

Temperature in C.	Natrolite		Scolecite		Mesolite		
	1	2	1	2	1	2	3
67°	0.08	0.02	0.02	0.01	0.01	0.03	0.13
82°	0.04	0.05	0.05	0.01	0.02	0.07	0.27
101°	0.11	0.13	0.05	0.06	0.22	0.15	0.41
121°	0.14	0.16	0.05	0.09	0.22	0.23	0.59
147°	0.30	0.19	0.33	0.10	0.62	0.25	0.62
162°	0.30	0.24	0.94	0.12	1.01	0.31	0.93
184°	0.30	0.32	2.84	0.94	2.57	1.03	1.79
200°	—	0.42	—	3.80	—	2.89	3.61
205°	0.36	—	4.06	—	3.23	—	—
222°	0.48	0.50	4.07	3.99	3.52	3.58	3.96
262°	2.70	1.00	4.56	4.15	6.00	5.41	5.92
300°	8.40	—	4.89	—	7.02	—	—
310°	—	8.47	—	4.85	—	5.94	7.21
325°	9.45	9.28	5.14	5.04	8.30	9.46	11.27
350°	9.50	9.01	7.40	5.82	9.81	10.82	11.36
400°	9.55	—	10.47	9.79	11.10	11.30	11.92
450°	9.31	9.42	10.90	10.88	11.48	11.69	12.44
500°	9.07	—	11.59	10.99	11.83	12.11	12.49
570°	9.36	9.21	12.61	11.94	12.48	12.54	12.90
610°	9.45	9.24	12.84	12.62	12.51	12.71	12.99
655°	9.62	—	13.23	—	12.74	—	—
670°	—	9.34	—	13.16	—	12.86	13.08
700°	9.81	9.41	13.58	13.41	12.82	12.86	13.04
765°	9.88	—	13.75	—	12.84	—	—
770°	—	9.43	—	13.53	—	12.90	13.13
800°	9.92	—	13.81	—	12.85	—	—
810°	—	9.63	—	13.56	—	12.92	13.19
865°	9.92	9.72	13.83	13.59	12.85	12.96	13.23

Natrolite: 1. Giant's Causeway, Ireland; 2. Auvergne, France.
Scolecite: 1. Bombay, India; 2. Moore, N. J.
Mesolite: 1. Peter's Point, Nova Scotia; 2. Same as 1; 3. Cape d'Or, Nova Scotia.

gree and may be explained as being due to the relatively small differences in volatility between the water molecules given off in the three stages so that the shoulders are not always well defined and sometimes may even fail to show up.

(*B*) *Differential Thermal Analysis*

The only published *DTA* data for zeolites are the study of natrolite by Sveshnikovr and Kuznetsov (1946), but no details of their work are available. In the present investigation, four specimens of natrolite and

three each of scolecite and mesolite from different localities have been examined by the *DTA* method. The specimens were fractioned into three particle-size groups: (1) minus 80 mesh, (2) minus 80 and plus 200 mesh, and (3) minus 200 mesh. The *DTA* curves of the three fractions of each specimen are essentially identical (Fig. 3 and Fig. 4). Some endothermic peaks showed a small shift in peak temperature, but the variations are so irregular that it would be impossible to state definitely

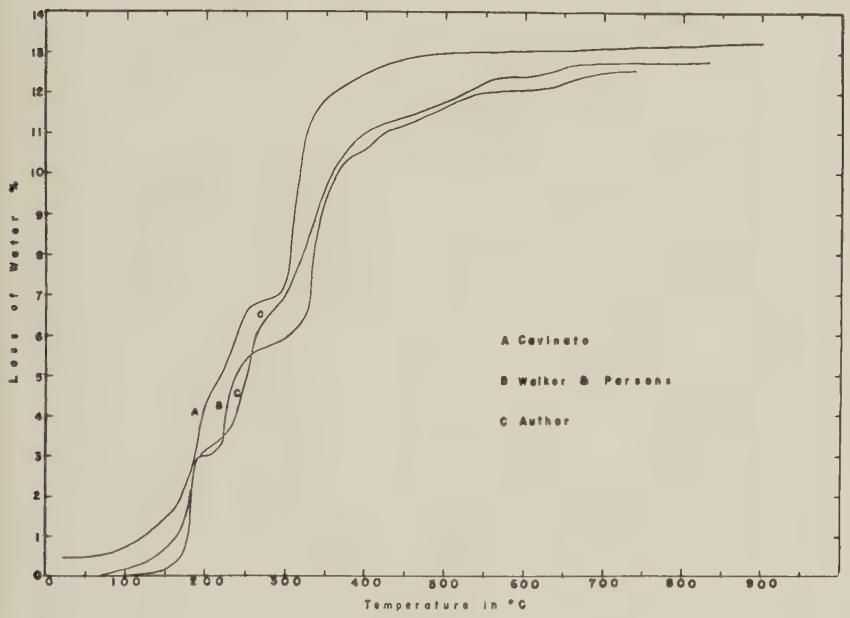

FIG. 2. Dehydration curve of mesolite.

whether they are due to the factor of particle size or not. However, the effect of grain size on the sharpness of an endothermic peak is more distinct, since almost all endothermic peaks shown by the minus 200 mesh fractions are sharper than the coarser ones. Furthermore, the endothermic doublets were also only shown by the finer fractions. Since particles of smaller grain-size should react thermally more uniformly, the sharpness of the endothermic peaks seems to be expected.

The *DTA* curves of both natrolite and mesolite show a high-temperature exothermic peak just above 1000° C. but experimental work showed that this peak on both curves varied considerably in shape and peak temperature. The exothermic reaction on the natrolite curve has a very small intensity and was shown only by the minus 80 mesh fractions. It results from recrystallization, but the small intensity clearly indicates

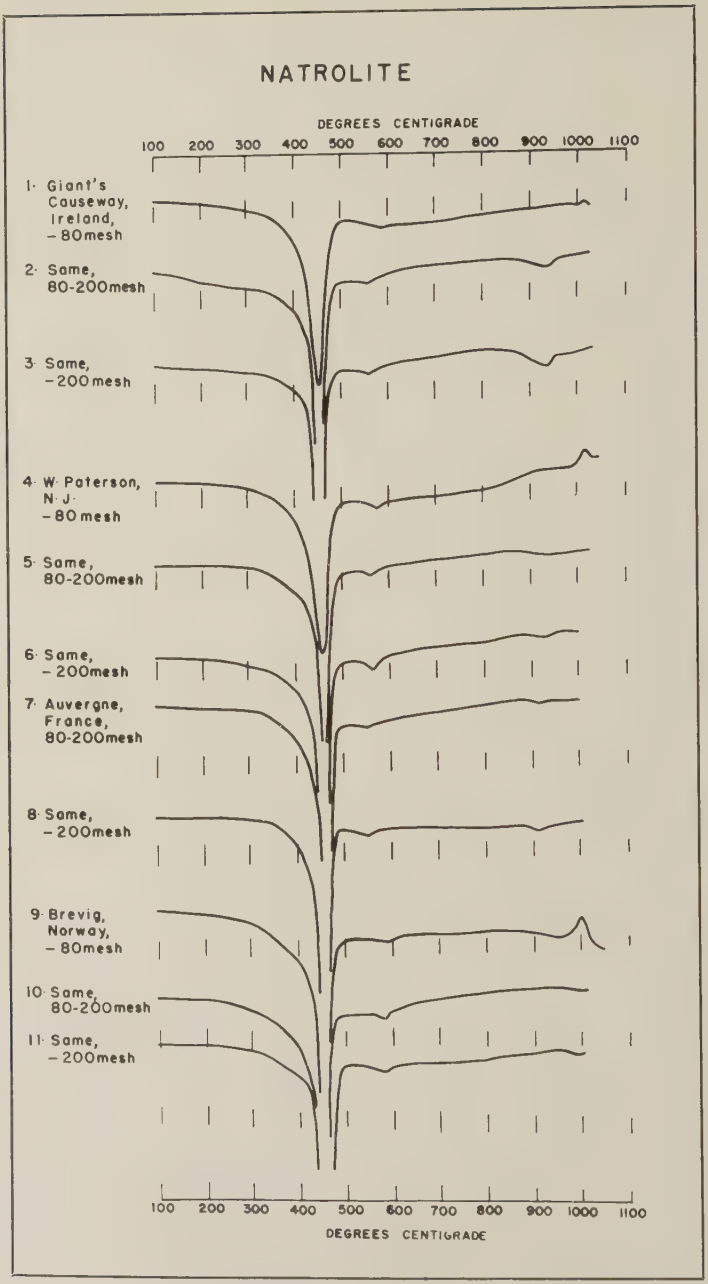

FIG. 3. Differential thermal analysis curve of natrolite.

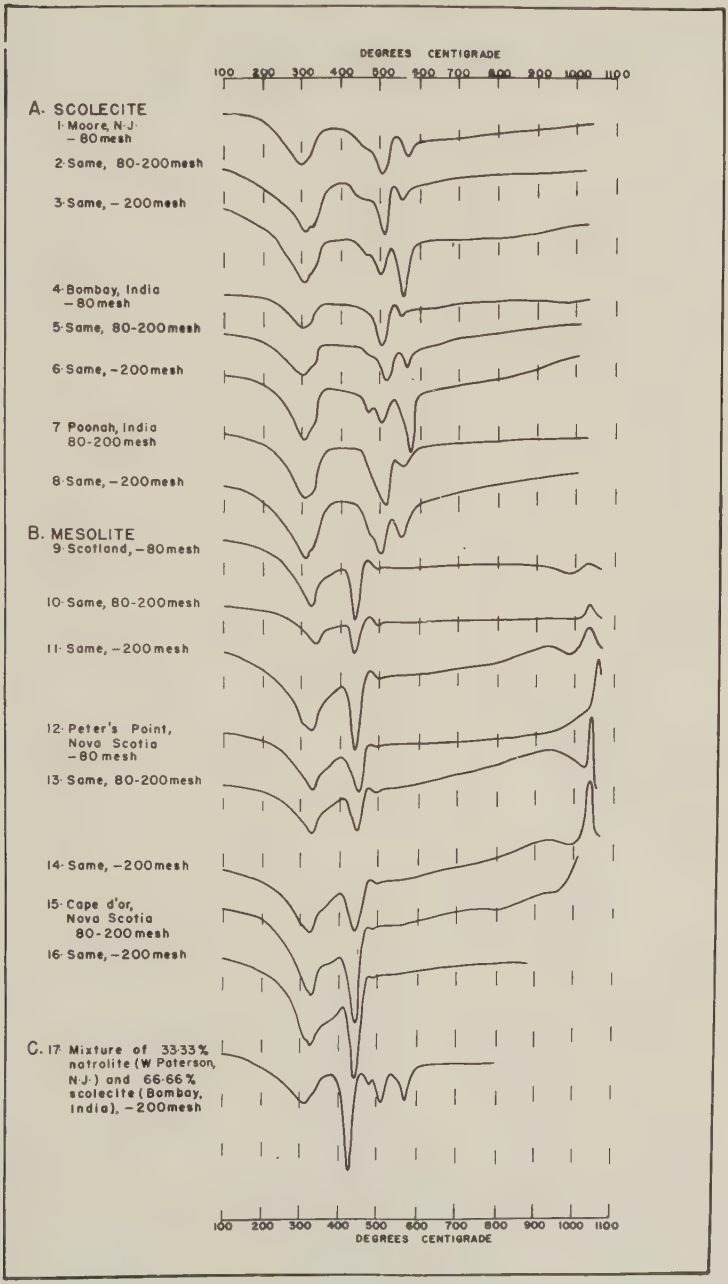

FIG. 4. Differential thermal analysis curves of scolecite and mesolite.

that the thermal effect must not be strong. In other words, the reaction may be a simple and easy one so that not much heat is evolved. Since finer particles should facilitate recrystallization, then this weak thermal effect may have been so subdued in the fractions of smaller grain sizes as to be unable to show up on the *DTA* curves.

The exothermic peak on the mesolite curve is a sharp and strong one. While it appeared at a constant peak temperature but showing increasing sharpness with decreasing particle size on the curves of the Scotland specimen, it occurred at a higher temperature on the curve of the coarse fraction of the Peter's Point specimen than on the curves of its finer fractions. Since the results are not consistent, the evidence for the effect of grain size on the exothermic peak does not seem conclusive.

Other factors may have also contributed to the variations of the reaction peaks. A reaction may be delayed if the sensitivity and position of the thermocouple head in the sample hole cannot be maintained reasonably constant in comparative runs, as often occurred in the present work as previously pointed out. Any change in the sample packing conditions in the sample holes may also impose some irregularities on the peak shape and temperature of reactions. Since limited ionic substitutions are known for the zeolites as discussed in an early section, shift of reaction peaks due to the presence of certain "impurities" is thus possible.

In spite of the aforesaid variations, the *DTA* curves of the three zeolites are as consistent and distinguishing as their dehydration curves. Each of the curves consists of a series of thermal reaction peaks due to loss of water and/or structural changes, but the intensity and temperatures at which they take place are markedly different for the three silicates. Further, those endothermic effects due to loss of water can be well correlated with the shoulders of corresponding dehydration curves, although they are found at higher temperatures for the reasons previously discussed. Also, the sharpness of these reaction peaks and their relative high temperatures indicate that the water is relatively firmly bound in the structures of the zeolites.

The *DTA* data and interpretations of the thermal reactions are given below:

(1) *Natrolite*

The natrolite curve is characterized by an extremely sharp and strong endothermic peak at 455° C. Sveshnikovr and Kuznetsov (1946) reported the peak as at 350° C., but there is no way to determine the cause of their lower peak temperature because of lack of detailed information. The reaction starts at about 300° C. and ends abruptly at 490° C. It is obviously consistent with the sharp break on the dehydration curve of

the zeolite and both are due to the release of the two water molecules. The dehydrated material showed little changes in appearance and optical properties, but there was some lattice expansion (Table 3).

Table 3. Interplanar Spacing for Natrolite and Its Modifications, $\lambda CuK_{\alpha 1} = 1.5405$ Å

Line No.	Natrolite		Anhydrous natrolite, at the first endothermic peak temperature (455° C.)		Metanatrolite, at the second endothermic peak temperature (565° C.)	
	d(Å)	*I.*	*d*(Å)	*I.*	*d*(Å)	*I.*
1	6.44	10	6.46	8	6.38	8
2	5.81	10	5.85	8	5.79	10
3	4.57	3	4.62	3	4.42	2
4	4.32	10	4.35	8	4.30	10
5	4.10	6	4.14	5	4.09	4
6	3.48	1	3.48	.5	—	—
7	3.18	10	3.18	7	3.13	10
8	—	—	3.14	5	—	—
9	—	—	3.09	2	—	—
10	2.93	4	2.94	4	2.93 D	3
11	2.83	10	2.85	10	2.83	10
12	2.66	1	—	—	—	—
13	2.57	3	2.57	3	2.56	3
14	2.43	3	2.44	1	2.42	2
15	2.41	2	2.41	1	—	—
16	2.32	2	2.32	.5	2.32	1
17	2.25	2	2.25 In	1	2.24 D	.5
18	2.17	6	2.18	5	2.18	2
19	2.06	1	2.06	.5	2.05 In	.5
20	1.96	1	1.96	.5	1.96 In	.5
21	1.87	2	1.93	1	1.88	1
22	1.80	4	1.80	4	1.80	3
23	1.75	1	—	—	—	—
24	1.73	1	1.72	.5	—	—
25	1.70 In	1	1.70 In	.5	—	—
26	1.68 In	1	1.68	.5	1.69	.5
27	1.65 In	1	1.65	.5	—	—
28	1.62 In	1	1.62	.5	—	—
29	1.60 In	1	1.60	.5	1.60 In	.5
30	1.57 In	1	1.57	.5	1.57 In	.5
31	1.53 In	2	1.53	1	1.53 In	1
32	1.46	4	1.46	3	1.45 In	1
33	1.42	1	1.42	.5	1.42	.5
34	1.39	2	1.39	1	1.39	1
35	1.37	.5	1.37 In	.5	—	—
36	1.35	.5	1.34 In	.5	1.35	.5
37	1.32	.5	1.33 In	.5	1.32 In	.5
38	1.31	2	1.31	1	1.30 In	.5
39	1.29	.5	—	—	—	—
40	1.27	.5	—	—	—	—
41	1.24	.5	—	—	—	—
42	1.22	3	1.22	2	1.22 In	1
43	1.19	1	1.19 In	.5	1.19 In	.5
44	1.16	.5	—	—	—	—
45	1.14	.5	1.14 In	—	—	—

In—Indistinct; D—Diffuse.

At 565° C. there is a very small but persistent endothermic peak. Optical and x-ray diffraction data of the Giant's Causeway specimen heated up to that temperature indicate the presence of a new phase which may correspond to Rinne's metanatrolite (1890) and hence, the endothermic reaction may represent the transformation.

After the 565° C. endothermic effect, the curve is almost level until between 910° and 940° C. where there is a small rounded endothermic trough with an immediately preceded small hump. Since the x-ray powder photograph of the materials heated to that temperature showed only a few diffuse bands, the thermal reaction may be properly identified with structural destruction.

The zeolite shows a small exothermic reaction peak at about 1010° C. as mentioned previously. Samples heated up to the peak temperature were essentially isotropic but with scattered weakly birefringent granules. Nevertheless, they all gave a distinct x-ray powder pattern. Most lines are those of nepheline, although some could not be accounted for (Table 4). It is thus clear that the exothermic reaction must be caused by recrystallization of fused natrolite into nepheline and probably another phase, although glass is still dominant at that temperature. The formation of nepheline and glass from natrolite was reported by C. Doelter long ago (1890) and the exothermic reaction was also noted by Sveshnikovr and Kuznetsov (1946), but the latter did not identify the products and the peak temperature given by them is much lower, namely, between 895° and 960° C.

(2) *Scolecite*

The *DTA* curve of scolecite shows three sharp endothermic peaks. The first reaction starts at about 170° C. and produces a broad V-shaped peak at 310° C. But the large breadth of the peak and its strange change in slope on the high-temperature side suggest that it may be a doublet with a small and poorly defined subsidiary peak at about 320° C. (Fig. 4). The major peak may be well correlated with the first shoulder on the dehydration curve of the zeolite ending around 200° C., if about 100° is allowed for the temperature difference between these two kinds of thermal curves. Thus it would represent a loss of one of the three water molecules in the mineral. The possible small subpeak may be due to the transformation of the mineral to metascolecite, which has long been recognized as a high-temperature form resulting from the removal of one water molecule from the zeolite (Rinne, 1890; Cavinato, 1927; Hey & Bannister, 1936). It seems probable that since these two reactions, partial dehydration and phase transition, are so closely related, their thermal effects may overlap and hence cannot be well separated on the *DTA* curve.

TABLE 4. POWDER DIFFRACTION DATA FROM NATROLITE HEATED TO 1010° C. AND NEPHELINE, $\lambda CuK_{\alpha 1}=1.5405$ Å

Line	Nepheline (A.S.T.M.)		Natrolite heated to 1010° C.		Nepheline, Magnet Cove, Ark.	
	d(Å)	I.	d(Å)	I.	d(Å)	I.
1	—	—	8.694	7	—	—
2	—	—	4.989	7	4.958	1
3	—	—	—	—	4.634	1
4	4.210	8	4.256	10	—	—
5	—	—	4.141	10	4.187	8
6	3.83	8	3.830	10	3.839	10
7	3.59	4	—	—	3.644	1
8	3.27	7	3.260	10	3.267	9
9	3.17	2	—	—	—	—
10	3.01	10	2.999	10	3.019	10
11	2.87	7	2.876	6	2.888	8
12	2.58	6	2.567	6	2.582	6
13	2.48	4	2.486	4	2.502	4
14	2.38	4	—	—	2.405	3
15	2.34	8	2.336	10	2.356	6
16	2.29	7	—	—	2.316	3
17	2.11	2	—	—	2.175	1
18	—	—	—	—	2.132	1
19	2.08	6	2.077	8	2.105	3
20	2.03	2	2.026	1	—	—
21	1.98	4	1.974	1	1.980	1
22	1.93	6	1.923	4	1.931	3
23	1.88	4	1.881	1	1.896	2
24	1.84	2	—	—	1.850	1
25	1.81	6	1.791	1	1.810	2
26	—	—	1.786	1	1.775	1
27	1.76	4	1.753	1	—	—
28	1.72	6	1.704	4	1.704	2
29	1.69	4	—	—	—	—
30	1.64	2	1.663	1	1.643	1
31	1.62	6	1.629	1	1.627	2
32	1.60	2	1.612	4	1.610	1
33	—	—	1.595	1	—	—
34	1.56	6	1.557	8	1.573	6
35	1.53	6	1.523	2	1.535	1
36	1.47	5	1.467	3	1.478	2
37	1.46	7	1.455	1	1.468	1
38	1.43	6	1.426	6	1.440	3
39	1.39	8	1.380	8	1.393	5
40	1.38	4	1.370	1	1.384	1
41	1.35	4	1.335	1	1.355	1
42	1.35	2	—	—	—	—
43	1.32	4	1.312	6	1.325	2
44	1.31	2	—	—	—	—
45	1.28	7	1.278	7	1.288	3
46	1.26	4	1.265	1	1.276	1
47	1.26	5	1.263	1	1.266	2
48	1.25	2	—	—	—	—
49	1.24	4	1.233	1	1.244	1
50	1.22	6	—	—	1.227	1
51	1.21	7	1.218	1	1.213	2
52	1.19	8	1.201	6	1.195	3
53	1.18	2	1.182	7	1.163	1
54	1.16	4	1.151	1	1.148	1
55	1.14	6	1.137	−1	1.141	1
56	—	—	1.028	−1	—	—

The second endothermic effect starts at about 440° C. and forms a doublet with a small auxiliary peak at about 470° C. and a sharp major peak at 500° C. It may be correlated with the final shoulder on the dehydration curve due to the liberation of the other two water molecules. Its doublet form also seems to be in accord with the appearance of the shoulder which has a secondary break and both suggest differing volatilities of the two water molecules.

The third endothermic peak merges with the second doublet at about 525° C. and reaches its maximum at about 560° C. The powder x-ray diffraction photograph of the Bombay specimen heated up to that temperature gave only a few diffuse lines, thus indicating the reaction as a result of structural disintegration (Table 5).

Then the curve levels off until the final firing temperature at 1050° C. used in the present study. Heated samples were a porous porcellaneous mass, isotropic between crossed nicols, and yielded no diffraction lines. Hence, melting of the zeolite resulting in glass and anorthite as reported by Doelter (1890) cannot be proved.

(3) *Mesolite*

The *DTA* curve of mesolite features two major and one minor endothermic reactions and two exothermic peaks. As in the case of scolecite, thermal decomposition of this zeolite starts at a relatively low temperature, probably in the neighborhood of 150° C. and then proceeds slowly until it reaches the first endothermic peak. The latter is a doublet with a minor subpeak at about 310° C. and a major one at 325° C., but the minor subpeak is not always developed. The second endothermic reaction takes place sharply at 400° C. and reaches its peak at about 440°C. It is a strong symmetrical peak, but the base line shifts to higher level on the high temperature side, probably due to a change in the thermal conductivity and specific heat of the material.

As demonstrated by the dehydration curve presented above, mesolite gives off its water successively in three stages with 2, 2, and 4 molecules respectively. If about 100° is assumed as the temperature difference between the two kinds of thermal data, the first endothermic doublet would be correlative with the first two shoulders on the dehydration curve and the second sharp endothermic peak with the last large shoulder. Then, it would follow that the first and second endothermic reactions may be attributed to the loss of (2+2) and 4 water molecules respectively. Samples heated up to the peak temperatures of the two thermal effects showed an increase in the refractive indices, but little changes in appearance. The heated material just after the first endothermic peak, like natrolite, had an expanded lattice, but after the second endothermic peak it showed some contraction (Table 6).

TABLE 5. INTERPLANAR SPACING FOR SCOLECITE AND MODIFICATIONS AT VARIOUS PEAK TEMPERATURES, $\lambda CuK\alpha_1 = 1.5405$ Å

Line	Scolecite		First endothermic peak (320° C.)		Second endothermic peak (500° C.)		Thrid endothermic peak (550°–570° C.)	
	d(Å)	*I.*	*d*(Å)	*I.*	*d*(Å)	*I.*	*d*(Å)	*I.*
1	6.53	3	6.52	3	6.41 B	4	Diffuse	Band
2	5.81	4	5.81	8	5.75 B	8		
3	4.69	3	4.61	5	4.64	1		
4	4.37	5	4.35	8	4.32	6		
5	4.19	1	4.16	1	4.16	1		
6	3.63	1	3.63	1	3.61	3	Diffuse	Band
7	3.15	2	3.17	5	3.16	3		
8	3.09	1	3.07	2	3.06	1		
9	2.86	10	2.87	10	2.86	10		
10	2.68	.2	—	—	—	—		
11	2.58	1	2.57 B	2	2.56 B	.5		
12	2.47	1	2.44	2	2.42 B	1		
13	2.42	1	—	—	—	—		
14	2.32	1	—	—	—	—		
15	2.26	1	2.25	.5	2.27	.5		
16	2.20	3	2.18 D	4	2.19	2		
17	2.17	.2	2.15 D	.5	—	—		
18	2.07	1	2.04	1	2.04 B	1		
19	2.03	.5	—	—	—	—		
20	1.99	2	1.96	2	1.95	1	Diffuse	Band
21	1.95	2	1.87	2	1.86	1		
22	1.90	.5	—	—	—	—		
23	1.86	1	—	—	—	—		
24	1.80 B	3	1.80	2	1.80 D	1		
25	1.75	2	1.75 B	1.5	1.75	.5		
26	1.72	.5	1.73 B	.5	—	—		
27	—	—	1.68	1	1.68	.5		
28	1.66 B	.5	1.66	.5	—	—		
29	1.64 B	1	1.63	3	1.63	.5		
30	1.61	1	1.62 In	.5	—	—		
31	1.60	.3	1.60	1	1.58 D	.5		
32	1.52	.5	1.51 In	.5	1.52 D	.5		
33	1.50	.2	—	—	—	—		
34	1.47	2	1.48	3	1.47 D	2		
35	1.43	1	1.43	1	1.43 D	.5		
36	—	—	1.40	1	—	—		
37	1.38	1	1.39	1	1.38 D	.5		
38	—	—	1.37	.5	—	—		
39	1.33	1	1.33	1	1.33	.5		
40	—	—	1.31 B	2	1.31	.5		
41	1.31	1	1.29	.5	1.27	.2		
42	—	—	1.28 In	.5	1.24	.5		
43	1.27	.5	—	—	—	—		
44	1.24	2	1.23	.5	—	—		
45	1.22	.5	—	—	1.21	.5		
46	1.21	.5	1.21 In	.5	—	—		
47	1.19	.5	1.19 In	.5	1.18	.5		
48	1.17	.5	1.17 In	.5	—	—		
49	1.15	.5	1.14	.5	—	—		
50	1.15	.2	—	—	—	—		

B—Broad; In—Indistinct; D—Diffuse.

Table 6. Interplanar Spacing for Mesolite and Its Modifications at Various Thermal Reaction Peak Temperatures, $\lambda CuK\alpha_1 = 1.5405$ Å

Line	Mesolite		First endothermic peak temperature, 325° C.		Second endothermic peak temperature, 440° C.		Third endothermic peak temperature, 490° C.	
	d(Å)	I.	d(Å)	I.	d(Å)	I.	d(Å)	I.
1	6.44 B	4	6.54	4	6.44	4		
2	5.79	7	5.81	6	5.81	6		
3	5.46	−1	—	—	—	—		
4	4.66	3	4.62	4	4.66	1		
5	4.35 B	5	4.37 D	6	4.33 D	4	Diffuse	Weak
6	4.16	1	4.17	2	4.09	2		
7	3.89	−1	3.66	−1	—	—		
8	3.18 D	3	3.18 D	4	—	—		
9	3.08 D	2	3.09	2	3.07	2		
10	2.86	10	2.88	10	2.85 D	10	Diffuse	Weak
11	2.57 D	1	2.58	2	2.55 B	−1		
12	2.47	1	2.48 B	2	2.41 D	−1		
13	2.41	1	2.44	2	—	—		
14	2.34	−1	2.33	−1	—	—		
15	2.27	−1	2.27	−1	—	—		
16	2.19 D	3	2.21	3	2.18 D	−1		
17	—	—	2.09	−1	2.06 D	−1		
18	2.05	−1	2.05	1	—	—		
19	—	—	2.00	−1	—	—		
20	1.95	−1	1.96	1	—	—		
21	1.86	−1	1.86	2	—	—		
22	1.81	3	1.81 D	2	1.81 D	2		
23	1.75	1	1.76 D	2	—	—		
24	1.72	−1	1.73 D	−1	—	—		
25	1.68	−1	1.69	−1	—	—		
26	—	—	1.67	−1	—	—		
27	1.64	1	1.64	2	1.64 D	−1		
28	1.59	−1	1.60	−1	1.61 D	−1		
29	1.54	−1	1.55 D	−1	—	—		
30	1.52	−1	1.53	−1	—	—		
31	1.47	3	1.48	2	1.47	−1		
32	1.43	1	1.44	1	—	—		
33	1.40	1	1.41	−1	—	—		
34	1.39	1	1.39	1	1.38 D	−1		
35	1.35	−1	1.37 D	−1	—	—		
36	—	—	1.35 D	−1	—	—		
37	—	—	1.33	1	1.31 D	−1		
38	1.30	−1	1.32	1	—	—		
39	—	—	1.30	−1	—	—		
40	—	—	1.28	−1	—	—		
41	1.24 B	1	1.24	1	—	—		
42	1.21	−1	1.22	−1	—	—		
43	1.19	−1	1.19	−1	—	—		
44	—	—	1.18 D	−1	—	—		
45	1.15	−1	1.16	−1	—	—		
46	1.15	−1	1.15	−1	1.13 D	1		
47	1.15	−1	—	—	1.10	1		

B—Broad; In—Indistinct; D—Diffuse.

Another endothermic peak occurs at 490° C. and is of small intensity. Since the Peter's Point specimen heated to that temperature gave no distinct diffraction lines, the reaction is interpreted as a structural breakdown. Just prior to this peak there is a very small swell at 470° C. indicative of a weak exothermic reaction, but its explanation is not clear.

A strong exothermic reaction takes place at about 1040° C., giving rise to a sharp peak with an immediately preceding dip. It is associated with recrystallization of fused mesolite, since specimens heated to the peak temperature comprised a mixture predominantly of glass with some cryptocrystalline plagioclase, probably labradorite, as shown by the diffraction pattern (Table 7).

It has been well established that the three zeolites are independent species but isostructural and mesolite is not an intermediate mixture (Gorgey, 1909; Bowman, 1909; Winchell, 1925; Cavinato, 1926; Hey & Bannister, 1932–33–36; Taylor *et al.*, 1933; Wyart, 1933; Berman, 1937). This is fully confirmed by the present study. Both their dehydration and *DTA* curves are distinctive and the *DTA* curve of mesolite does not appear to be a combination of the natrolite and scolecite curves. Additional evidence is provided by the *DTA* curve of an artificial mixture of one part of natrolite and two parts of scolecite proportional to the composition of mesolite (Fig. 4, No. 17). It produced a typical composite curve of the two components showing no resemblance whatever to the mesolite curve. However, although the overall shape of the mesolite curve is characteristic, its first endothermic peak well matches the first endothermic peak of scolecite and its second endothermic peak falls almost within the same temperature range as the intense endothermic peak of natrolite. Since all of the peaks mainly result from dehydration, it appears that the water molecules in the three zeolites released during corresponding endothermic reactions may be structurally of the same type so that upon heating they behave in the same manner.

Crystal Structure and Thermal Behavior

The fundamental cause of thermal decomposition of a mineral is the disruption of certain bonds within its crystal structure. Since the bonds which hold atoms to their lattice positions have specific energy values, a definite activation energy is required for their dislocation. Hence, the decomposition temperature may be regarded as a measure of the bond strengths involved. On this account, the thermal behavior of a mineral may be better understood in terms of structural concepts and thermal analysis data in turn should provide useful information on the structure.

According to both Pauling (1930) and Taylor *et al.* (1933), scolecite and mesolite have essentially the same framework structure as that of

TABLE 7. POWDER DIFFRACTION DATA FROM MESOLITE HEATED TO 1040° C. AND LABRADORITE, $\lambda CuK\alpha_1 = 1.5405$ Å

Line	Labradorite (A.S.T.M.)		Mesolite heated to 1040° C.		Labradorite, Labrador	
	d(Å)	I.	d(Å)	I.	d(Å)	I.
1	—	—	—	—	6.488	1
2	—	—	—	—	4.689	1
3	4.07	4	3.975	7	4.038	5
4	—	—	—	—	3.885	1
5	3.77	1.3	3.678	6	3.763	5
6	3.64	1.1	—	—	3.683	4
7	—	—	3.378	−1	3.488	1
8	—	—	—	—	3.365	1
9	3.20	10	3.163	10	3.215	10
10	3.00	1.1	—	—	3.020	1
11	2.92	1.1	2.888	−1	2.940	3
12	2.84	0.5	2.787	−1	2.845	2
13	2.64	0.5	2.649	−1	2.660	2
14	2.53	2.7	2.498	−1	2.500	3
15	2.40	1	2.401	−1	—	—
16	2.29	5	—	—	2.300	1
17	2.21	1	—	—	—	—
18	2.12	0.7	2.130	4	2.128	1
19	2.01	0.5	—	—	2.025	1
20	—	—	1.999	1	1.996	1
21	1.92	0.4	1.912	2	1.925	1
22	—	—	—	—	1.890	1
23	1.83	0.7	1.829	4	1.835	3
24	—	—	—	—	1.800	1
25	1.77	0.5	1.765	4	1.765	2
26	—	—	—	—	1.750	1
27	1.71	0.3	1.708	−1	1.725	1
28	1.62	0.3	1.605	−1	1.608	1
29	1.56	0.1	1.560	−1	1.545	1
30	1.53	0.1	1.525	−1	—	—
31	1.48	0.4	1.480	2	1.463	2
32	1.37	0.1	—	—	1.388	1
33	1.35	0.4	1.350	4	1.355	2
34	1.32	0.1	1.319	−1	1.328	1
35	1.29	0.1	—	—	—	—
36	1.27	0.2	1.271	−1	1.272	1
37	1.25	0.1	1.253	−1	—	—
38	1.21	0.4	1.219	−1	1.224	1
39	1.16	0.3	—	—	—	—
40	1.13	0.3	—	—	1.135	1
41	1.07	0.1	—	—	—	—

natrolite, probably with the same cavities filled. But since they have different water contents and cations, they must differ in certain details of their arrangements. These structural differences are believed to be chiefly responsible for the differing thermal behavior of the zeolites.

The diagnostic feature of the thermal behavior of natrolite is the intense endothermic effect at 455° C. with its two water molecules removed at the same time. Evidently, the two must occupy equivalent lattice positions so that they have the same volatility. This is in perfect agreement with the structure suggested by Taylor *et al.* (Fig. 5*a*). After dehydration the structure is essentially preserved and will not break down until about 940° C.

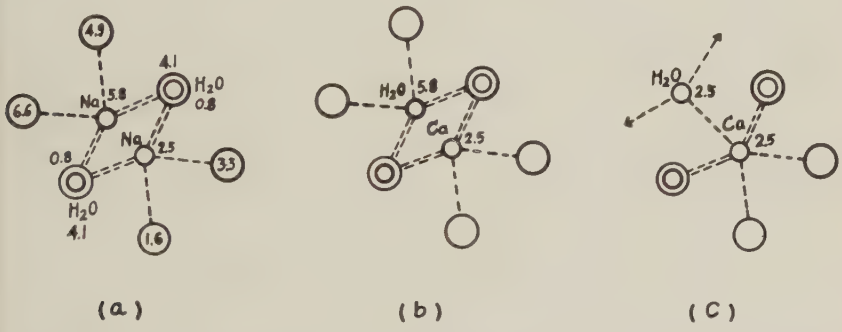

FIG. 5. The arrangement of cations and water molecules in natrolite by W. H. Taylor et al. (*a*), in scolecite by L. Pauling (*b*), and in scolecite by Taylor et al. (*c*). The large circles represent oxygen atoms in the SiO_4 and AlO_4 tetrahedra. The figures denote heights in Angstrom units above the plane of projection. (After W. H. Taylor *et al.* 1933)

The dehydration of scolecite proceeds discontinuously with one water molecule coming off during the 310° C. endothermic reaction and the other two in the 500° C. endothermic doublet, indicating that the former must be more loosely bound in the structure than the latter. This tends to bear out Pauling's arrangement of the water in the zeolite (Fig. 5*b*) in which one molecule is placed at 3.6 Å from the single cation of Ca while the other two are 2.5 Å away as in the natrolite structure. It is, however, at variance with the structure proposed by Taylor *et al.* (Fig. 5*c*) in which one water molecule is a little closer to the cation than the other two at distances of 2.3 Å and 2.5 Å respectively, and hence the single water molecule would come off later than the other two. But Hey (1936) found it satisfactory to explain his dehydration data of the zeolite. Another point brought up by the present study is that both the *DTA* and static curves suggest that even the other two water molecules may not occupy exactly the same lattice positions as they do in the structure suggested

either by Pauling or by Taylor *et al.*, since they are removed in a doublet reaction. Further structural study thus seems desirable.

While the natrolite structure persists up to about 940° C. as already discussed, scolecite begins to show signs of structural collapse after final dehydration at 500° C. and breaks down completely at 560° C. Their different structural stability cannot be explained by the nature of the cations, since Ca and Na ions are almost of the same size and the strength of the Ca-H_2O bond (2/7) is even stronger than that of the Na-H_2O bond (1/6) according to the structures of the two zeolites worked out by Taylor *et al.* It seems certain that the much lower stability of scolecite may result from the introduction of the extra water molecule into the natrolite structure, which, according to Pauling's suggestion (Fig. 5*b*), takes up one of the two Na positions in natrolite. Since it must be much more loosely bound to other ions than the corresponding Na ion in natrolite, the entire structure would be weakened accordingly. Furthermore, since it is more readily driven out upon heating than the other two water molecules, its removal would further damage the structure. But the other two water molecules are given off at slightly higher temperatures (about 500° C.) than the two in natrolite (at 455° C.) although they probably occupy similar lattice positions. This is explained as being due to the strength difference between the Ca-H_2O and Na-H_2O bonds.

No detailed *x*-ray analysis has yet been made of mesolite. Since its *x*-ray diffraction pattern is almost identical to that of both natrolite and scolecite and it has a composition corresponding to one natrolite and two scolecite molecules, Taylor *et al.* (1933) have suggested that the mesolite structure must be similar in all its essentials to that of the other two zeolites except that its cell size is three times as large. Further, 6 of the 8 water molecules occupy the general positions as in natrolite and the other two are more strongly tied to the Ca ions as in scolecite. Such an arrangement of the water molecules fails, however, to explain the mode of dehydration of the zeolites as revealed by their thermal curves, which show that 2 water molecules each are removed earlier in two closely spaced stages and the other 4 in a single higher-temperature reaction. It is thus indicated that the water in mesolite may comprise two volatile groups of two molecules each and one less volatile group of four. Further, as has been noted above, the two volatile groups come off in about the same temperature range as the first water molecule of scolecite and the less volatile one at about the peak temperature of the intense endothermic effect of natrolite. Then it may be reasonably assumed that only 4 of the 8 water molecules may occupy the general positions as in natrolite and the other 4 may be placed in similar positions as the extra water molecule in scolecite. In the absence of detailed structural data at present, however, it would be merely speculative to assign any specific positions to the water.

After final dehydration at 440° C. mesolite has already shown considerable optical and structural changes and breaks down completely at 490° C. The still lower stability of the zeolite may be similarily explained as for scolecite as being due to addition of extra water molecules to the natrolite structure. Thus, it appears that the higher the water content of a zeolite, the smaller is its stability range, which seems to be in line with the view of J. W. Gruner (1950) as to the reaction energies of silicates.

Conclusions

The distinctive shoulders on the dehydration curves and their corresponding endothermic peaks on the *DTA* curves of the three zeolites clearly indicate that the water must hold definite lattice positions. Although the three are isostructural, they give off their water at different temperatures and in different amounts. The conclusion is irresistible that the water occupies different positions in their structures. On the basis of their thermal data, it is suggested that natrolite contains a single group of two water molecules of equal volatility, scolecite has a volatile group of one molecule and another less volatile group of two, and mesolite comprises two groups of two molecules each of high and slightly different volatilities and a group of four molecules of equal and lower volatility. This confirms the validity of the methods to arrange water molecules in natrolite and scolecite proposed by Taylor *et al.* and by Pauling. But it is assumed by Taylor *et al.* that the water in mesolite consists of a group of six molecules and another group of two.

The physical properties of the three zeolites show marked changes during the course of dehydration and upon heating up to about 1050° C. They do not, however, undergo the same kind of changes at the same temperature. While natrolite shows only slight changes in the optical properties and crystal structure after complete dehydration at 455° C. and retains its structure until about 940° C, the structures of scolecite and mesolite are completely destroyed respectively at about 560° C. and 490° C. immediately after their final dehydration. Their stability ranges thus seem to depend upon the degree of hydration —apparently the higher the water content of the mineral, the lower is its stability.

The thermal curves of the three zeolites are so characteristic that they should prove to be a useful means of identification. Further, they may serve as an additional proof that the three do not constitute an isomorphous series but are independent species.

References

1. *Am. Soc. Testing Materials & Nat'l Res. Council* (1950), *X*-ray Diffraction Data Cards (in three sets).

2. Ashcroft, F. N. (1916), The natrolite occurring near Kinbane (White Head), County Antrim: *Mineral. Mag.*, **17,** 307.
3. Berman, H. (1937), Constitution and classification of the natural silicates: *Am. Mineral.*, **22,** 374.
4. Bowman, H. L. (1909), On the identity of poonahlite with mesolite: *Mineral. Mag.*, **15,** 216.
5. Cavinato, A. (1926), Sulla mesolite: *Atti Coc. Ital. Sci. Nat.*, **65,** 104–114.
6. ——— (1927), Nuove osservazioni sulle zeoliti del gruppo della natrolite: *Mem. Rend. Accad. Lincei. cl. sci. fis. mat. nat. Roma, ser. 6,* **2,** 320–350.
7. Doelter, C. (1890), Über die künstliche Darstellung und die chemiche Constitution einiger Zeolithe: *Neues Jahrb. Mineral.*, **1,** 134–137.
8. Gonnard, F. (1891), Sur le groupe mésotype dans le Puy-de-Dome: *Bull. Soc. Franc. Mineral.*, **14,** 170.
9. Gorgey, R. (1909), Über Mesolith: *Ibid.*, **28,** 77–106.
10. Gruner, J. W. (1950), An attempt to arrange silicates in the order of reaction energies at relatively low temperatures: *Am. Mineral.*, **35,** 143.
11. Heddle, M. F. (1883), On a new mineral locality: *Mineral. Mag.*, **5,** 118.
12. Hey, M. H., and Bannister, F. A. (1932), Studies on the zeolites, Pt. 3, Natrolite and metanatrolite: *Ibid.*, **23,** 243–289.
13. ——— (1933), Studies on the zeolites, Pt. 5, Mesolite: *Ibid.*, **23,** 421–447.
14. ——— (1935), Studies on the zeolites, Pt. 8, A theory of the vapour pressure of the zeolites and of the diffusion of water or gases in a zeolite crystal: *Ibid.*, **24,** 110–130.
15. ——— (1936), Studies on the zeolites, Pt. 9, Scolecite and metascolecite: *Ibid.*, **24,** 227–253.
16. Kerr, P. F., and Kulp, J. L. (1948), Multiple differential thermal analysis: *Am. Mineral.*, **33,** 387–419.
17. Milligan, W. O., and Weiser, H. B. (1937), The mechanism of the dehydration of zeolites: *Jour. Phys. Chem.*, **41,** 1029–1040.
18. Pauling, L. (1930), The structure of some sodium and calcium aluminosilicates: *Proc. Nat. Acad. Sci., U.S.A.*, **16,** 453–459.
19. Pelacani, L. (1908), Studio chemico delle zeoliti de Montresta (Sordegna): *Atti. Accad. Lincei. Rend. cl. fis. mat. nat., ser. 5,* **17,** sem. 2, 66–68.
20. Rinne, F. (1890), Über Umänderungen, welche die Zeolithe durch Erwärmen bei und nach dem Trübewerden erfahren: *Sitzungsber. d. k. preuss, Akadem. d. Wissensch. z. Berlin,* **46,** 1163.
21. Sveshnikovr, V. N., and Kuznetsov, V. G. (1946), Structural relations between zeolites and natural kaolin and their transformations on heating: *Izvest. Akad. Nauk, U.S.S.R. Otdel, Khim. Nauk,* **1946,** 25–36; *Chem. Abst.*, **42,** 6200 (1948).
22. Taylor, W. H., Meek, C. A., and Jackson, W. W. (1933), The structures of fibrous zeolites: *Zeits. Krist.*, **84,** 373–398.
23. Tschermak, G. (1917–1918), Der chemische Bestand und das Verhalten der Zeolithe, I. Teil.: *Sitzungsber. Akad. Wiss. Wien, Math.-naturwiss. Kl., Abt. I,* **126,** 541–606; II Teil.: *Ibid.*, **127,** 177–289.
24. Walker, T. L., and Parsons, A. L. (1922), The zeolites of Nova Scotia: *Univ. Toronto Studies, Geol. Ser.*, **14,** 14–22.
25. Winchell, A. N. (1925), A new theory of the composition of the zeolites: *Am. Mineral.*, **10,** 112–116; 171–174.
26. Wyart, J. (1933), Recherches sur les zeolites: *Bull. Soc. Franc. Mineral.*, **56,** 81–187.
27. Zambonini, F. (1908), Contributo allo studio dei silcati idrati: *Atti. d. Reale Accad. d. Sci. fis. e. mat. d. Napoli,* **16,** 1.

Manuscript received July 26, 1954.

WULFENITE SYMMETRY AS SHOWN ON CRYSTALS FROM JUGOSLAVIA*

CORNELIUS S. HURLBUT, JR., *Department of Mineralogy, Harvard University, Cambridge, Mass.*

ABSTRACT

Wulfenite crystals from Schwarzenbach, Jugoslavia, are in two distinct habits; (1) Pyramidal crystals indicating that [001] is polar. (2) Tabular crystals twinned on $\{00\bar{1}\}$. The morphology, etch tests and the presence of piezoelectricity indicate that wulfenite symmetry is tetragonal-pyramidal (4).

In the summer of 1953, the Harvard Mineralogical Museum purchased a fine collection of wulfenite specimens that came from the Helena Mine, Schwarzenbach, Jugoslavia. They are beautifully crystallized and of a rich orange-yellow color. The crystals are essentially of two distinct habits, Figs. 1 and 2, both of which indicate that wulfenite crystallizes in the tetragonal-pyramidal crystal class.

Morphology. Considerable uncertainty exists regarding the symmetry of wulfenite. From the morphology of most crystals one would conclude that the symmetry is tetragonal-dipyramidal ($4/m$). A few crystals have

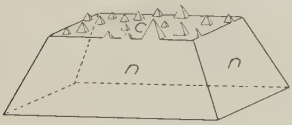

FIG. 1

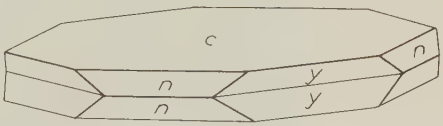

FIG. 2

FIG. 1. Pyramidal wulfenite crystal.
FIG. 2. Wulfenite twinned on $\{00\bar{1}\}$.

been described that indicate tetragonal-pyramidal (4) symmetry. In Volume II of the *System of Mineralogy* (1951), the symmetry is accepted as (4) on rather unconvincing evidence.

The crystals from Jugoslavia, as illustrated in Figs. 1 and 3, range in maximum dimension from 1 millimeter to 2 centimeters. They have a simple habit with the only important forms being $n\{011\}$, $c\{001\}$ and $\bar{c}\{00\bar{1}\}$. The $\{001\}$ form on the larger crystals is covered with overgrowths of small pyramids, $\{011\}$; the $\{00\bar{1}\}$ form is a plane surface. This habit indicates that the [001] axis is polar but the evidence is no more convincing than that supplied by the pyramidal crystals from

* Contribution No. 354, Department of Mineralogy, Harvard University, Cambridge, Massachusetts.

Inverness-shire, Scotland, described by Russell (1946); and wulfenite from various other localities described by Bach (1926).

The second habit, as illustrated in Figs. 2 and 4, is platy with the crystals flattened on {001}. The maximum dimension across the plates is 3 centimeters, and the ratio of width to thickness is about 10:1. All of the crystals of this platy type are twinned on $\{00\bar{1}\}$ and show re-entrant angles where the faces of $\bar{y}\{11\bar{3}\}$ join one another. The only other forms are $n\{011\}$ and $c\{001\}$. Hlawatsch (1925) also noted re-entrant angles on wulfenite from Mies, Carinthia.

Etching. This twinning definitely indicates that [001] is polar but is contrary to the conclusions reached by Honess (1927) and Royer (1936)

FIG. 3. Pyramidal wulfenite crystals. $\times\frac{1}{2}$.

by etching wulfenite. These earlier works showed that etch pits on (001) and $(00\bar{1})$ were identical, indicating a horizontal symmetry plane.

To check these etching results, planes corresponding to (001) and $(00\bar{1})$ were ground and polished on one of the pyramidal crystals from Jugoslavia. Also, the broad opposing faces of one of the twins were ground and polished. These crystals were then etched in dilute nitric acid for 12 hours. The pyramidal crystal showed a marked difference in the etching on (001) and (001), whereas the etching on the opposite faces of the twin was identical and similar to that on (001) face of the single individual. As a further check, one of the individuals was completely ground from a twin and the broad faces of the remaining part polished. After

etching in nitric acid for 12 hours, the appearance of the faces corresponded to the (001) and (00$\bar{1}$) faces of the etched pyramidal crystal.

The etching produced on the (001) face of each crystal is a dull irregular pitted surface crossed by shallow grooves producing a square pattern. The grooves make an angle of about 15° to the trace of (011) on (001). On the opposite surfaces etching produced square pits, the pyramidal sides of which give brilliant reflections. The edges of the etch pits make an angle of about 15° with the intersection of (01$\bar{1}$) on (00$\bar{1}$). The etch pits described by Honess (1927) on wulfenite crystals from the Red Cloud Mine, Arizona, are similar to this second type.

FIG. 4. Wulfenite crystals twinned on 001. $\times\frac{1}{2}$

Etching of a tabular crystal from the Red Cloud Mine gave results similar to those reported by Honess; that is, the etching on the two basal faces was the same. This crystal and a pseudocubic crystal from the Ahumada Mine, Mexico, were then cut in half along what appeared to be the horizontal symmetry plane. Etching half of each crystal gave dissimilar patterns on (001) and (00$\bar{1}$). From the results of etching, one must conclude that wulfenite belongs in the tetragonal-pyramidal symmetry class and that most crystals are twinned on a pedion, either {001} or {00$\bar{1}$}.

If we consider that the crystal represented in Fig. 1 is in the correct position with {001} at the top, the etching indicates that the twin (Fig. 2) has {00$\bar{1}$} as the composition plane. This is contrary to all other wulfenite crystals examined by etching, in which {001} is the composition plane. There is insufficient evidence to make a broad generalization but

it may well be that twins with composition plane $\{00\bar{1}\}$ have re-entrant angles, whereas those with composition plane {001} have a pseudo-dipyramidal symmetry.

Piezoelectricity. The absence of positive tests for piezoelectricity in wulfenite has argued for the symmetry $4/m$. However, one could not expect to detect it in a crystal twinned on a plane normal to [001]. Since most wulfenite is twinned in this manner, it is likely that the test may never have been made on a single individual. Using one of the pyramidal crystals from Jugoslavia, a feeble but definite piezoelectric response was obtained. A similar response was also given by one individual of a twin pair. The positive electrical pole of these crystals is at the (001) face.

References

Bach, Ludwig, Über Wulfenit: *Neus Jahab. Min., Abt. A, Beil. Bd.* **54,** 380–419.

Dana, J. D., and E. S. (1951), *System of Mineralogy* II, ed. 7. by C. Palache, H. Berman, and C. Frondel. New York.

Hlawatsch, K. (1925), Mineralogischen Notizen I–II: *Am. Naturhist. Mus. Vien,* **38,** 15–19.

Honess, A. P. (1927), The Nature, Origin and Interpretation of the Etch Figure on Crystals. New York.

Russell, Arthur (1946), An account of the Stury lead mines, Inverness-shire and of wulfenite, harmotome and other minerals which occur there: *Mineral. Mag.*, **27,** 147–154.

Manuscript received Sept. 11, 1954.

A CRYSTAL CHEMICAL STUDY OF MONTROSEITE AND PARAMONTROSEITE*

HOWARD T. EVANS, JR., AND MARY E. MROSE,
U. S. Geological Survey, Washington 25, D. C.

ABSTRACT

Montroseite, (V, Fe)O(OH), has been shown by Evans and Block to have a structure analogous to that of diaspore, AlO(OH). Altered crystals of montroseite give multiple x-ray patterns showing one sharp orthorhombic lattice corresponding to the host crystal and two diffuse lattices of similar symmetry and dimensions in parallel orientation. The more prominent of the diffuse phases is interpreted as a metastable form of VO_2, resulting from the oxidation of the host crystal, and is given the name "paramontroseite". Paramontroseite has $a=4.89$, $b=9.39$, and $c=2.93$ A., with space group *Pbnm*. The structure of both montroseite and paramontroseite has been completely refined by electron density synthesis and least squares analysis. The outstanding difference between the two structures lies in the length of the oxygen-oxygen distance corresponding to the hydrogen bond in montroseite. This length increases from 2.63 to 3.87 A., in going from montroseite to paramontroseite, indicating the loss of hydrogen during the alteration. The concept of an alteration process involving a migration of ions and electrons through an unbroken oxygen framework is thus directly supported by the crystal structure analyses, and also by other x-ray diffraction and chemical information. The postulated alteration mechanism is illustrated by certain other examples, notably the alteration of lepidocrocite and magnetite to maghemite, and of goethite to hematite.

INTRODUCTION

In a recent communication Weeks, Cisney, and Sherwood (1953) described the discovery, properties, and mode of occurrence of a new mineral, montroseite, from the Colorado Plateaus region. The material forms submetallic, grayish-black bladed crystalline masses. In cavities it forms small lathlike crystals with a perfect (010) cleavage. The specific gravity was measured on one sample as 4.00. The essential constitution of montroseite was demonstrated by means of a detailed crystal structure analysis by Evans and Block (1953), to consist of a vanadium oxide hydrate with the basic formula VO(OH), analogous to diaspore, AlO(OH). These authors pointed out that diffraction patterns obtained from apparently single crystals of montroseite are multiple, showing the presence of at least three phases. The multiple diffraction patterns show three orthorhombic lattices in parallel position, with slightly varying lattice constants, one characterized by sharp diffraction spots, the other two by diffuse spots. Figure 1 shows part of a Buerger precession photograph of the ($0kl$) plane on which the sharp and the "diffuse B" lattices are clearly visible. The data given for these lattices by Evans and Block are reproduced in Table 1.

* Publication authorized by the Director, U. S. Geological Survey.

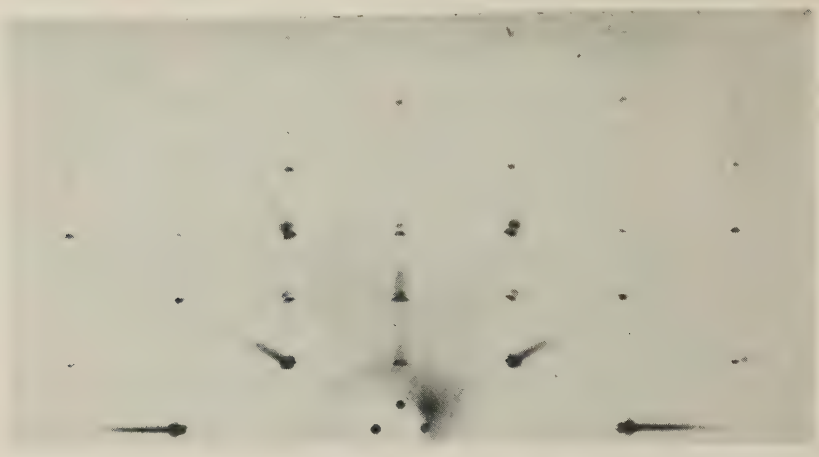

FIG. 1. Buerger precession photograph of the (0*kl*) net plane of a montroseite crystal showing sharp and diffuse spots.

It was tentatively suggested by Evans and Block that the sharp lattice (for which the structure analysis was carried out) represents the original host phase which subsequently alters by atmospheric action to give rise to the diffuse phases. New information has now been obtained concerning this alteration process as a result of a complete structure analysis of the the "diffuse B" phase, which is described in this paper. The evidence is sufficient to define the chemical nature of the "diffuse B" phase and to establish it as a new mineral. Therefore, because of the paramorphic relationship that it has to the host mineral montroseite, as described more fully below, we propose for the "diffuse B" phase the name *paramontroseite.*

TABLE 1. LATTICE DATA FOR MONTROSEITE PHASES

	Montroseite	"Diffuse A"	Paramontroseite "Diffuse B"
Formula	VO(OH)	$V_2O_3(OH)$(?)	VO_2
a (A)	4.54	4.80	4.89
b (A)	9.97	9.63	9.39
c (A)	3.03	2.93	2.93
V (A^3)	136.9	135.4	134.4
d (calc. for 8% FeO)	4.11	4.15	4.18
Z (formula units)	4	2	4
Space group	*Pbnm* (D_{2h}^{16})	*Pb*2_1*m*(?) (C_{2v}^{2})	*Pbnm* (D_{2h}^{16})

As a result of the study described here, it has been possible to show by the direct methods of x-ray diffraction and crystal structure analysis that the naturally occurring crystals of the mineral are entirely, or part or wholly, pseudomorphs of the new mineral paramontroseite after the original montroseite. The anomalous and variable results of chemical analysis are fully explained and, furthermore, the mechanism of alteration by oxidation and de-hydrogenation is revealed.

The work described in this paper was carried out on behalf of the Division of Raw Materials of the Atomic Energy Commission.

Source of the Data

Crystals of montroseite from the Burner Creek mine, Paradox Valley, Colorado, were used for the structure investigation. The best crystal to be photographed showed all three phases present, the montroseite and paramontroseite lattices being about equally intense, the "diffuse" lattice much the weakest. The spots were streaked in a manner to indicate a distortion of the crystal around the c axis of 10° or more, a feature that is apparently characteristic of montroseite crystals. The intensity data for montroseite were measured by visual estimates of 90 observed $(hk0)$ reflections from this crystal registered on a Weissenberg pattern using Mo$K\alpha$ radiation, as described by Evans and Block (1951). A second altered crystal of montroseite gave a nearly pure paramontroseite pattern, with only slight traces of the strongest reflections of the montroseite lattice still discernible. This crystal was used to measure 84 observed $(hk0)$ reflections by visual estimates made on a Weissenberg pattern made with Cu$K\alpha$ radiation. No corrections were made for absorption.

Despite the distortions inherent in the crystals, the data for montroseite give excellent agreement with those calculated for the proposed structure, but those for the diffuse phase are of very poor quality. Both sets of data have been treated by the method of least squares as described below, in order to insure the determination of the most likely structures and at the same time derive the standard errors appropriate to each.

Determination of the Crystal Structure of Paramontroseite

The distribution of intensity among the $(hk0)$ reflections for paramontroseite is quite similar to, though differing markedly in detail from, that of montroseite as reported by Evans and Block (1951). On the assumption that the structure of paramontroseite is similar to that of montroseite, the Patterson projection along [001] was partly computed in order to locate the V-V interatomic distance vectors. Peaks were found near the expected positions, and from them vanadium parameters were obtained from which the first set of structure factors was calculated

(oxygen atoms omitted). These structure factors for vanadium yielded probable Fourier phases for the 34 observed ($hk0$) terms, permitting the synthesis of the electron density projected along the c axis. Peaks corresponding to oxygen atoms were clearly apparent in this map, and the second set of calculated structure factors included all atoms in the cell, with coordinates read from the electron density map. The usual electron density synthesis-structure factor cycle was repeated twice more, until the map coordinates were consistent with all the phases. The final electron density projection is shown in Fig. 2*a*. Fig. 2*b* shows the corresponding electron density projection of montroseite from Evans and Block (1953) for comparison. The atom coordinates as measured from these maps by parabolic interpolation are given in Table 2.

Refinement of the Montroseite and Paramontroseite Structures by the Method of Least Squares

Because of the distortions in the electron density maps caused by inaccuracies in the intensity measurements and series termination effects, the method of least squares was used to derive the most likely structure consistent with the original data. The method was applied in a straightforward manner as described in several other places. (See, for example, Shoemaker, Donahue, Schomaker, and Corey, 1950.) The analysis is based on the structure factor function:

$$F_{calc} = e^{-Bs^2} \sum_j f_j \cos 2\pi(hx_j + ky_j + lz_j)$$

where B is the temperature coefficient, $s = (\sin\theta)/\lambda$, f_j is the scattering factor for the atom j, and x_j, y_j, are z_j are coordinates of each atom j. The seven parameters to be determined are $x(\mathrm{V})$, $y(\mathrm{V})$, $x(\mathrm{O_I})$, $y(\mathrm{O_I})$, $x(\mathrm{O_{II}})$, $y(\mathrm{O_{II}})$, and B. As all atoms are well separated in the c axis projection, all nondiagonal terms in the normal equations were neglected. The only matter of judgment concerns the manner in which the observations should be weighted in deriving the normal equations. Using these considerations, the normal equations reduce to a series of independent linear equations in terms of correction terms Δx, to be applied to each of the structure parameters:

$$\left[\sum w\left(\frac{\partial F}{\partial x}\right)^2\right]\Delta x = \sum w\left(\frac{\partial F}{\partial x}\Delta F\right)$$

where $\Delta F = (F_{obs} - F_{calc})$, x is the structure parameter $x(\mathrm{V})$, $y(\mathrm{V})$, $x(\mathrm{O_I})$, etc., and $\sqrt{w}$ is the weight given to each observation. If intensity as measured is a logarithmic function of film density in which errors of estimate by the eye are assumed to be distributed normally, it can easily be shown that the appropriate weighting factor is

$$\sqrt{w} = \frac{1}{|F|}.$$

Although experience seems to show that such an assumption is somewhere near the truth, the point is controversial, and we have carried out analyses with both

$$\sqrt{w} = \frac{1}{|F|} \text{ (weighted) and}$$

$$\sqrt{w} = 1 \text{ (unweighted).}$$

We accept the structures derived from the weighted analysis as the best,

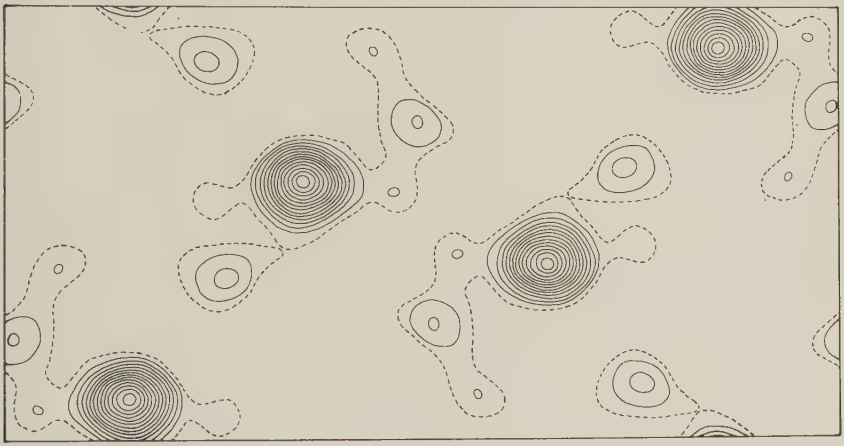

(*a*)

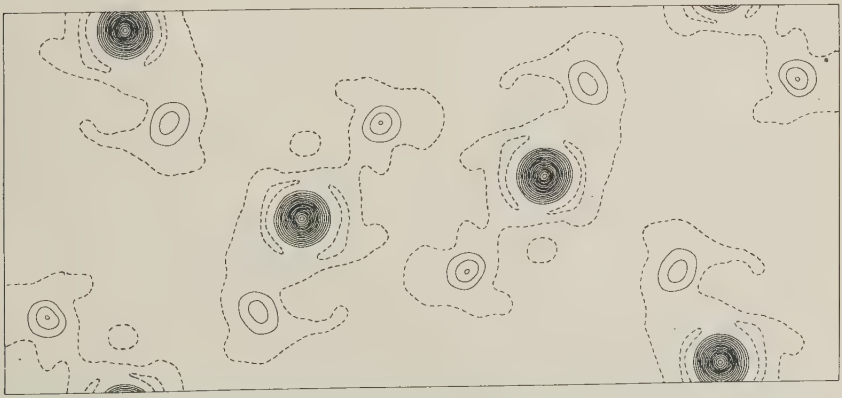

(*b*)

FIG. 2. Electron density projections along the *c* axis of (*a*) paramontroseite and (*b*) montroseite. Dotted contour represents 2 electrons per Å.^{2}; other contours at intervals of 2 *e*/Å^2.

TABLE 2. LEAST SQUARES DETERMINED PARAMETERS AND STANDARD ERRORS FOR MONTROSEITE AND PARAMONTROSEITE

Parameter	Montroseite					Paramontroseite				
	From electron density	From least squares analysis				From electron density	From least squares analysis			
		Unweighted		Weighted*			Unweighted		Weighted	
		Parameter	ϵ	Parameter	ϵ		Parameter	ϵ	Parameter	ϵ
$x(v)$	−0.051	−0.0511	0.00086	−0.0517	0.00054	0.094	0.091	0.0048	0.088	0.0034
$y(v)$	0.145	0.1457	0.00035	0.1455	0.00019	0.145	0.144	0.0027	0.143	0.0015
$x(O_I)$	0.297	0.300	0.0034	0.301	0.0021	0.127	0.091	0.0174	0.106	0.0181
$y(O_I)$	−0.197	−0.201	0.0016	−0.197	0.0011	−0.243	−0.254	0.0099	−0.235	0.0054
$x(O_{II})$	−0.197	−0.199	0.0030	−0.198	0.0021	−0.232	−0.231	0.0197	−0.227	0.0157
$y(O_{II})$	−0.051	−0.053	0.0016	−0.054	0.0011	−0.012	−0.018	0.0097	−0.013	0.0039
B		0.49	0.033	0.32	0.041		2.12	0.398	2.42	0.867

* The reflection (970) has been omitted from this analysis because of its disproportionately high weighting factor.

but it is observed that the difference between the weighted and unweighted results is generally less than the calculated standard errors. The standard error of F is

$$\epsilon_F = \sqrt{\frac{\sum w(\Delta F)^2}{n - p}}$$

where n is the number of observations (99 for montroseite, 34 for paramontroseite) and p the number of parameters (7, including the temperature factor, B). The standard error of x, ϵ_x, is given by

$$\epsilon_x^2 = \frac{\epsilon_F^2}{\sum w \left(\frac{\partial F}{\partial x}\right)^2}.$$

The ΔF values were obtained by scaling F_{obs} by multiplying by

$$k = \frac{\sum |F_{calc}| \cdot |F_{obs}|}{\sum |F_{obs}|^2}$$

for unweighted calculations, and

$$k = \frac{1}{n} \sum \frac{|F_{calc}|}{|F_{obs}|}$$

for weighted calculations. Acutally, the value of k is not very critical, except in the weighted calculations of ΔB for the temperature corrections where it was found necessary to take account of the cross-product terms between ΔB and Δk.

The results of all calculations for both montroseite and paramontroseite

are given in Table 2. The final parameters for montroseite and paramontroseite used to determine bond lengths in the following section are listed under the columns labeled "weighted" in this table.

The reliability factor

$$R = \frac{\sum | \Delta F_i |}{\sum | F_{obs} |}$$

obtained with

$$k = \frac{\sum | F_{calc} |}{\sum | F_{obs} |}$$

has a value $R = 0.113$ for 99 observed reflections for montroseite and $R = 0.24$ for 34 observed reflections for paramontroseite. Observed and calculated structure factors for montroseite and paramontroseite are listed in Table 3.*

Structural Features of Montroseite and Paramontroseite

The interatomic distances defined in Fig. 3 are tabulated for both structures in Table 4. The standard errors of the lengths shown are derived from those associated with the parameters given in Table 2. It is found that the errors in location of most atoms are practically isotropic and have magnitudes shown in Table 5. Errors on interatomic distances r between atoms A and B are given by:

$$\epsilon_r^2 = \epsilon_A^2 + \epsilon_B^2 + (\epsilon_L' r)^2$$

where ϵ_L' is the error of lattice measurement in per cent.

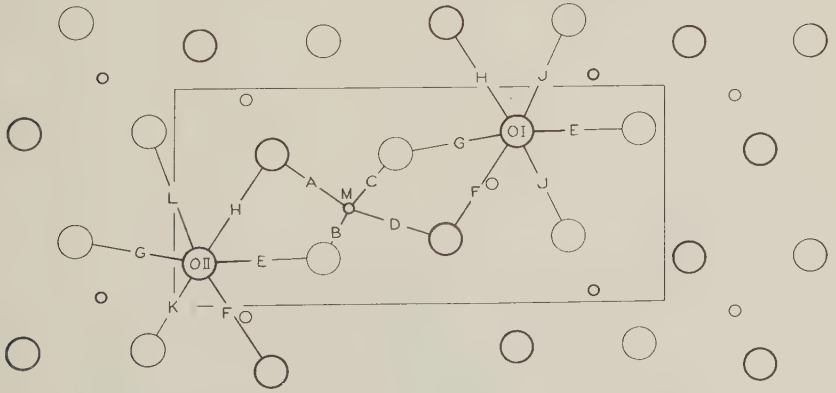

Fig. 3. Interatomic distance vectors in montroseite and paramontroseite (see Table 4).

* Because of an error made in the calculations, the values of F_{calc} for reflections with k odd in Table 2 of the paper by Evans and Block (1953) are incorrect. This error does not affect any other data given in that paper, except that $R = 0.11$ instead of 0.21.

TABLE 3. OBSERVED AND CALCULATED STRUCTURE FACTORS FOR MONTROSEITE AND PARAMONTROSEITE

hkl	Montroseite		Paramontroseite		*hkl*	Montroseite		Paramontroseite	
	$F_{obs.}$	$F_{calc.}$	$F_{obs.}$	$F_{calc.}$		$F_{obs.}$	$F_{calc.}$	$F_{obs.}$	$F_{calc.}$
020	18.9	−19.5		13	2,10,0	21.0	−25.5	7	− 8
040	42.2	−46.0	8	−14	2,11,0	8.7	−11.8		
060	32.3	36.6	14	27	2,12,0		5.0		
080	5.1	5.6	17	26	2,13,0	6.3	− 6.2		
0,10,0	27.4	−34.8	11	−17	2,14,0	17.4	18.8		
0,12,0	9.6	−10.7			2,15,0	13.6	14.7		
0,14,0	28.6	23.6			2,16,0	10.8	−10.3		
0,16,0		− 4.3			2,17,0		2.6		
0,18,0	12.6	−13.6			2,18,0	11.6	− 9.6		
0,20,0	14.6	18.7			2,19,0		− 6.1		
					2,20,0				
110	56.2	51.7	34	43					
120	33.9	22.2	46	−40	310	11.0	10.1	8	− 9
130	53.9	−48.9	46	−48	320	42.2	37.0	48	−35
140	52.2	−44.6	5	7	330	37.6	−37.0		3
150	14.0	−13.2		− 1	340	5.1	− 5.3	7	17
160	9.6	−11.9		13	350		4.0		− 3
170	42.2	43.1	26	26	360	20.6	−24.4	11	22
180		1.9	16	−17	370	20.2	21.0		− 4
190	11.8	−15.7		− 3	380	26.5	28.7	10	−15
1,10,0		2.6		− 4	390		0		− 1
1,11,0	28.0	−29.0		−12	3,10,0	7.4	8.0		
1,12,0		− 1.0			3,11,0	8.7	− 6.8		
1,13,0	17.7	19.7			3,12,0	22.3	−25.2		
1,14,0		1.3			3,13,0		8.7		
1,15,0	11.4	8.4			3,14,0		3.7		
1,16,0	11.8	13.2			3,15,0		8.2		
1,17,0	17.3	−15.5			3,16,0	11.4	9.5		
1,18,0		− 2.3			3,17,0	14.6	−13.3		
1,19,0		1.7			3,18,0		− 8.3		
1,20,0		− 4.2			3,19,0		− 2.9		
1,21,0	13.8	12.7							
					400	17.0	17.0	24	−22
200	19.3	17.7	16	3	410	39.4	40.7	14	−16
210	14.4	19.0	15	−24	420		− 3.7	16	17
220	11.2	−11.7	32	−21	430	17.0	17.0		−10
230	12.6	9 8	32	−34	440	8.1	− 8.0	10	15
240	52.6	−42.8	19	−27	450	23.4	−27.4	18	16
250	38.4	−35.8	35	44	460	7.5	7.1		− 3
260	24.2	23.8		0	470	9.1	12.3		− 2
270	5.9	− 6.2	7	− 9	480		1.4		− 6
280	25.6	28.2		2	490	22.2	21.6	6	− 7
290	20.6	24.5	10	−14	4,10,0		− 6.6		

TABLE 3—(*continued*)

hkl	Montroseite		Paramontroseite		*hkl*	Montroseite		Paramontroseite	
	$F_{obs.}$	$F_{calc.}$	$F_{obs.}$	$F_{calc.}$		$F_{obs.}$	$F_{calc.}$	$F_{obs.}$	$F_{calc.}$
4,11,0	10.8	−12.2			720	17.1	16.0		
4,12,0		− 2.6			730	8.1	6.7		
4,13,0	22.3	−19.0			740	12.6	−13.0		
4,14,0		5.2			750		6.1		
4,15,0		10.0			760	12.0	−12.8		
4,16,0		− 0.8			770	12.8	−12.6		
4,17,0		3.3			780	10.8	9.8		
4,18,0		− 3.7			790		7.1		
4,19,0	14.8	−17.1			7,10,0		3.7		
					7,11,0	11.0	12.4		
510		3.7		−10	7,12,0		− 8.3		
520	30.7	32.1	7	− 4					
530	10.8	10.3	19	19	800	20.8	−21.7		
540	13.8	−15.0		1	810	9.5	11.1		
550	7.4	− 6.2		15	820		2.9		
560	21.0	−20.1		1	830		3.8		
570			6	−10	840	12.6	10.7		
580	22.7	21.9			850		− 7.3		
590		− 5.1			860	11.0	− 9.3		
5,10,0	10.4	7.0			870		4.1		
5,11,0		− 6.1			880		− 1.4		
5,12,0	18.9	−20.2			890		5.1		
5,13,0		1.6			8,10,0	11.8	11.9		
5,14,0		2.6							
5,15,0		− 3.7			910	10.0	− 8.5		
5,16,0	17.4	13.4			920		3.5		
					930	15.5	14.3		
600		− 6.0	15	−14	940		5.0		
610	14.4	13.4		2	950		0.5		
620		3.3		3	960		− 2.1		
630	6.5	8.7			970	5.7	11.8		
640		8.5							
650	28.4	−27.0			10,0,0	9.5	5.7		
660		− 5.8			10,1,0		− 0.9		
670		− 4.6			10,2,0		2.9		
680		− 6.6			10,3,0		0.5		
690	22.0	21.7			10,4,0	11.6	11.9		
6,10,0		5.4			10,5,0		1.3		
6,11,0	10.2	−11.9			10,6,0	8.5	− 7.6		
6,12,0		− 1.5			10,7,0		0		
6,13,0		− 5.4			10,8,0	10.0	−10.4		
6,14,0		− 5.3							
6,15,0	12.8	16.4			11,1,0		− 4.7		
					11,2,0		− 3.6		
710	10.6	−10.3			11,3,0	9.1	9.5		

TABLE 4. INTERATOMIC DISTANCES IN MONTROSEITE AND PARAMONTROSEITE

(See Fig. 3)

Atoms	Vector	Montroseite (A)		Paramontroseite (A)	
$V\text{-}O_I$	A	1.94	±0.017	1.88	±0.07
	B(2)	1.96	±0.017	1.91	±0.07
$V\text{-}O_{II}$	C(2)	2.10	±0.017	2.00	±0.07
	D	2.10	±0.017	2.13	±0.07
$O_I\text{-}O_{II}$	E(2)	2.91	±0.02	2.88	±0.10
	F	2.68	±0.02	2.65	±0.10
	G(2)	2.96	±0.02	2.79	±0.10
	H	2.63	±0.02	3.87	±0.10
$O_I\text{-}O_I$	J(4)	2.93	±0.02	2.86	±0.10
	c-axis (2)	3.03	±0.01	2.93	±0.02
$O_{II}\text{-}O_{II}$	K(2)	2.59	±0.02	2.65	±0.10
	L(2)	3.31	±0.02	3.04	±0.10
V-V		3.306	±0.011	3.16	±0.03

It is clear that the essential principles of coordination and vanadium-oxygen bonding are the same in both montroseite and paramontroseite. The main difference between these structures, as shown by the *c* axis elevations in Fig. 4, lies in the fact that the zigzag octahedron chains have rotated about 28° around the *c* axis during the change from montroseite to paramontroseite. This process has been accompanied by two important changes in the structure:

(1) Most important, the interoxygen distance, *H*, is short (2.63 Å) in montroseite, but very long (3.87 Å) in paramontroseite. The former value is very reasonable for a hydrogen bond, as suggested by Evans and Block (1953), but the latter is far too large for such a bond. As hydrogen has no other logical place in the structure, the conclusion must be drawn that it is absent in paramontroseite.

(2) The vanadium-oxygen distances are slightly, but probably significantly shorter in paramontroseite than in montroseite. The change is

TABLE 5. STANDARD ERRORS OF ATOMIC POSITIONS IN MONTROSEITE AND PARAMONTROSEITE

	Montroseite	Paramontroseite
ϵ_V	0.0037A.	0.015A.
ϵ_O	0.015A.	0.070A.
ϵ_L'	0.3 per cent	0.5 per cent

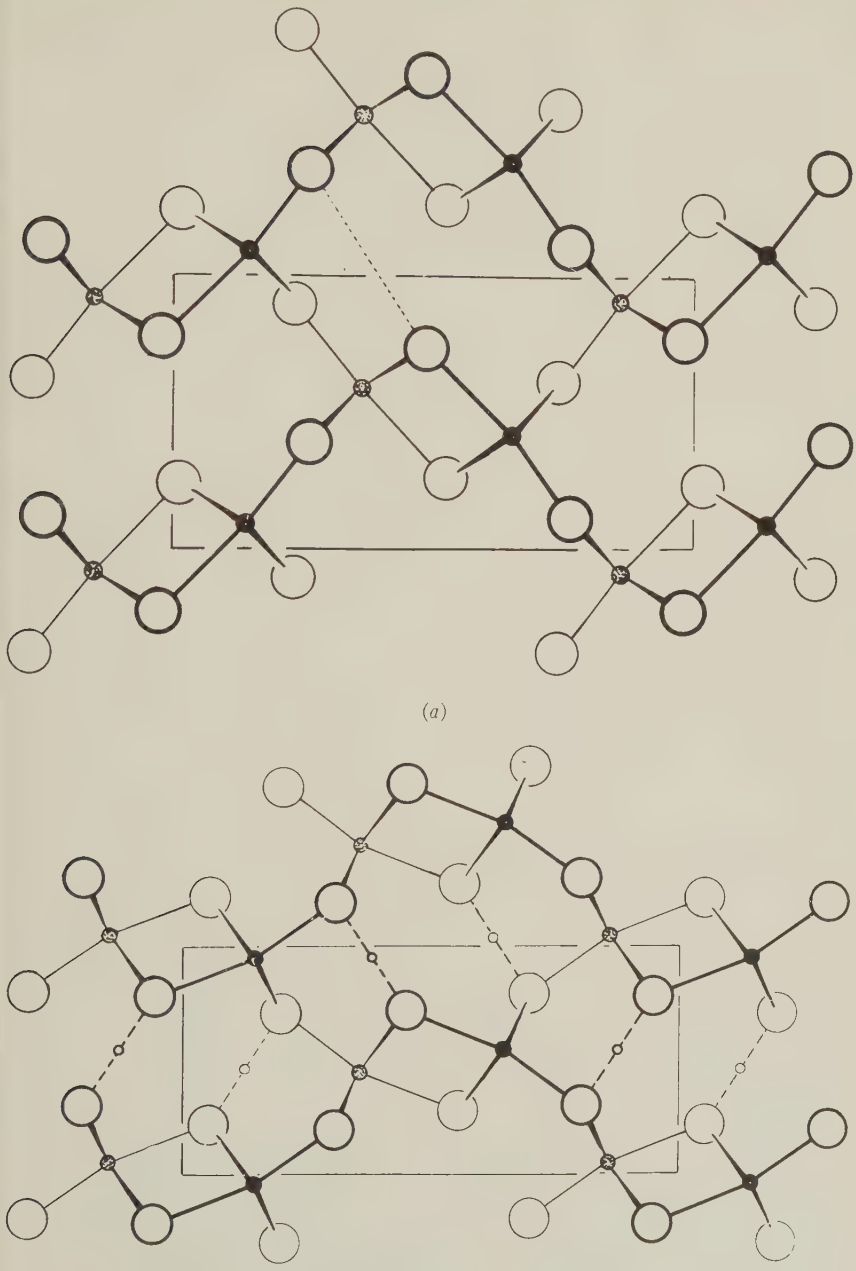

(*a*)

(*b*)

FIG. 4. View of crystal structure along the *c* axis of (*a*) paramontroseite, and (*b*) montroseite showing hydrogen bonds.

close to that which would be expected when one electron pair is added to the montroseite vanadium bond coordination system; that is, when vanadium is oxidized from +3 to +4 through the loss of hydrogen.

Solid State Alteration of Montroseite

In light of the known facts, the history of the mineral montroseite may be outlined as follows:

(*a*) The mineral montroseite, VO(OH) with some Fe usually replacing V, is deposited in crystalline masses, by an unknown process, in a sandstone matrix.

(*b*) The crystallized montroseite is oxidized by oxygen in the atmosphere or in ground water to paramontroseite, at temperatures below 50° C., according to the reaction:

$$\underset{\text{(Montroseite)}}{2VO(OH)} + \tfrac{1}{2}O_2 \rightarrow \underset{\text{(Paramontroseite)}}{2VO_2} + H_2O$$

(*c*) The oxidation process is accomplished by a migration of the hydrogen atoms through the montroseite crystal structure to the crystal surface, where they combine with oxygen. The close-packed oxygen framework is slightly shifted in this process but is not broken down. The process may pass through an intermediate stage involving the "diffuse A" phase.

(*d*) The end product of this solid state alteration process, paramontroseite, is itself unstable and is subsequently destroyed by weathering action and replaced by the corvusite type of minerals.

These conclusions are drawn from the following established facts:

1. The montroseite phase gives rise to a sharp diffraction pattern, suggesting normal crystal growth of a primary phase.

2. The paramontroseite diffraction pattern is diffuse, suggesting that this phase occurs as alteration nucleii finely disseminated through the host crystal, as would be expected to result from the postulated diffusion of hydrogen atoms.

3. The structure of montroseite and paramontroseite, especially the nearly hexagonal close-packed oxygen framework, is the same.

4. The crystal lattices of montroseite and paramontroseite are in parallel position.

5. The average temperature vibration amplitude for montroseite ($=\sqrt{B/8\pi^2}$) is 0.21 Å, indicating a firmly bound, stable structure, whereas the average amplitude of paramontroseite is 0.53 Å, indicating a much less stable structure. The difference in temperature vibration accounts for the much larger and more diffuse appearance of the vanadium atoms in the electron density map of paramontroseite as compared with montroseite (Fig. 2).

6. The length of the hydrogen bond in montroseite is much less than the corresponding distance in paramontroseite, indicating loss of hydrogen.

7. The vanadium-oxygen distances in montroseite are longer than in paramontroseite, indicating oxidation of the vanadium.

8. The powder patterns of montroseite can be indexed on a lattice that conforms most closely with the paramontroseite lattice(Weeks, Cisney, and Sherwood, 1953). In fact, calculated and observed interplanar spacings show fair agreement, if lattice parameters intermediate between the "diffuse A" and "B" lattices are used.

9. Chemical analyses (Weeks, Cisney, and Sherwood, 1953) show extensive, in some cases nearly complete, replacement of V_2O_3 by V_2O_4. Also, the water content is decreased consistently with the oxidation of VO(OH) to VO_2.

It has been mentioned that there is evidence that a third phase is present in montroseite crystals, referred to as the "diffuse A" phase. The true nature of the "diffuse A" phase is unknown. Its relation to the montroseite and paramontroseite suggests that it may represent an intermediate step in the alteration of one into the other. If this is so, the "diffuse A" phase may be $V_2O_3(OH)$, having the space group $Pb2_1m(C_{2v}^2)$ or $P2_1nm$ (C_{2v}^7), with 2 formula units per cell. This noncentrosymmetric phase would correspond to the montroseite structure with half the hydrogen atoms removed. Alternatively, the "diffuse A" phase may represent some sort of separated Fe-rich phase, but its constants are not the same as those of goethite.

Other Examples of Solid State Alteration Phenomena

It is well known that the cubic polymorph of Fe_2O_3 can be prepared by warming magnetite (Fe_3O_4) in a stream of oxygen at low temperatures ($<250°$ C.). At higher temperatures the cubic γ-Fe_2O_3 is converted to the rhombohedral α-Fe_2O_3. It is understood that the oxidation occurs without disturbing the cubic close-packed oxygen framework of the spinel structure of magnetite. The oxygen lattice grows at the crystal surface, and the Fe atoms diffuse outward until the spinel-type unit cell contents $Fe_{24}O_{32}$ is reduced to $Fe_{21\frac{1}{3}}O_{32}$. Evidently γ-Fe_2O_3 is wholly metastable and can only exist as a result of a low-temperature chemical change in the solid state from a stable phase.

This phenomenon probably accounts for the observation by Newhouse (1929) that magnetite crystals from Magnet Cove, Ark., are coated with an oriented overgrowth of maghemite (γ-Fe_2O_3). Maghemite also is known (Sosman and Posnjak, 1925) as an alteration product of lepidocrocite, FeO(OH), which has a structure based on a cubic close-packed

oxygen lattice, whereas hematite (α-Fe_2O_3) is a common alteration product of goethite, which has the diaspore structure like montroseite. These two examples do not involve oxidation, but the alteration process is probably similar to that of montroseite and magnetite.

Artificial vanadium dioxide does not have the parmontroseite structure, but rather a distorted rutile structure (Andersson, 1953). Paramontroseite is probably also metastable like maghemite and can only exist through solid state alteration from the stable montroseite at low temperatures. These minerals are most nearly analogous to groutite, MnO(OH), and ramsdellite, MnO_2, both having the diaspore structure, but unfortunately no study has been made of the paragenetic relationships of the two manganese minerals which would enable us to compare our conclusions regarding the vanadium minerals.

Summary

The crystal structures of montroseite, VO(OH), and paramontroseite, VO_2, have been refined by the method of least squares. The structures of both minerals are based on the diaspore structure type. Montroseite crystals give multiple x-ray diffraction patterns—a sharp pattern, which has yielded the data for montroseite, and a diffuse pattern, which gave the data for paramontroseite. An outstanding difference between the two phases revealed by the structure analysis is that the structure of montroseite includes a hydrogen bond, whereas this bond is absent in the paramontroseite structure. Thus, the chemical nature of the two phases is confirmed, and paramontroseite is established as a new mineral. In addition, the paramorphic relationship between the two is well explained.

Crystal structure data, lattice studies, certain diffraction phenomena and chemical data have all led to the conclusion that montroseite alters to paramontroseite through weathering action, by means of a solid state reaction at low temperature. This process involves the migration of hydrogen atoms through an unchanged hexagonal close-packed oxygen framework. Paramontroseite is evidently a metastable phase. The alteration of montroseite to paramontroseite is apparently analogous with that of magnetite to maghemite, lepidocrocite to maghemite, and goethite to hematite.

References

Andersson, G. (1953), X-ray studies on vanadium oxides: *Research*, **6**, 455–465.

Evans, H. T., Jr., and Block, S. (1953), The crystal structure of montroseite, a vanadium member of the diaspore group: *Am. Mineral.*, **38**, 1242–1250.

Newhouse, W. H. (1929), The identity and genesis of loadstone magnetite: *Econ. Geology*, **24**, 62–67.

Shoemaker, D. P., Donahue, J., Schomaker, V., and Corey, R. B. (1950), The crystal structure of Ls-threonine: *Jour. Am. Chem. Soc.*, **72**, 2328–2349.

Sosman, R. B., and Posnjak, E. (1925), Ferromagnetic ferric oxide, artificial and natural: *Washington Acad. Sci. Jour.*, **15**, 329–344.

Weeks, A. D , Cisney, E., and Sherwood, A. M (1953), Montroseite, a new vanadium oxide from the Colorado Plateaus: *Am. Mineral.*, **38**, 1235–1241.

Manuscript received Oct. 9, 1954.

A PRECISION *X*-RAY POWDER CAMERA*

CLIFFORD FRONDEL, *Harvard University, Cambridge, Massachusetts.*

INTRODUCTION

In the cylindrical camera here described, the sample is successively photographed on the peripheral positions at opposite ends of a diameter, the film remaining unmoved during the operation. This gives two back-reflection photographs that are symmetrically opposed on the same strip of film (Fig. 1). This technique has the fundamental advantage over other back-reflection camera designs in that it permits the effective camera diameter to be computed directly from film measurements. The manner of film mounting is immaterial.

The construction of the camera is apparent from Figs. 1–4. The *x*-ray beam is sharply collimated by a long narrow rectangular slit system that is permanently fixed in a diametral position within the body of the camera itself. There is no focussing, as in conventional back-reflection cameras. The powder sample is prepared as a flat disc. The disc is mounted on the end of a tubular, removable, rotating fixture so that its surface is tangent to the (projected) inner surface of the film at the end of the diameter where *x*-ray beam impinges. The fixture sample is mounted on ball bearings (Fig. 4). The sample in reality is located between the open ends of the film or within a hole punched in the film. The opposite, or inlet, end of the slit system is covered by a removable tubular shield inserted through the inlet port to prevent scattering from the end of the slit system. In practice, the sample is first photographed at one port. The sample-fixture and slit shield are then interchanged (in the dark), the camera rotated 180° on its axis, and the sample rephotographed. The film, strongly clamped in place by steel rings along its sides, is not moved during the operation. A removable, cylindrical shield of suitable dimension can be mounted around the sample at each port inside the camera for the purpose of shielding off reflections below some predetermined angle of θ. The shields are not needed if there is no undesirable overlap of lines on the front and back patterns.

The method employed for rotating the camera 180° between the two exposures can be described with reference to Fig. 3. The annular ring *A*, secured to the camera body by four machine screws within slots, contains two diametrically opposite key holes, *D*. The camera is lined up for use as follows: axle lock *B* and the screws holding ring *A* are loosened and the camera rotated until the *x*-ray beam passes with maximum intensity

* Contribution from the Department of Mineralogy and Petrography, Harvard University, No. 356.

through the slit system. The camera is then clamped by lock B and the annular ring turned until one of the key holes D is engaged by the positioning pin C. The annular ring is then permanently fastened; the camera can now be turned 180° by withdrawing pin C, loosening lock B and turning until the opposite key hole is engaged.

The slit system is of rectangular cross-section and has a length of roughly two-thirds the camera diameter. It is made by clamping a channeled brass plate against a flat plate, the whole assembly being rotatable on a centrally positioned axle. Precision machining is required. Fine-adjustment of the rotation is effected by a small screw cam set into the base of the slit assembly. Set screws are provided for locking the slit assembly permanently in the position at which the x-ray beam strikes

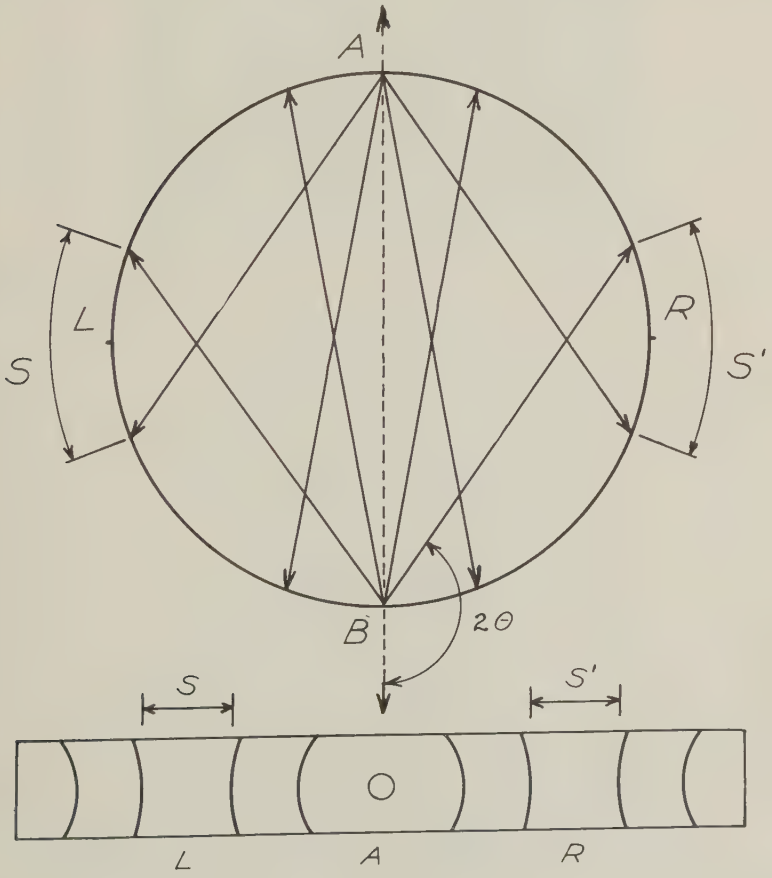

FIG. 1

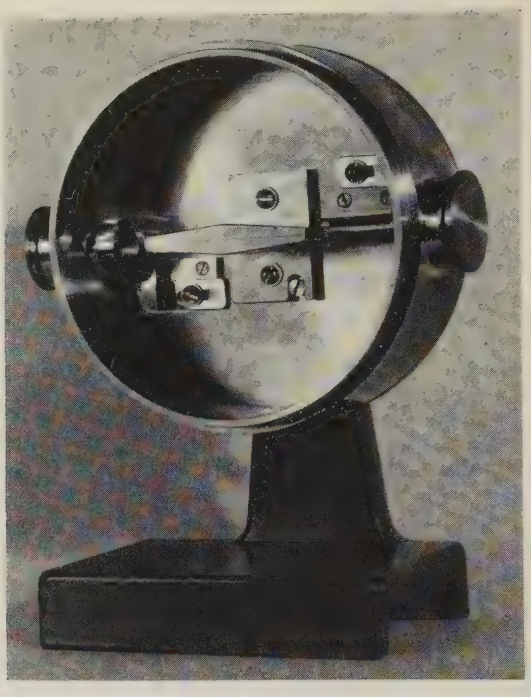

FIG. 2. Front view of camera, showing central slit system, ring shields for limiting angle of reflection (one retracted), rotating sample holder (left) and shield for end of inlet slit (right).

the flat powder mount at its point of tangency to the film. This also is the position at which the diametral slit system and the axis of rotation of the sample are parallel, the latter axis being offset about 0.020 inch from the center of the camera to provide greater randomness in the irradiated area of the mount.

The diametral position of the slit system and the accuracy of the 180° rotation can be determined experimentally by measurement of the film distances S and S' (Fig. 1). These distances are equal in a well constructed and well aligned camera.

The powder sample disc can be adjusted to tangency with the film in several ways: by pushing the sample-fixture through its bearing until contact is made with a mandrel held against the inner surface of the film, by visual sighting under a safe-light or, if the thickness of the sample disc is held constant, by pushing the sample-fixture against a fixed stop. The error introduced in line position by a difference between the camera diameter and the effective sample to sample distance decreases to zero as θ increases to 90° and can be removed, together with absorption errors, by an extrapolation method.

Several different methods of film mounting can be employed. If the open end of the film is placed at a port, A or B in Fig. 1, the effective camera half-circumference can be determined from the average positions of the lines symmetrical about R and L. The angle θ for each line can be obtained from the averaged film distances S and S' of these lines, using the relation

$$\theta_{hkl} = \left(\frac{\text{half-circumf.} - S_{hkl}/2}{2}\right) \text{X}^\circ, \quad \text{where} \quad \text{X}^\circ = \frac{180}{\text{half circumf.}}.$$

The open end of the film can also be placed at R or L, with the x-ray beam entering and leaving through holes in the film, but there is no advantage in so doing. In actual practice it is desirable to average results from several films, and these should be taken alternately with the open end at A and B.

Camera Specifications

A single solution to the problem of the ideal camera diameter, slit dimensions and sample thickness can not be found. The principal matters involved are the angular dispersion and the line quality. The line quality,

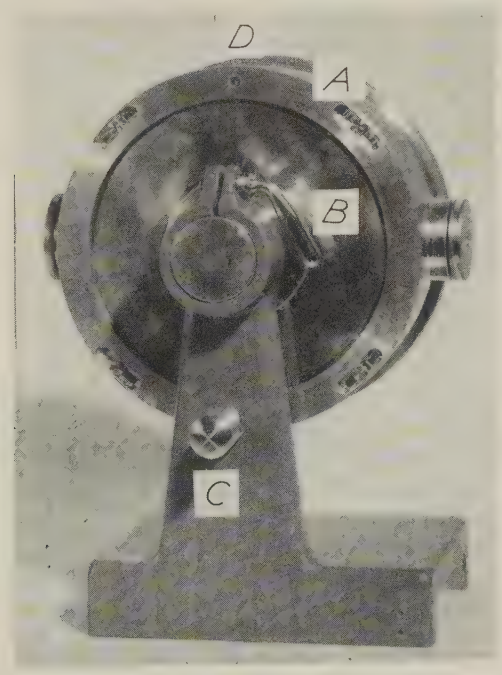

Fig. 3. Rear view of camera, showing annular positioning ring A, axle lock B, positioning pin C, and positioning key holes D.

on which the camera precision largely depends, is affected by a number of factors. These include the particular substance to be photographed, the manner of preparation and particle size of the sample, the x-ray dosage, the amount of sample that is irradiated, absorption in the sample, air scatter and the slit specifications. The camera precision that is realized also depends on the nature of the measuring scale employed, the degree of temperature control and the manner of treatment of the line measurements.

Two cameras 9 and 16 cm. (3.5 and 6.3 in.) in diameter were constructed and were each tested with NaCl, ThO_2, Ag, quartz and diamond to determine the slit dimensions and the sample thickness that gave the best line quality. The effect of variation in sample position also was investigated. The line quality was evaluated primarily by the precision to which the unit cell dimensions could be determined under standardized conditions of film measurement, sample preparation, etc.

The 9 cm. camera was found to afford greater precision than the 16 cm. camera under all slit and sample conditions in spite of its smaller angular dispersion. This was due to much better line quality. In the 9 cm. camera, with a slit length of 6.3 cm. and a slit height of 0.76 mm. it

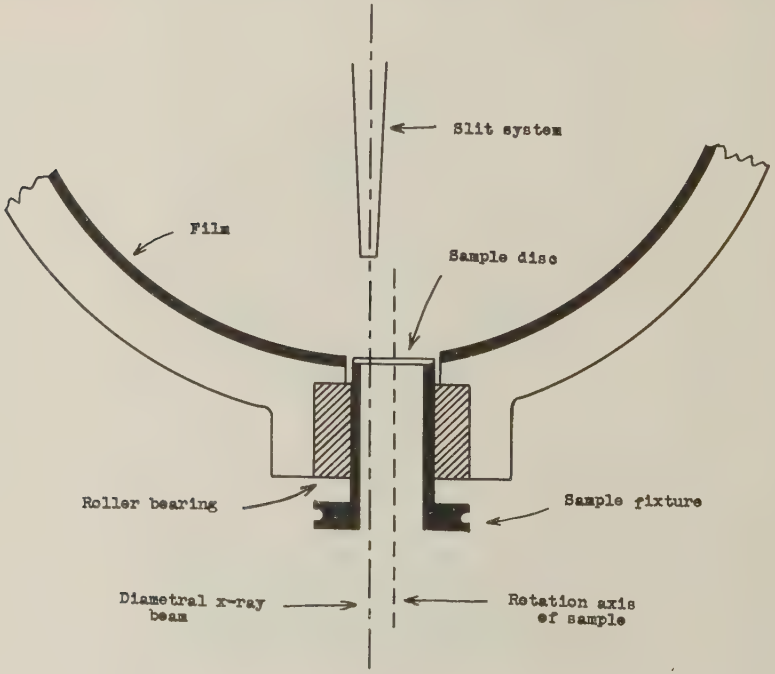

FIG. 4

was found that at slit widths below about 0.127–0.152 mm. (0.005–0.006 in.) the precision was rapidly reduced due to increasing line graininess (small volume of sample irradiated). At widths over about 0.305–0.381 mm. (0.012–0.015 in.) precision was slowly lost due to increasing line width. The optimum slit width for Ag and diamond was larger than for quartz, due principally to difficulty in obtaining sufficient randomness in the sample. The optimum diameter for the camera independent of slit dimensions is not known. Increase in the precision of the measuring scale would tend to reduce the optimum diameter. Increase in line quality beyond a point that can be realized by the scale employed would tend to increase the optimum diameter. Variation in sample thickness between about full thickness to half thickness (0.127–0.254 mm.) of the x-ray film was not found to materially affect line quality, but faint and grainy films were afforded at lesser thickness. Variation in the sample to sample distance over a range of about 3.81 mm. did not affect line quality, but did markedly influence the extrapolation graphs and thereby the camera precision. A variation of less than about 0.2 mm., easily effected experimentally, did not materially affect the camera precision. The experimental data reported beyond were obtained in the 9 cm. camera with a 0.127 mm. slit. This narrow slit requires careful sample preparation to ensure randomness. A slit width of 0.177–0.0203 mm. would be more generally serviceable with little loss in precision.

Experimental Data

Measurements of a_0 made on NaCl and ThO_2 may be reported to illustrate the precision of the 9 cm. camera with a rectangular slit $65 \times 0.76 \times 0.127$ mm. ($2.56 \times 0.030 \times 0.005$ inch) in dimensions. NaCl affords films in general of below-average quality, with rather unfavorable extrapolation conditions, and offers a relatively severe test of any powder camera. ThO_2 affords films of very good quality, with the advantage of several sharp lines at high θ angles, but is relatively strongly absorbing. A value of a_0 was calculated for each line and these values were graphically extrapolated to $\theta = 90°$ using the function

$$\frac{1}{2}\left(\frac{\cos^2\theta}{\sin\theta} + \frac{\cos^2\theta}{\theta}\right)$$

of Nelson and Riley.[1] This function, originally developed for cylindrical samples, was found to give a linear graph. The NaCl graphs had an upward slope of about 1 part in 17, and the ThO_2 graphs of about 1 part in 8. The films were taken in copper radiation filtered through nickel foil. The x-ray wave-lengths used in the calculations were:

[1] Nelson, J. B., and Riley, D. P.: *Proc. Phys. Soc.*, **57**, 160 (1945).

$$\text{Cu } K_{\alpha_1} = 1.537395 \text{ kX}$$

$$\text{Cu } K_{\alpha_2} = 1.541232.$$

The camera was housed in an air bath in which a resistance heater was controlled by a capillary mercury-bulb thermometer in a thyratron circuit.[2] The variation in air temperature over the run was 0.25° C. This variation had roughly a 10 minute cycle. The variation in temperature within the camera was less than 0.1°. The films were measured on a Hilger and Watts Film Measuring Rule, No. L85, ruled to 1 mm. with a precision of 0.001 mm. and fitted with a vernier ruled to 0.05 mm. The vernier could be read, however, to about 0.02 mm. by interpolation. Each line was measured 6 or more times and the results averaged. A magnification of 2× was employed; it was clearly established that magnification was advantageous with dark and sharp lines, but that the unaided eye was superior with diffuse lines. Double-coated film was employed, but the outer surface of the film strip was shielded by adhesive tape during development. The *x*-ray reflections enter the film at angles decreasing from 90° at $\theta = 90°$, so that if both sides of the film are developed there is a slight offset of the line on opposite sides of the film. If the average line position is measured an erroneous film distance is obtained that causes a very steep slope in the extrapolation graph.

ThO_2

The ThO_2 was prepared by ignition of a thorium salt and gave good photographs without being powdered. The material contained an undetermined amount of other elements in solid solution and the value for a_0 can not be taken as representative of pure ThO_2. The coefficient of

Table 1. Unit Cell Dimensions of ThO_2

Temperature 31.6°. 9 cm. diameter camera. 16 films.
Copper radiation

Open end of film	a_0 in kX	Open end of film	a_0 in kX
R	5.58396	A	5.58417
A	5.58405	B	5.58417
B	5.58408	R	5.58417
L	5.58412	A	5.58420
A	5.58413	A	5.58420
A	5.58414	L	5.58423
B	5.58415	L	5.58424
B	5.58415	R	5.58425

Arithmetic mean a_0 5.58415. Average deviation ±0.00005.

linear thermal expansion is not known, and the cell size is cited as of the camera temperature, 31.6° C. The values of a_0 obtained from the measurement of 16 separate films are given in Table 1. Eleven of the values

[2] Strong, J.: Procedures in Experimental Physics, New York, Fig. 18, p. 446 (1945).

are based on single measurements of the film, two are an average of two measurements, and three an average of three measurements. The range of values is 0.00028 kX. The arithmetic mean is $a_0 = 5.58415$ kX and the calculated average deviation is ± 0.00005 kX, about one part in 55,000. An independent check of this material[3] on a 16 cm. diameter precision central-mount camera using the same film measuring and extrapolation procedures gave $a_0 = 5.5842$ kX at 31.6°.

NaCl

The NaCl used had been prepared from material of high initial purity by precipitating a saturated solution in HCl with HCl gas, centrifuging, and repeating the operation three times in platinum ware. The precipitate, too coarse to use directly, was powdered, sieved, annealed at 400° C. for 12 hours and sieved again without crushing. It is difficult to prepare NaCl in small particle size free from strain, and the present films were

Table 2. Unit Cell Dimensions of NaCl

Reduced to 25°, corrected for refraction. 9 cm. camera. 9 films. Copper radiation

No.	Open end of film	a_0 in kX
1	B	5.62921
2	B	5.62912
3	A	5.62910
4	A	5.62907
5	R	5.62902
6	B	5.62899
7	B	5.62892
8	A	5.62885
9	A	5.62882

Arithmetic mean a_0-5.62901. Average deviation ± 0.0001.

visibly inferior in line quality to those of ThO_2 and quartz. It may be noted that the characteristic impurity present in solid solution, KCl, increases a_0 by 0.00058 kX per 0.1 weight per cent KCl,[4] so that it is important to use material of the highest purity for comparative work.

The values of a_0 obtained from the measurement of nine separate films are given in Table 2. Values 2–5 and 8 represent averages of 5 to 9 film measurements, the others of three. The range of values is 0.00039

[3] By Mr. Brian Skinner, Department of Mineralogy, Harvard University, April, 1954.

[4] Straumanis, M., and Ievinš, A.: Die Präzisionsbest. von Gitterkonst. Berlin (1940), p. 95.

kX. The arithmetic mean is $a_0 = 5.62901$ and the calculated average deviation is ± 0.0001 kX, about one part in 28,000. Four of the films, numbers 2–5, were of perceptibly better line quality than the others; the arithmetic mean of these films is $a_0 = 5.62908$ kX. Both of the above values for a_0 are close to the values for NaCl reported by Straumanis (Table 3). The present data were reduced from the camera temperatures (31.6° and 30.7°) to 25° using the coefficient of linear thermal expansion of 40.5×10^{-6} of Straumanis instead of the value 40.40×10^{-6} (at 20°) of

TABLE 3. LITERATURE VALUES OF a_0 FOR NaCl

a_0 in kX at 25°. Corr. for refr.	Material and Method	Reference
5.62906 ± .00003	Natural rock-salt (Wieliczka), of high purity. Central-mount camera	Straumanis and Ieviņš, footnote 4.
5.62907 ± .00003	Average of rock-salt from four localities, not analyzed. Central-mount camera.	Straumanis and Ieviņš, footnote 4.
5.62894 ± .00002	Kahlbaum, high purity. Central-mount camera.	Straumanis and Ieviņš: *Zeit. Phys.*, **102**, 353 (1936).
5.62933 ± .0001	No details on sample. Spectrometer method.	Tu: *Phys. Rev.*, **40**, 662 (1932).
5.6298 ± .0001	"Pure NaCl." Unicam 19 cm. central-mount camera.	Rymer and Hambling: *Acta Cryst.*, **4**, 565 (1951).
5.62983 ± .00006	Merck, 99.98% pure. Spectrometer method of Kossel, *Ann. Phys.*, **26**, 553 (1936).	van Bergen: *Ann. Phys.*, **39**, 553 (1941).

Fizeau. Straumanis' values were obtained in a central mount camera by averaging the high-order lines, without extrapolation, using an extremely thin mount to minimize absorption. The reported precision values of a_0 for NaCl show a remarkably wide spread (Table 3).

ACKNOWLEDGMENTS

The writer wishes to express his appreciation to Miss Mary E. Mrose for assistance in computation, and to her and Mr. George Robinson and Mr. Peter Piston for aid in film measurement. The cameras were constructed by Mr. Harold Ames, Dunbar Laboratory, Harvard University. Certain costs were paid under a contract with the Frequency Control Branch, (Quartz Crystal), U. S. Signal Corps, Fort Monmouth, New Jersey.

Manuscript received July 20, 1954

THE STRUCTURAL SCHEME OF SEPIOLITE*

Bartholomew Nagy† and W. F. Bradley,‡
The Pennsylvania State University, State College, Pennsylvania, and the Illinois State Geological Survey, Urbana, Illinois.

Abstract

An idealized structure for sepiolite is deduced from the zero layer x-ray diffraction effects from natural fibers. Linked hydrous $H_6Mg_8Si_{12}O_{30}(OH)_{10}+Aq$ chains are disposed in centered array in a cell of 13.4×27Å cross section.

Sepiolite is a hydrous magnesium silicate mineral, often referred to in textbooks by the approximate chemical formula of $3SiO_2 \cdot 2MgO \cdot xH_2O$. It is a fine grained material which may occur occasionally in the form of macroscopic fibers. Sepiolite can be classified as one of the clay minerals. A summary of the available x-ray diffraction data of sepiolite, together with the results of the physical, thermal and chemical investigations, have recently been reviewed in an authoritative manner by Caillere (1951).

The excellence of development of fibrous habit in several natural occurrences permits registration of x-ray fiber diagrams from which the probability of proper indexing of sufficient numbers of reflections, especially in the zero layer, seems high enough to justify a schematic analysis of the structure.

Fibers from Little Cottonwood, Utah, were used to obtain the x-ray diffraction data. The sample consisted of $1\frac{1}{2}$–2 cm. long, light gray colored fibers. Viewed at high magnification under the electron microscope the fibers appeared to have a lath or ribbon-like particle morphology. The fibrous habit of the Little Cottonwood sample is illustrated in Fig. 1. No certain diffraction maxima for any extraneous accessory minerals were observed on the x-ray patterns. Other sepiolite fibers, notably those from Ampandrandrava, Madagascar, are often associated with some opaline silica. The chemical analysis of the sample that was used for obtaining the diffraction data is listed in Table 1.

The c axis periodicity of about 5.3 Å has been recorded by Migeon (1936) and Longchambon (1937). The present analysis is limited to the establishment of an orthogonal net in the zero layer, which provides lat-

* An abstract of this paper was presented at the Third General Assembly of the International Union of Crystallography, held in Paris, France, July 21–28, 1954.

† Present address: Stanolind Oil and Gas Company, Research Center, Tulsa, Oklahoma.

‡ Published with the permission of the Chief, Illinois State Geological Survey, Urbana, Illinois.

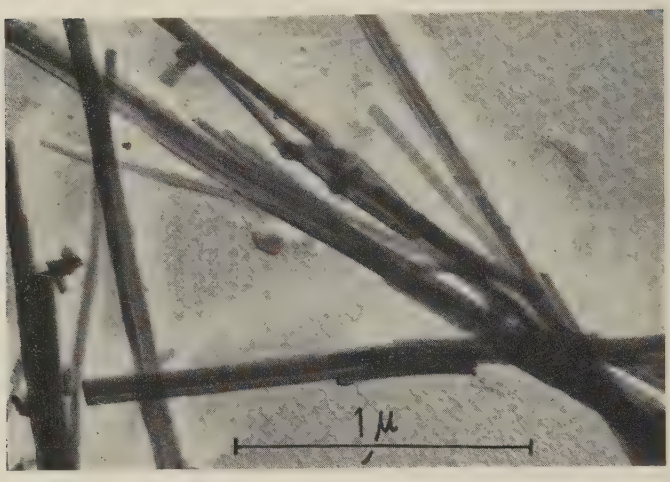

FIG. 1. Electron micrograph of the Little Cottonwood, Utah, sepiolite showing the fibrous and lath shaped morphology of sepiolite particles. Magnification 39,200×. Platinum shadowed.

tice parameters consistent with the dimensions of some reasonable model based on other known hydrous magnesium silicate crystal structures. Such a section has been found with $a_0 \sin\beta = 13.4$ and $b_0 = 27.0$ Å, for which all observed reflections are of the form $h+k=2n$. This net provides a b/c ratio of approximately $3\sqrt{3}$, consistent with the obvious pseudo-hexagonal character of the bc plane.

In these particulars the structure is analogous with an earlier schematic

TABLE 1. CHEMICAL ANALYSIS OF LITTLE COTTONWOOD SEPIOLITE

	Weight Per cent	Relative mol. populations	
SiO_2	52.97	12.00	
MgO	22.50	7.62	
Al_2O_3	0.86	.23	
Fe_2O_3	0.70	.12	8.67
Mn_2O_3	3.14	.55	
CuO	0.87	.15	
H_2O^+	9.90	7.50	
H_2O^-	8.80	6.64	
Total	99.74		

Additional spectrographically determined components: CaO: 0.14; K_2O: 0.17; BaO: 0.024; P_2O_5: 0.1; others: 0.01.

Idealized empirical formula: $12SiO_2$, 8–9 octahedral metal oxides, $14H_2O$.

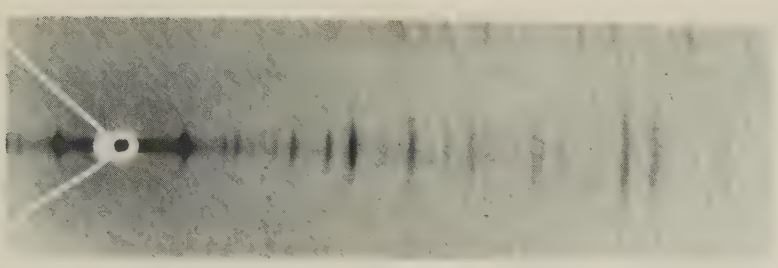

FIG. 2. The zero layer line of a sepiolite fiber x-ray diffraction diagram. Filtered Cu radiation. Camera radius = 6.35 cm.

analysis of the related mineral attapulgite, described by Bradley (1940). A projection of a model was therefore arranged, using centered amphibole-like chains of one and one half times the b dimension of chains found for attapulgite, and the zero layer diffraction effects were synthesized for the chemical components of a typical analysis distributed in accordance with the model. It is interesting to note one of the differences that exists between the attapulgite and sepiolite models. In the former one the chains are amphibole-type chains composed of two pyroxene-type chains. In the sepiolite model, however, the chains contain *three* instead of two pyroxene chain components; therefore, they are basically not amphibole-like in character but rather they represent a new silicate structure type.

Figure 2 is a reproduction of the zero layer diffraction effects of a Little Cottonwood sepiolite fiber. Figure 3 illustrates the proposed idealized structure with the angular plane coordinates indicated along the margins.

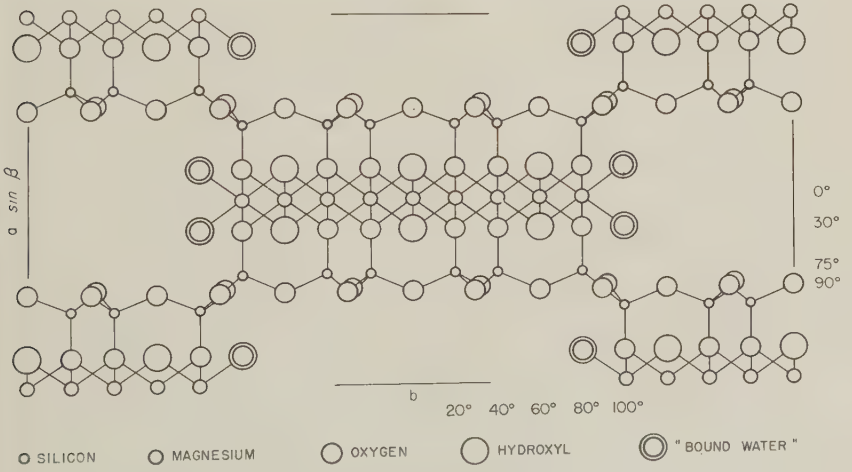

FIG. 3. Idealized proposed structure for sepiolite projected onto 001.

The ideal density is 2.2, comparing favorably with determined values ranging from 2.0 to 2.1. In Table 2 are assembled the calculated F factors for all possible reflections out to about 1.5 Å; a few additional entries for smaller periodicities are also included in order to match observed values below the 1.5 Å limit. In the table each entry on the left side of the columns is for the skeleton alone; a second entry at the right side of the columns includes the water allowance, and it refers to those small-angle reflections near a^* and b^* for which water contribution could be fairly estimated. For these F values octahedral ion occupants were taken as 8/9 Mg in view of the apparent octahedral deficiency which will be discussed later. The largest apparent departures between calculated and observed entries are concentrated systematically about the $b=6$, 12 and 18 levels, and are attributable to the arbitrary use of exact submultiples of the cell parameters as coordinates. In Table 3 the estimated observed, relative intensities are compared with the calculated intensities derived from Table 2; the calculated intensities include multiplicity, polarization and Lorentz corrections.

The general quality of the agreement is such that the gross features of the structure can be viewed with some confidence. The large number of coincident reflections, the large number of ions, mostly in general positions and the analytical uncertainties of actual chemical composition of any specific fiber seem to render pointless any attempts at further refinements.

Speculative aspects of the crystal chemistry can be outlined as follows: the scheme (per half cell) provides sites for twelve tetrahedral ions, nine octahedral ions, forty articulated oxygens and hydroxyls and room for about six molecules of low temperature water. Ideal occupation of tetrahedral sites by silicon and the octahedral ones by magnesium would lead to the formula $H_4Mg_9Si_{12}O_{30}(OH)_{10}\cdot 6H_2O$. It can be assumed that the four "extra" protons are associated with the edges of the brucite ribbons, indicated in Fig. 3 as OH_2 or "bound water." The chemical analyses indicate that fewer than nine octahedral sites are actually occupied, especially if allowance is made for aluminum ions in tetrahedral positions, for the uncertainty of the actual valence state of the minor constituents and for the possibility that the minor constituents may actually be accessory. Neutrality is maintained by the presence of sufficient additional protons and/or exchange ions to balance any residual charge deficiency. A practical rationalization of the formula is therefore written as $H_6Mg_8Si_{12}O_{30}(OH)_{10}\cdot 6H_2O$. This formula allows for water of four separate bonding energies; namely, (1) molecular water; (2) water bound on brucite ribbon edges; (3) hydroxyls analogous with those of various layer mineral structures; and (4) balancing protons

TABLE 2. CALCULATED *hk*0 STRUCTURE FACTORS PER ¼ CELL FOR THE IDEALIZED SEPIOLITE MODEL

b \ a	0	1	2	3	4	5	6	7	8	9	10	11	12
0			−43 −21		+95 +110		−75 −65		+24		+50		+36
1		+80 +65		− 2 −14		+31 +25		−34		+39		+20	
2	− 15		− 7		+ 6		+10		+ 4		− 3		− 5
3		−21 −14		− 2		−12		+ 5		−11		− 5	
4	+ 11		+ 6		− 5		− 8		− 3		+ 2		+ 4
5		+ 3 −11		+11		0		+12		0		+ 4	
6	− 61 −45		+42 +47		−30		+20		+ 2		− 8		+ 7
7		− 9 −15		+17		−36		+17		−18		+ 4	
8	+ 2		+ 1		− 1		− 2		− 1		0		+ 1
9		+ 4		− 9		+25		− 7		+13		− 1	
10	+ 2		+ 1		− 1		− 2		− 1		0		+ 1
11		− 8		+16		−32		+16		−17		+ 3	
12	+ 16		−26		+33		−34		+47		−41		+33
13		+ 2		+ 9		0		+ 9		0			
14	+ 7		+ 4		− 3		− 6						
15		−13		− 1		−10							
16	− 8		− 4		+ 3		+ 6						
17		+46		0		+27							
18	+104		+20		+20		+ 2						
19		+39											

TABLE 3. SUMMARY OF CALCULATED RELATIVE INTENSITIES FOR THE SEPIOLITE FIBER DIAGRAM IN THE ZERO LEVEL

Indices	d in Å	$nF^2\phi(\theta)\times10^{-3}$	Estimated relative intensity in the fiber diagram
020	13.5	3.8	m
110	12.0	128.0	sss
130	7.5	3.7	m-w
040	6.7	.3	w
200		3.7	
220	6.0	.8	ww
150	5.0	1.5	w
240	4.75	.4	ww
060	4.50	11.2	m
310	4.40	2.1	w
330	4.00	.2	?
260	3.73	20.0	s
170	3.71	2.0	
350	3.45	1.0	w
080	3.35	.02	ss
400		48.0	
420	3.25	.3	?
440	3.00	.2	ww
370	2.93	2.0	w
190		.1	
460	2.69	5.6	s
510	2.68	3.9	
530	2.56	.8	w
2,10,0	2.50	.01	ww
390		.5	
550	2.40	.0	w
1,11,0	2.39	.4	
0,12,0	2.25	.6	m
600	2.24	10.0	
620	2.21	.5	m
570		6.2	
3,11,0	2.15	1.2	
2,12,0	2.13	3.1	w
640	2.12	.3	
1,13,0	2.05	.02	
660	2.00	1.7	ww
590		2.6	
710	1.91	4.5	w
3,13,0	1.88	.3	
730	1.87	.05	w
680		—	
4,12,0		4.2	
5,11,0	1.81	3.6	w
750	1.80	.5	

TABLE 3—(*continued*)

Indices	d in Å	$nF^2\phi(\theta)\times10^{-3}$	Estimated relative intensity in the fiber diagram
1,15,0	1.78	.6	ww
6,10,0	1.73	.01	ww
770	1.71	1.0	ww
800	1.68	1.0	ww
840	1.63	.03	ww
790	1.61	.1	ww
6,12,0	1.58	3.5	s
1,17,0	1.57	6.3	
0,18,0	1.50	15.0	m-s
8,8,0		.0	
910	1.48	3.9	w
1,19,0	1.41	3.7	w
970	1.385	.8	
4,18,0	1.375	1.0	m
5,17,0	1.365	1.8	
8,12,0	1.345	5.3	m
10,0,0	1.34	3.0	
10,12,0	1.15	3.4	w
12,0,0	1.12	1.3	w
12,12,0	1.00	2.3	m

analogous with exchange ions. These categories are in the ratio of 6:4:3:1, and with some tolerance they can be regarded to be not in serious conflict with the results of the weight loss studies reported by Migeon and Caillere.

It is to be noted that oxygen ions at $\frac{1}{4}$, $\frac{1}{4}$, z, etc. positions which join chains in this structural scheme are double links as compared with the single link oxygen of the attapulgus. It is quite possible that both structures are actually alike, and that an improper choice of model was made in one case or the other. If the difference is real, however, it can be speculated that this is the factor which renders the sepiolite II modification, described by Longchambon, more stable than the comparable high temperature modification of attapulgite.

The entire structure could be either orthorombic or monoclinic. It seems more probable that it belongs to the space group $C\ 2/m$.

Dr. A. F. Moodie of C.S.I.R.O., Melbourne, Australia, and Drs. G. W. Brindley and W. R. Büssem of the Pennsylvania State University, State College, Pennsylvania, took active interest in this investigation; this is hereby gratefully acknowledged.

References

1. Bradley, W. F. (1940), The structural scheme of attapulgite: *Am. Mineral.*, **25**, 405–410.
2. Caillere, S. (1951), Sepiolite, *X*-ray Identification and Structures of Clay Minerals, Chapter VIII, 224–233, Taylor and Francis, London.
3. Longchambon, H. (1937), Sur certaines characteristiques de la sepiolite D'Ampandrandava: *Bull. Soc. Franc. Min.*, **60**, 232–276.
4. Migeon, G. (1936), Contribution a l'etude de la definition des sepiolites: *Bull. Soc. Franc. Min.*, **59**, 6–133.

Manuscript received July 30, 1954.

CRYSTALLOGRAPHY OF MONOCALCIUM AND DICALCIUM PHOSPHATES

James P. Smith, James R. Lehr, and Walter E. Brown,
Division of Chemical Development, Tennessee Valley Authority, Wilson Dam, Ala.

Abstract

Optics and lattice constants are reported for three triclinic calcium orthophosphates. The lattice constants are: anhydrous monocalcium phosphate, $Ca(H_2PO_4)_2$, $a=5.55$ Å, $b=7.60$ Å, $c=9.07$ Å, $\alpha=121°\ 54'$, $\beta=108°\ 48'$, $\gamma=87°\ 28'$; monocalcium phosphate monohydrate, $Ca(H_2PO_4)_2\cdot H_2O$, $a=5.67$ Å, $b=11.92$ Å, $c=6.51$ Å, $\alpha=99°\ 50'$, $\beta=118°\ 31'$, $\gamma=83°\ 9'$; and anhydrous dicalcium phosphate, $CaHPO_4$, $a=6.91$ Å, $b=6.66$ Å, $c=7.02$ Å, $\alpha=96°\ 7'$, $\beta=103°\ 53'$, $\gamma=89°\ 11'$. A structural similarity between monocalcium phosphate monohydrate and dicalcium phosphate dihydrate is postulated.

Introduction

Primary and secondary calcium orthophosphates are major components of most of the phosphate fertilizer used in the world and are present also in other products of the chemical industry. The primary or monocalcium salt occurs in the anhydrous form, $Ca(H_2PO_4)_2$, and as the monohydrate, $Ca(H_2PO_4)_2\cdot H_2O$. The secondary or dicalcium salt occurs in anhydrous form, $CaHPO_4$, and as the dihydrate, $CaHPO_4\cdot 2H_2O$. Both forms of the dicalcium salt are found as natural minerals—the anhydrous form as monetite and the hydrate as brushite.

X-ray studies of single crystals have been reported for only one of these crystalline calcium phosphates. Hill and Hendricks (1936) and Terpstra (1937) predicted from their *x*-ray study of single crystals that dicalcium phosphate dihydrate would be found essentially isostructural with gypsum—a prediction confirmed recently by Beevers and Raistrick (1954). *X*-ray powder diffraction patterns and refractive indices of the mono- and dicalcium phosphates were reported by Hill and Hendricks (1936) and by Bale *et al.* (1945). Haushofer (1883) and Schulten (1904) reported axial ratios and interaxial angles of monocalcium phosphate monohydrate and anhydrous dicalcium phosphate from goniometric measurements.

The results of *x*-ray measurements on single crystals of monocalcium phosphate—anhydrous and monohydrated—and of anhydrous dicalcium phosphate are presented here. The optical properties of the three compounds also are covered more completely than has been done heretofore.

Optical and *X*-ray Examinations

The crystals were synthetic. Their refractive indices were measured at 25° C. with calibrated oils and Corning filters. Optic angle 2V was computed from the refractive indices.

The x-ray photographs were made with a Weissenberg camera 57.3 mm. in diameter and with copper K_α radiation ($\lambda = 1.54$ Å). To the extent possible, the reciprocal angles were determined by the method of triangulation (Buerger, 1942). The axial lengths were determined to within ± 0.2 per cent and the angles to within $\pm 0.3°$.

Single-crystal x-ray data and some of the optical data for the three compounds are shown in Table 1. Several additional points about the crystallography of each compound are given in the text. The optical descriptions are in terms of the axes selected from x-ray measurements.

TABLE 1. OPTICAL AND SINGLE-CRYSTAL X-RAY DATA FOR ANHYDROUS MONOCALCIUM PHOSPHATE, MONOCALCIUM PHOSPHATE MONOHYDRATE, AND ANHYDROUS DICALCIUM PHOSPHATE

	$Ca(H_2PO_4)_2$	$Ca(H_2PO_4)_2 \cdot H_2O$	$CaHPO_4$
Symmetry	Triclinic, pinacoidal	Triclinic, pinacoidal	Triclinic, pinacoidal
Refractive indices:			
425 mμ N_α	1.543	1.492	1.586
425 mμ N_β	1.567	1.512	1.613
425 mμ N_γ	1.596	1.526	1.635
610 mμ N_α	1.548	1.496	1.588
610 mμ N_β	1.572	1.515	1.616
610 mμ N_γ	1.602	1.529	1.640
Birefringence (610 mμ)	.054	.033	.052
Optic sign	Biaxial (+)	Biaxial (−)	Biaxial (−)
Optic angle 2V (610 mμ)	85° 14′	81° 30′	84° 4′
Dispersion	$r<v$, very weak	$r>v$, very weak	$r>v$, weak
Cleavage	None observed	(100) imperfect (001) imperfect	None observed
Space group	$P\bar{1}$ or $P1$	$P\bar{1}$ or $P1$	$P\bar{1}$ or $P1$
a	5.55 Å	5.67 Å	6.91 Å
b	7.60	11.92	6.66
c	9.07	6.51	7.02
α	121° 54′	99° 50′	96° 7′
β	108 °48′	118° 31′	103° 53′
γ	87° 28′	83° 9′	89° 11′
Cell contents	$2[Ca(H_2PO_4)_2]$	$2[Ca(H_2PO_4)_2 \cdot H_2O]$	$4[CaHPO_4]$
Density- calc.	2.55	2.19	2.89
obs.[a]	2.546	2.22	2.89_2

[a] Bassett (1908).

Anhydrous Monocalcium Phosphate

This salt crystallizes as colorless triclinic rods that are elongated parallel to the a-axis and as elongated tablets with $(01\bar{1})$, and sometimes (010), as the tabular face. Twinning was not observed.

The N_α–N_β plane is perpendicular to (010) and essentially parallel to the a-axis, with N_β (the optic normal) inclined to (010) by 15° in obtuse γ.

The x-ray data in Table 1 are based upon rotation photographs and Weissenberg photographs (zero, first, and second layers) for the three primitive axial directions. The interaxial angles measured microscopically are in satisfactory agreement with those given in Table 1.

In a moist atmosphere the anhydrous crystal alters slowly to randomly oriented crystallites of the monohydrate. This observation and the apparently unrelated unit-cell dimensions of the two crystals indicate an absence of structural similarity.

Monocalcium Phosphate Monohydrate

This salt crystallizes as colorless triclinic (010) plates that are elongated parallel to the c-axis. Polysynthetic twinning according to the albite law is common, with (010) as the composition plane. Contact twinning on (001) with a as the twin axis, sometimes seen as penetration forms, is less common.

The obtuse bisectrix, N_γ, is parallel to (010) and is inclined to the a-axis by 2° 40′ in acute β. The N_α–N_β plane is perpendicular to (010), with N_α inclined to (010) by 37° in obtuse α.

The lattice constants shown in Table 1 are based upon a rotation photograph and Weissenberg photographs (zero, first, second, and composite zero-second layers) from a c-axis setting. The tabulated values agree with those determined from a rotation pattern and a zero-layer Weissenberg photograph from an a-axis setting.

Haushofer (1883) reported the following interaxial angles and axial ratios for monocalcium phosphate monohydrate: $\alpha = 98° 40'$, $\beta = 118° 21'$, $\gamma = 83° 16'$, $a:b:c = 0.4753:1:0.5448$. With the exception of the value for α, agreement with the x-ray values in Table 1 is good. The x-ray value for α was obtained from two different settings and is considered reliable.

Several of the crystals that were examined by the Weissenberg technique were twinned, and their reciprocal lattices proved that the twins were of the albite type.

A determination of the crystal structure may not be too difficult. If the usual dimensions of the phosphate ion are assumed and the positions of the hydrogens are ignored, a maximum of 18 parameters must be determined to specify the positions of the phosphate ions, calcium ions, and water molecules. The dimensions of the unit cell in the a and c

directions are relatively small, and most of the atoms therefore will be resolved clearly in Fourier projections. The weak intensities of the $0k0$ reflections for odd values of k suggest pseudosymmetry—a twofold screw axis or a layer-type structure with the layers perpendicular to b and with two similar but not identical layers for each unit cell. Monocalcium phosphate monohydrate, dicalcium phosphate dihydrate, and gypsum have very similar lattice constants a, c, and β, as shown in Table 2. Haushofer (1883) also recognized a similarity between morphological elements of the two phosphates.

The structure of gypsum is known to comprise alternate layers of calcium sulfate and water molecules (Wooster, 1936). The a and c

Table 2. Comparison of the Lattice Constants of Monocalcium Phosphate Monohydrate, Dicalcium Phosphate Dihydrate, and Calcium Sulfate Dihydrate

Lattice Constant	$Ca(H_2PO_4)_2 \cdot H_2O$	$CaHPO_4 \cdot 2H_2O$[a]	$CaSO_4 \cdot 2H_2O$[b]
a	5.67 Å	5.812 Å	5.67 Å
b	11.92	15.180	15.15
c	6.51	6.239	6.51
β	118° 31′	116° 25′	118° 23′

[a] Beevers and Raistrick (1954).
[b] Simple alternative cell suggested by Bragg (1937).

directions of gypsum lie parallel to the plane of the calcium sulfate layers. The structure of monocalcium phosphate monohydrate apparently comprises similar layers—the shorter b resulting from an absence of two layers of water molecules. The stacking of the layers presumably results in a slight lateral displacement that shifts angles α and γ from 90°. The analogy may be extended to the striking similarity in the twinning of the two compounds. Both form contact twins with a as the twin axis. Gypsum does not form albite twins, because the twinning axis corresponds to one of its symmetry axes.

The similarities in crystallographic properties suggested a study of the overgrowth of the phosphate on gypsum. The phosphate was crystallized upon suspended blanks of gypsum that were cleaved along (010) from selected selenite stock. Thick, oriented overgrowths formed over large areas of the (010) faces of the gypsum. The overgrowths were predominantly of a type with the a and c axes of the two crystals parallel, and thus the (010) could be a composition plane. The relation of some of the

overgrowths to the substrate was analogous to the contact twinning exhibited by both compounds.

The confirmation of a close structural relation between the phosphate and gypsum would facilitate greatly a determination of the structure of the phosphate. Speculation on the basis of this structural analogy leads to a possibility that in monocalcium phosphate monohydrate the water of hydration occupies positions similar to the calcium sites, instead of the water sites, of gypsum—also that the phosphate structure comprises alternate layers with the respective compositions $CaHPO_4$ and $H_3PO_4 \cdot H_2O$.

Anhydrous Dicalcium Phosphate

This salt crystallizes as colorless triclinic (010) tablets that are elongated parallel to the *a*-axis. Prismatic and rod habits also occur. The crystals are brittle with hackly fracture. Twinning was not observed.

The acute bisectrix, N_α, is oriented nearly perpendicular to $(11\bar{1})$ and is inclined 52° to the normal to (010). The trace of the optic plane on $(11\bar{1})$ is inclined to the trace of (010) by 32° in obtuse γ. The extinction angles on the (010) are 15° with the (101) trace and 38° with the $(01\bar{1})$ trace. When the crystal is lying on (010), a slight tilt in the direction of the fast component changes the extinction angle from 15° through the 23°-value reported by Hill and Hendricks (1936).

The *x*-ray data shown for this salt in Table 1 are based upon rotation and zero-layer Weissenberg photographs obtained from the three axes of the primitive cell. In addition, first- and second-layer Weissenberg photographs were obtained from the *c*-axis rotation. The *x*-ray data are brought into satisfactory agreement with Schulten's (1904) goniometric study of natural monetite through a transformation involving an assumption that the cell reported by him is *b*-centered with a *b*-axis twice that of the primitive cell. The comparison is shown in Table 3.

Hill and Hendricks (1936) noted a similarity between the powder patterns of anhydrous dicalcium phosphate and the orthorhombic anhydrous calcium sulfate (anhydrite). An additional similarity is evident from a comparison of the axial lengths:

	a	*b*	*c*
$CaHPO_4$	6.91 Å	6.66 Å	7.02 Å
$CaSO_4$	6.96	6.22	6.97

The similarity does not extend, however, to the axial angles. Although the general features of coordination in the two compounds may prove to be the same, considerable differences in structural details likely will be found.

Table 3. Comparison of Lattice Constants of Anhydrous Dicalcium Phosphate as Determined from Morphology and from *X*-ray Measurements

Lattice Constant	Schulten Cell	Transformed *X*-ray Cell
$a:b:c$	0.647:1:0.824	0.645:1:0.824
α	84° 57′	85° 35′
β	90° 17′	90° 56′
γ	94° 22′	94° 20′

Quality of Synthetic Materials

The chemical compositions of the synthetic crystals are compared with the theoretical compositions in Table 4. With the exception of liquid inclusions of negligible volume in the crystals of anhydrous monocalcium phosphate, extraneous phases were not detected in microscopic examinations.

Anhydrous monocalcium phosphate was crystallized over a 4-day period at 130° C. from a filtered solution that was prepared by dissolving 500 grams of recrystallized monocalcium phosphate monohydrate in 2000 ml. of an 81.5 per cent solution of phosphoric acid at the boiling point. The crystals were washed free of acid with anhydrous acetone on a heated funnel. They were oven-dried for 3 hours at 85° C. and then vacuum-dried for 4 days over anhydrous magnesium perchlorate.

Monocalcium phosphate monohydrate was thrice recrystallized from a 50 per cent solution of phosphoric acid. The final crystallization was done with slow cooling and constant stirring. The crystals were washed with acetone and vacuum-dried.

Anhydrous dicalcium phosphate was crystallized by slow interdiffusion of calcium nitrate and ammonium phosphate through a barrier of nitric acid at pH 3. Prepared from recrystallized reagents, the reactant solutions were 20 per cent $Ca(NO_3)_2 \cdot 4H_2O$ (adjusted to pH 3 with nitric

Table 4. Chemical Composition of Synthetic Crystals

	CaO, per cent		P_2O_5, per cent	
	Found	Theoretical	Found	Theoretical
$Ca(H_2PO_4)_2$	23.92[a]	23.96	60.63[a]	60.65
$Ca(H_2PO_4)_2 \cdot H_2O$	22.38[b]	22.24	56.24[b]	56.31
$CaHPO_4$	41.22[a]	41.21	52.14[a]	52.16

[a] Average of four determinations.

[b] Average of three determinations.

acid) and 20 per cent $NH_4H_2PO_4$. After 43 days of diffusion at 83° C. the resultant crystals were washed with hot water and then with acetone. They were dried at 105° C. for 72 hours. A chemical analysis showed an absence of nitrogen. The only significant impurity found in a spectrographic analysis was 0.03 per cent silica.

Acknowledgments

W. E. Cate and Z. T. Wakefield prepared the synthetic crystals. Inez J. Murphy and B. B. Luff made the chemical analyses and Frances M. Youngblood the spectrographic analyses.

References

Bale, W. F., Bonner, J. F., Hodge, H. C., Adler, H., Wreath, A. R., and Bell, R. (1945), *Ind. Eng. Chem., Anal. Ed.*, **17**, 491–495.

Bassett, H., Jr. (1908), *Zeit. anorg. Chem.*, **59**, 1–55.

Beevers, C. A., and Raistrick, B. (1954), *Nature*, **173**, 542–543.

Bragg, W. L., (1937), Atomic Structure of Minerals, p. 129–31, Ithaca, Cornell Univ. Press.

Buerger, M. J. (1942), *X*-Ray Crystallography, New York, John Wiley and Sons.

Haushofer, K. (1883), *Zeit. Kryst.*, **7**, 265, reported in Groth, P. (1908), Chemische Krystallographie, Vol. 2, Leipzig, Wilhelm Engelmann.

Hill, W. L., and Hendricks, S. B. (1936), *Ind. Eng. Chem.*, **28**, 440–447.

Johannsen, A. (1918), Manual of Petrographic Methods, 2nd ed., New York, McGraw-Hill.

Schulten, A. de (1904), *Bull. soc. franc. mineral.*, **27**, 120, reported in Groth, P. (1908), Chemische Krystallographie, Vol. 2, Leipzig, Wilhelm Engelmann.

Terpstra, P. (1937), *Zeit. Krist.*, **97**, 229–233.

Wooster, W. A. (1936), *Zeit. Krist.*, **94**, 375–396.

Manuscript received Sept. 3, 1954

BULTFONTEINITE FROM CRESTMORE, CALIFORNIA

JOSEPH MURDOCH, *University of California at Los Angeles, Los Angeles, California.*

ABSTRACT

The rare mineral bultfonteinite has been found in the contact zone at Crestmore, California, in association with afwillite and scawtite. It occurs with these as microscopic, twinned individuals, much finer grained than the enclosing minerals. Optical and microchemical observations indicated that it is bultfonteinite, and this is confirmed by *x*-ray powder pattern, which matches that of the type material. This is the first locality for this mineral outside of South Africa The powder pattern shows the following spacings and intensities for the strongest lines: 8.16 Å-7; 3.51 Å-5; 3.46 Å-5; 2.92 Å-10; 2.885 Å-10; —1.93 Å-10.

X-ray measurements on a crystal sliver from the type locality give cell-dimensions and angles as follows:

$a_0=8.34$ Å	$b_0=11.18$ Å	$c_0=5.68$ Å
$\lambda=88°\ 24'$	$\mu=86°\ 06'$	$\nu=90°\ 00'$

These agree very closely with morphological measurements by Wright, provided his *a* and *b* axes are exchanged, and the value for the new *b* axis is doubled. The transformation formula, Wright to Murdoch is 010/200/001.

The rare mineral Bultfonteinite was discovered about 1903 or 1904 in the Bultfontein mine, in the Kimberley District, South Africa. Several years later it appeared in the Dutoitspan mine in the same district, and shortly before 1932 it was found also at the Jagersfontein mine in the Orange River Colony, some hundred miles southeast of Kimberley. When first collected, it was thought to be natrolite, but was later recognized by A. F. Williams as a new mineral, and as such described by Parry, Williams, and Wright (1932). It is a hydrous, fluorine-bearing calcium silicate, close to $11Ca(OH, F)_2 \cdot 5SiO_2$ in composition, and quite similar in many properties to afwillite. The new mineral was originally called dutoitspanite, Williams (1932, p. 171), but later changed to bultfonteinite.

On examining some specimens of massive afwillite, and later also of scawtite, from the 910′ level of the Commercial quarry at Crestmore, California, the writer observed some patches and stringers of a fine-grained, sugary-textured material in the coarser matrix. This suggested a different mineral, and microscopic examination showed these areas to be composed of a granular aggregate of stout prismatic grains showing multiple twinning like that of a plagioclase. Selected material showed them to be biaxial positive with 2V near 70° and with a beta index close to 1.59. Grains with sharply defined twin lamellae showed a symmetrical extinction angle of 27–28°. Microchemical tests gave CaO, SiO_2, H_2O and F. Leaching with water produced an alkaline solution. These properties correspond with those of bultfonteinite, which is easily dis-

tinguished from the optically similar custerite by the extinction angle, which in the latter is only about 6° (Tilley 1928), and from afwillite which does not have multiple twinning. Incidentally, the fluorine noted by Switzer and Bailey (1954) in their analysis of afwillite from Crestmore, was probably due to the unsuspected presence of bultfonteinite, since there is no practical difference, other than grain size, in appearance between the two minerals.

A thin section of one massive afwillite-bultfonteinite vein showed that the latter mineral occurs as an irregular stringer roughly along the center line of the vein, in part replacing afwillite. This relationship is shown in the photomicrograph (Fig. 1), taken with crossed nicols.

X-Ray Study

A good *x*-ray powder photograph was obtained from the Crestmore material, showing a distribution of spacing and intensities which matched no published pattern. Fortunately, through the kindness of Professor C. E. Tilley of Cambridge University, a little of the type mineral from South Africa was made available, and a reference pattern recorded. The two patterns showed a close correspondence, with the exception of a few lines in the Crestmore film which could be accounted for by the presence of a small amount of calcite impurity in the sample. All bultfonteinite lines down to a spacing of 2.45 Å have been readily indexed, using the unit cell data given below. Table 1 lists the powder data, using the average of several Crestmore specimens, and compared with the type material.

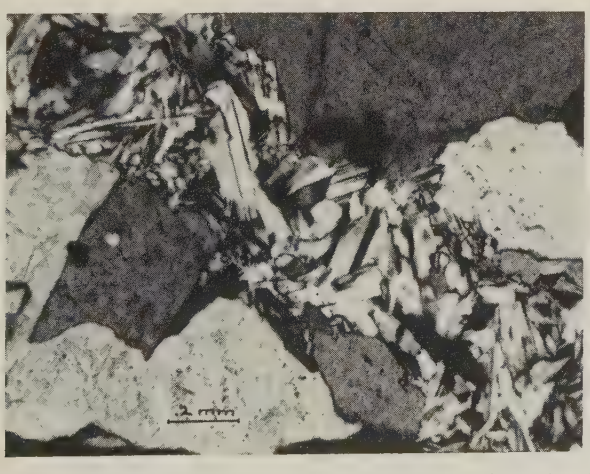

Fig. 1. Vein of bultfonteinite in afwillite. Magnification shown by .2 mm. scale. Crossed nicols, showing multiple twinning.

TABLE 1. X-RAY POWDER DATA FOR BULTFONTEINITE, IRON RADIATION, MANGANESE FILTER, IN ANGSTROM UNITS. $FeK_\alpha = 1.9373$

Crestmore		South Africa			
d/n measured	*I*	*d/n* measured	*I*	*d/n* calcul.	*hkl*
10.29	½			11.18	010
8.16	7	8.12	6	8.33	100
6.53	3	6.51	2	6.71	110
5.46	3	5.47	2	5.59	020
				4.16	200
4.065	3	4.06	4	4.14	111
3.98	½	3.95	½	4.02	02̄1
3.83	½			3.89	021
3.65	½	3.636	½	3.69	1̄21
3.59	½	3.60	½	3.615	1̄21
3.51	5	3.50	4	3.48	121
3.46	5	3.44	4	3.44	2̄01
				3.40	130
3.35	½	3.33	½	3.34	220
				3.337	2̄11
3.27	½	3.26	½	3.268	2̄11
				3.244	201
3.11	½			3.111	21̄1
2.92	10	2.92	6	2.958	2̄1̄1
2.885	10	2.88	6	2.913	2̄21
2.825	4	2.825	2	2.834	22̄1
2.78	4	2.77	4	2.785	2̄21
				2.775	300
2.75	3	2.743	3	2.757	01̄2
2.72	½	2.72	2	2.718	012
2.625	½	2.634	½	2.637	140, 1̄12
2.48	½			2.467	041
2.45	½			2.441	231
2.355	½	2.36	½		
2.34	½	2.333	½		
2.28	½	2.272	½		
2.21	1				
2.19	½	2.195	3		
2.12	3				
2.093	2	2.118	4		
2.037	4	2.037	5		
1.99	3	1.988	2		
1.956	½	1.953	½		
1.93	8	1.93	10		
1.91	½	1.912	½		
1.89	1	1.887	½		
1.855	½	1.847	½		
1.73	1	1.751	½		
		1.729	½		
1.714	3	1.709	5		
1.687	½	1.686	½		
1.667	1	1.665	½		
1.63	1	1.638	3		
		1.614	½		
1.60	1	1.60	½		
1.54	½	1.541	½		
1.48	2	1.487	2		
1.426	2	1.413	2		
1.375	½	1.371	1		
1.35	2	1.348	2		
1.31	½	1.306	1		
1.07	½	1.074	1		

TABLE 2. BULTFONTEINITE
ANGLE TABLE

Triclinic; Pinacoidal $\bar{1}$. $a:b:c=0.7461:1:0.5078$, $\alpha=91°36'$, $\beta=93°53'$, $\gamma=89°54\frac{1}{2}'$, $p_0:q_0:r_0=0.6805:0.5067:1$. $\lambda=88°24'$, $\mu=86°06'$, $\nu=90°00'$, $p_0'=0.6823$, $q_0'=0.5081$, $x_0'=0.06815$, $y_0'=0.0280$.

Forms			ϕ	ρ	A	B	C
Old		New					
001	c	001	67°40′	4°13′	86°06′	88°24′	0°00′
100	b	010	0 00	90 00	90 00	0 00	88 24
010	a	100	90 00	90 00	0 00	90 00	86 06
210		140	18 34½	90 00	71 25½	18 34½	87 14½
110		120	33 53	90 00	56 07	33 53	86 29½
120	m	110	53 20	90 00	36 40	53 20	85 55
$1\bar{4}0$		$2\bar{1}0$	110 25	90 00	20 25	110 25	86 54½
$1\bar{2}0$	M	$1\bar{1}0$	126 40	90 00	36 40	126 40	87 55
$1\bar{1}0$		$1\bar{2}0$	146 07	90 00	56 07	146 07	88 09
$2\bar{1}0$		$1\bar{4}0$	161 25½	90 00	71 25½	161 25½	89 44
102	w	011	7 15	28 23	86 33½	61 52	26 32
101		021	3 42	46 34	87 19	43 33	44 51
$\bar{1}02$	W	$0\bar{1}1$	171 55	25 52	86 29	115 35½	25 08
$\bar{1}01$		$0\bar{2}1$	176 05½	45 00½	87 14½	134 52	46 28½
011	e	101	87 52	36 55	53 06½	88 43	33 00
$0\bar{1}1$	E	$\bar{1}01$	−87 23	31 35	121 33	88 38	35 26
112		122	37 22	34 00	70 10	63 37	30 25½
211		141	20 01	65 29	71 51	31 15	62 41
111		121	35 42½	52 07½	62 33	50 08	48 35
$\bar{1}11$		$1\bar{2}1$	142 47	51 08	61 44	128 19	50 10
$1\bar{1}1$		$\bar{1}21$	−30 28	50 27½	113 01	48 20½	51 11
$\bar{1}\bar{1}1$		$\bar{1}2\bar{1}$	−148 08	49 19	113 36	130 06	52 46

Transformation formula: Parry, Williams, Wright to Murdoch 010/200/001.

None of the Crestmore mineral was other than microscopic in grain size, but the type specimen from Professor Tilley was in the form of coarsely crystalline prismatic fragments. From these it was possible to select a relatively simple appearing sliver, which could be rather readily oriented on the c-axis, and since no x-ray determinative work had been done on the mineral, it was decided to see whether a satisfactory cell-determination could be made. Accordingly, a rotation photograph, and equator, first and second layer-line pictures, all about the prism-axis, were taken with filtered copper radiation.

These pictures were successful, and the reciprocal lattice plotted from the layer-lines showed a consistent pattern which appeared to be monoclinic. However, since Wright's optical study showed the mineral to be triclinic, this must be pseudomonoclinic, with $V=90°$ (within the limits of measurement). Twinning on both (100) and (010), is shown by the

presence of quadruplicate points on the plot, matching those shown by Wright (1932, p. 154), in the gnomonic projection of forms.

Cell dimensions, measured on the rotation picture for c_0, and calculated from the layer line pictures for a_0 and b_0, are as follows: $a_0 = 8.34$ Å, $b_0 = 11.18$ Å, $c_0 = 5.68$ Å, which reduce to an axial ratio of 0.7461 : 1 : 0.5078.

On comparing this ratio with the morphological data it is seen that agreement is very close, if Wright's a and b axes are exchanged and the new b axis taken at twice his value.

Parry, Williams & Wright original:	0.6756:1:0.6873
Parry, Williams & Wright re-valued:	0.7401:1:0.5087
Murdoch from x-ray:	0.7461:1:0.5078

The crystallographic work done on rather poorly terminated crystals, was remarkably accurate, and the newly chosen setting has been made on the basis of the x-ray findings, and to place the pole of (001) in the normally accepted triclinic position, i.e. forward and to the right of center in the gnomonic projection. The following Table 2 gives the revised crystallographic constants for the new position, the original forms, the new angles for reported forms, and the translation formula from old to new orientation.

The author wishes particularly to express his thanks to Professor C. E. Tilley, without whose kindness the measurements of cell dimensions and form would not have been possible.

References

Tilley, C. E. (1928), On a custerite-bearing contact rock from California: *Geol. Mag.*, **65**, 371–372.

Williams, A. F., (1932), The genesis of the diamond I, 352 pp. E. Benn, London.

Parry, J., Williams, A. F., and Wright, F. E., (1932), On bultfonteinite, a new fluorine-bearing hydrous calcium silicate from South Africa: *Mineral. Mag.*, **23**, 145–162.

Switzer, George, and Bailey, E. H. (1954), Afwillite from Crestmore, California: *Am. Mineral.*, **38**, 629–633.

Manuscript received Oct. 23, 1954

MURDOCHITE, A NEW COPPER LEAD OXIDE MINERAL*

Joseph J. Fahey, *U. S. Geological Survey, Washington 25, D. C.*

Abstract

Chemical analysis and *x*-ray structural studies (see following paper by C. L. Christ and J. R. Clark in this issue) establish as a new species a copper lead oxide from the Mammoth mine, Tiger, Ariz. The percentage composition, CuO 67.24, PbO_2 30.53, Fe_2O_3 0.17, SiO_2 0.05, and insoluble 1.11, yields the formula Cu_6PbO_8. The specific gravity is 6.47 at 4° C. The mineral forms in tiny lustrous black octahedra associated with wulfenite, dioptase, willemite, and fluorite.

The new mineral was found by Percy W. Porter, now deceased, of Cavecreek, Ariz., and at his request it is named in honor of Professor Joseph Murdoch of the University of California at Los Angeles.

Introduction

The new mineral, murdochite, described in this paper is an anhydrous oxide of copper and lead from the Mammoth mine, located at Tiger, Pinal County, Ariz. It has a composition that yields approximately the formula Cu_6PbO_8 and occurs as tiny black opaque octahedra, of which the largest is less than one millimeter in the longest dimension. The late Percy W. Porter, a mining engineer of Cavecreek, Ariz., collected this mineral with many others from the Mammoth mine. Spending approximately 300 hours and using a binocular microscope, he hand-picked the 401.5-mg. sample that he submitted for analysis.

Mr. Porter requested that if the mineral was found to be a new species it be named in honor of Professor Joseph Murdoch of the University of California at Los Angeles, in recognition of Professor Murdoch's many contributions to the science of mineralogy.

Locality and Associated Minerals

The Mammoth mine is about 46 miles northeast of Tucson. The deposit that was developed by this mine was discovered about 1880 and has been worked at various times for gold, molybdenum, and vanadium and more recently for lead, zinc, and silver in primary galena and sphalerite.

The tiny black octahedra of murdochite are found on the surface of and embedded within plates of wulfenite and on the surface of crystals of fluorite. Crystals of hemimorphite, willemite that fluoresces greenish-white, and quartz are also present.

Physical and Chemical Properties

The specific gravity of the sample of murdochite (401.5 mg) was found to be 6.47 as determined with a 5-ml fused-silica Adams-Johnston

* Publication authorized by the Director, U. S. Geological Survey.

pycnometer (see following article). The crystals have a hardness of 4 and give a black streak.

When the mineral was treated in a small beaker with cold (1+1)HNO_3, no reaction was noticed. Within one minute after the beaker was placed on the steam bath, a gas was evolved that continued coming off in good quantity until the mineral was dissolved. Owing to the paucity of sample, no quantitative measurement of the oxygen was made. Copper was determined electrolytically by deposition on a small platinum dish. Lead was weighed as $PbSO_4$.

Analysis and Formula of Murdochite

	Per cent
CuO	67.24
PbO_2	30.53
Fe_2O_3	0.17
SiO_2	0.05
Insol. in HNO_3	1.11
	99.10

Formula $Cu_{6.1}Pb_{0.9}O_{8.0}$.

The chemical analysis plus the structural analysis by Christ and Clark (1955) lead to the ideal formula Cu_6PbO_8.

A spectrographic report by K. J. Murata lists, in addition to the elements in the above analyses, Zn, Mn, As, Mo, and V each less than 0.1 per cent.

Acknowledgments

The author is indebted to Mr. Fred A. Hildebrand who took the first x-ray powder picture of the sample and suggested that it might be a new mineral.

Reference

Christ, C. L., and Clark, Joan R. (1955), The crystal structure of murdochite: *Am. Mineral.*, **40**, 907–916.

Manuscript received July 24, 1954

THE CRYSTAL STRUCTURE OF MURDOCHITE*

C. L. Christ and Joan R. Clark, *U. S. Geological Survey, Washington 25, D. C.*

Abstract

The crystal structure of the new mineral murdochite, Cu_6PbO_8, is shown to be of a new simple structure type. It is essentially a sodium chloride type with an ordered arrangement of the metal ions and vacant sites, and is the first crystal structure in which Cu^{++} is found to be octahedrally coordinated. The variable density found for murdochite and the occurrence of a second mineral of the same structure type, but with Pb > Cu, indicate a solid solution between Pb and Cu.

Introduction

Chemical analysis and *x*-ray structural studies have established as a new species a copper-lead oxide from Mammoth mine, Arizona. The new mineral has been named murdochite and is described by Fahey (see preceding article). Murdochite has a composition corresponding to the formula Cu_6PbO_8, and its structure is a simple new type that is essentially an ordered NaCl arrangement (Christ, Clark, and Fahey, 1953; Christ and Clark, 1954). A second example of this structure type, a synthetic compound Mg_6MnO_8, was discovered independently by Kasper and Prener (1954). A preliminary note on both these compounds has appeared (Kasper and Christ, 1953).

Crystal Structure Analysis

Preliminary investigations of murdochite were made through the use of Debye-Scherrer photographs. All reflections could be indexed for a cubic cell with $a_0 = 9.210 \pm 0.002$ Å, and systematic absences for *hkl* not all odd or all even were observed, indicating face centering. The special extinctions demanded by a spinel structure were not observed and this type of structure was therefore ruled out at the beginning of the analysis. *X*-ray powder data for murdochite are given in Table 1.

The length of the unit cell edge for murdochite is approximately twice, and the volume accordingly eight times, that expected for a simple NaCl structure. The data of the chemical analysis of Fahey (1955) yield the formula $Cu_{6.1}Pb_{0.93}O_{8.0}$, or ideally Cu_6PbO_8. These facts indicate that the structure of murdochite is based on a NaCl structure, with a unit cell containing 32 oxygen atoms in essentially close-packed arrangement and with the metal ions placed in the octahedral interstices, the doubling of the cell edge being accounted for by a special kind of ordering of the metal ions.

* Publication authorized by the Director, U. S. Geological Survey.

TABLE 1. *X*-RAY POWDER DATA FOR MURDOCHITE—Cu_6PbO_8
CUBIC $Fm3m$ (O_h^5); $a_0=9.210\pm0.002$ Å*

Measured†		*Calculated*	
Cu/Ni	$\lambda=1.5418$ Å		
I	d_{hkl}	d_{hkl}	*hkl*
10	5.30	5.318	111
7	4.59	4.605	200
8	3.25	3.257	220
8	2.776	2.777	311
10	2.659	2.659	222
9	2.303	2.303	400
9	2.109	2.113	331
7	2.059	2.059	420
5	1.880	1.880	422
7	1.772	1.773	511, 333
10	1.629	1.628	440
8	1.556	1.557	531
6	1.537	1.535	600, 442
4	1.457	1.456	620
4	1.404	1.405	533

Plus many additional lines.

* Lattice constant determined by the extrapolation method of Bradley and Jay (1932).

† Pattern corrected for shrinkage.

The postulated structure is appropriately described by the following crystallographic data:

4 Cu_6PbO_8 per unit cell
Space group: $Fm3m(O_h^5)$
Atomic parameters:

$(000; 0\frac{1}{2}\frac{1}{2}; \frac{1}{2}0\frac{1}{2}; \frac{1}{2}\frac{1}{2}0)+$
4Pb: (*a*) 000
8 O_I: (*c*) $\frac{1}{4}\frac{1}{4}\frac{1}{4}$; $\frac{3}{4}\frac{3}{4}\frac{3}{4}$
24 O_{II}: (*e*) x00; 0x0; 00x; $\bar{x}00$; $0\bar{x}0$; $00\bar{x}$; $x\fallingdotseq\frac{1}{4}$

The 24 Cu ions may alternatively be distributed over the 28 sites given by

4(*b*) $\frac{1}{2}\frac{1}{2}\frac{1}{2}$
24(*d*) $0\frac{1}{4}\frac{1}{4}$; $\frac{1}{4}0\frac{1}{4}$; $\frac{1}{4}\frac{1}{4}0$; $0\frac{1}{4}\frac{3}{4}$; $\frac{3}{4}0\frac{1}{4}$; $\frac{1}{4}\frac{3}{4}0$

or put into the 24(*d*) positions leaving four vacancies in the 4(*b*) positions. The model with the statistical distribution of Cu ions is designated the *disordered* structure, that with the ordered arrangement of Cu ions and holes, the *ordered* structure. Both models have been investigated.

Intensity measurements were first made by microphotometering Debye-Scherrer photographs. Although the agreement between the in-

tensities measured in this way and the intensities calculated from the postulated structure was sufficiently good to attest to the essential correctness of the structure, it was apparent that preferred orientation and particle size effects in the spindle sample were leading to poor data. Recourse was then made to single crystal patterns. Using a small crystal (ca. 0.2 mm. in largest dimension), multiple film Weissenberg patterns of the zero and second levels around [110] were prepared with Mo/Zr radiation. Intensities on these films were measured by comparing the densities of the reflections with those on a calibrated strip. The estimated intensities were converted to $|F_{hkl}|^2$ values through the use of the Lp chart of Cochran (1948). Structure factors, F_{hkl}, were calculated for both the disordered and the ordered structure models, setting the x parameter of the O_{II} atoms equal to $\frac{1}{4}$ in both cases. For these calculations the Hartree atomic scattering curve for $O^{=}$ was used for the oxygen atoms. For Pb^{++++} and Cu^{++}, scattering curves corresponding to the Thomas-Fermi values for Pb and Cu for $(\sin\theta)/\lambda \geqq 0.3$ A^{-1} and smoothed in to $f=78$ and $f=27$, respectively, for $(\sin\theta)/\lambda=0$ were used. All values of the scattering factors were taken from the International Tables (1935). An over-all temperature correction was made by multiplying the calculated structure factors by the modifying factor $\exp[-B(\sin^2\theta)/\lambda^2]$, according to the relationship $k|F_{obs.}| = |F_{calc.}| \exp[-B(\sin^2\theta)/\lambda^2]$, where k is a scaling constant. The values of k and B were found by plotting $\log(F_{calc.}/F_{obs.})$ *vs.* $(\sin^2\theta)/\lambda^2$, following the standard method of Wilson (1942). Corrections were not made for absorption effects in the crystal. The following expressions were used to calculate the structure factors:

I. h, k, l all odd

$F_{hkl}=4(f_{Pb}-6/7f_{Cu})$ *disordered* model

$F_{hkl}=4f_{Pb}$ *ordered* model

II. h, k, l all even

A. $h/2, k/2, l/2$ all even

$F_{hkl}=4(f_{Pb}+6f_{Cu}+8f_o)$ both models

B. $h/2, k/2, l/2$ all odd

$F_{hkl}=4(f_{Pb}+6f_{Cu}-8f_o)$ both models

C. $h/2, k/2, l/2$ mixed odd and even

$F_{hkl}=4(f_{Pb}-6/7f_{Cu})$ *disordered* model

$F_{hkl}=4(f_{Pb}-2f_{Cu})$ *ordered* model

A comparison of the calculated and observed structure factors for both models is given in Table 2. In order to assess the closeness of fit between the calculated and observed structure factors for each of the two models, discrepancy factors were calculated in several different ways. The discrepancy factor, R, is defined, as usual, as

$$R = \frac{\sum ||F_{obs.}| - |F_{calc.}||}{\sum |F_{obs.}|}.$$

TABLE 2. COMPARISON OF CALCULATED AND OBSERVED CRYSTAL STRUCTURE FACTORS FOR MURDOCHITE

(I—disordered model, II—ordered model; $x=\frac{1}{4}$)

hkl	sin θ	I		II	
		$F_{calc.}$	$F_{obs.}$	$F_{calc.}$	$F_{obs.}$
111	.067	52	*	72	*
002	.077	51	*	24	*
220	.109	49	52	24	47
113	.128	48	55	65	50
222	.134	137	142	141	125
004	.154	221	181	219	165
331	.168	45	88	61	80
402	.173	45	48	23	44
224	.189	43	35	22	32
333	.201	43	36	57	33
115	.201	43	57	57	53
440	.218	186	198	182	180
315	.228	40	57	54	52
442	.232	40	27	21	24
006	.232	40	47	21	42
620	.244	39	27	21	24
335	.253	39	49	51	45
226	.256	121	153	118	139
444	.267	162	142	157	130
551	.276	37	49	48	46
117	.276	37	61	48	56
406	.278	37	17	20	16
624	.289	36	31	19	28
553	.297	35	53	45	48
317	.297	35	37	45	55
008	.309	144	137	139	125
337	.316	34	61	43	56
446	.318	34	40	18	36
660	.328	33	37	18	34
228	.328	33	24	18	17
555	.334	33	49	42	45
517	.334	33	40	42	36
662	.337	102	125	97	114
408	.345	131	110	125	100
119	.352	31	35	40	32
735	.352	31	45	40	41
842	.353	31	25	17	23
664	.362	31	<24†	17	<22
319	.368	31	40	38	36
448	.378	120	118	114	108
771	.384	30	53	37	48
557	.384	30	45	37	41
339	.384	30	37	37	34
0.0.10	.386	29	<26	16	<24
628	.394	29	<23	15	<21
519	.399	29	32	36	29
737	.399	29	23	36	21
666	.401	87	54	82	50
2.2.10	.401	87	90	82	82
953	.414	28	29	34	27

* Reflection not recorded.
† Values preceded by < are threshold values.

TABLE 2—(*continued*)

hkl	sin θ	I		II	
		$F_{calc.}$	$F_{obs.}$	$F_{calc.}$	$F_{obs.}$
4.0.10	.416	28	23	15	21
846	.416	28	<24	15	<22
880	.437	106	105	98	96
559	.442	27	29	32	36
3.1.11	.442	27	33	33	30
4.4.10	.444	27	28	15	25
882	.444	27	<29	14	<26
668	.450	26	<29	14	<26
10.6.0	.450	26	<24	14	<22
739	.455	26	35	31	31
6.2.10	.457	78	85	71	77
884	.463	99	80	90	73
0.0.12	.463	99	89	90	81
777	.468	25	29	30	27
5.1.11	.468	25	35	30	32
2.2.12	.476	25	<25	14	<23
10.6.4	.476	25	<24	14	<23
957	.481	25	24	29	22
4.0.12	.488	93	75	84	68
886	.495	24	<31	13	<28
6.6.10	.506	69	76	63	69
4.4.12	.512	89	65	80	59
7.3.11	.517	23	27	27	24
779	.517	23	32	27	29
8.4.10	.518	23	<27	13	<24
6.2.12	.523	23	<27	12	<24
888	.535	83	75	74	68
0.0.14	.540	22	<33	12	<30
10.6.8	.546	22	<29	12	<27
10.10.2	.551	62	76	55	69
2.2.14	.551	62	59	55	53
12.8.0	.557	80	59	70	53
4.0.14	.562	21	<29	11	<27
8.4.12	.578	76	61	66	56
10.10.6	.593	56	61	48	56
6.2.14	.593	56	56	48	51
0.0.16	.618	69	57	59	52
2.2.16	.627	18	<29	10	<27
6.6.14	.632	51	52	43	47
4.0.16	.637	66	55	56	50
8.8.12	.637	66	64	56	58
12.12.0	.655	63	52	52	47
2.2.18	.703	42	48	34	44

The over-all R for the ordered model is 0.17, whereas that for the disordered model is 0.18, if in both cases only the non-zero observed reflections are included. If, however, each reflection observed to be zero is assigned a value equal to one-half its threshold value, the ordered model yields an R equal to 0.18, and the disordered model, an R equal to 0.21.

A possibly more significant way to consider these data is to examine

R as a function of sin θ, as suggested by Luzzati (1952). In Luzzati's method R', i.e. R for a chosen interval of sin θ, is plotted against the midpoint of that sin θ interval, all sin θ intervals for which there are data being plotted. The data for the disordered model together with the theoretical curve for a structure having a maximum mean absolute error in bond length of 0.05 Å ($\overline{|\Delta r|}=0.05$) as derived by Luzzati (1952), are shown in Fig. 1. It will be noted from this plot that for values of sin $\theta<0.35$, the R' increases with decreasing sin θ, in contradiction to the theoretical curve (the same effect holds for the ordered model, but in order to avoid confusion these data are not plotted). This deviation from the theoretical curve is undoubtedly due to absorption effects that are more important at smaller sin θ values. It is therefore of interest to consider the R factors for reflections having sin $\theta \geqq 0.35$. For the ordered model, if only the non-zero values are included, R is 0.15; if one-half the threshold value is used for the zero-observed reflections, R is also 0.15. The corresponding cases for the disordered model yield $R=0.16$ and $R=0.22$, respectively. The values of R calculated by different methods are collected in Table 3.

The evidence from the foregoing considerations is in favor of the

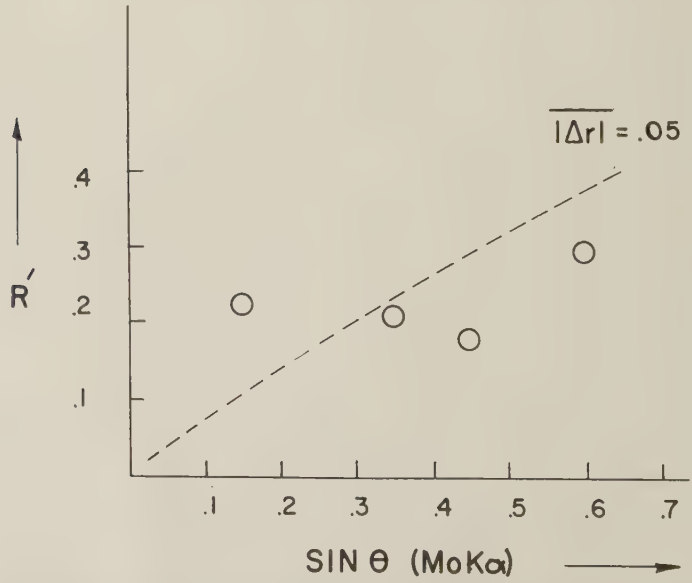

FIG. 1. Plot of R' *vs.* sin θ for murdochite. The circles represent experimental points for the disordered structure. R' is calculated omitting the non-observed $F_{obs.}$'s. The dashed line is the theoretical curve for a structure having a maximum mean error in bond length of 0.05 Å.

Table 3. Discrepancy Factors for Murdochite

Structure Model	R			
	I	II	III	IV
Ordered	0.17	0.18	0.15	0.15
Disordered	0.18	0.21	0.16	0.22

I—All reflections considered, $\Delta F = |F_{obs.}| - |F_{calc.}|$ omitted if $F_{obs.} = 0$.
II—All reflections considered, when $F_{obs.} = 0$ one-half its threshold value used.
III—Only reflections for which $\sin\theta \geqq 0.35$ considered, otherwise same as I.
IV—Only reflections for which $\sin\theta \geqq 0.35$ considered, otherwise same as II.

ordered model. This is in agreement with the findings of Kasper and Prener (1954) for Mg_6MnO_8. It is also in agreement with the results of Bertaut (1953), who has shown from energy considerations that, in general, ionic substances with vacancies would be ordered.

Discussion of the Structure

The postulated ordered structure of murdochite is illustrated in Fig. 2. Each Cu^{++} and each Pb^{++++} is surrounded octahedrally by eight $O^{=}$. No previous example of Cu^{++} in octahedral coordination is known, the usual coordination consisting of four oxygens equidistant from the Cu^{++} and lying in the same plane as the metal ion, as in tenorite, CuO (Tunell et al., 1935). Octahedrally coordinated Pb^{++++} occurs in Pb_3O_4 (Byström and Westgren, 1943).

On the basis of the parameterless model ($x = \frac{1}{4}$) all the Cu-O and Pb-O distances in murdochite are the same, namely 2.30 Å. In Pb_3O_4 the Pb-O bond length is 2.15 Å. It is quite possible that in murdochite the oxygen ions depart from the ideal close-packed arrangement, corresponding to a deviation from $x = \frac{1}{4}$, as has been found for Mg_6MnO_8, for which $x = 0.230$ (Kasper and Prener, 1954). For example, if $x = 0.235$, each Pb^{++++} would have six $O^{=}$ neighbors at a distance of 2.16 Å, and each Cu^{++} two $O^{=}$ neighbors at 2.30 Å and four at 2.33 Å. However, because of the lack of absorption corrections, the data at hand are not good enough to fix a more precise value of x. This point will be further investigated if it becomes possible to obtain sufficient material so that accurate intensities may be secured by the flat-plate reflection method of the diffractometer.

Density and Solid Solution

The calculated density for Cu_6PbO_8 is 6.1 gm. cm.$^{-3}$. The density of murdochite was measured in several ways. For the tube sample (0.4015

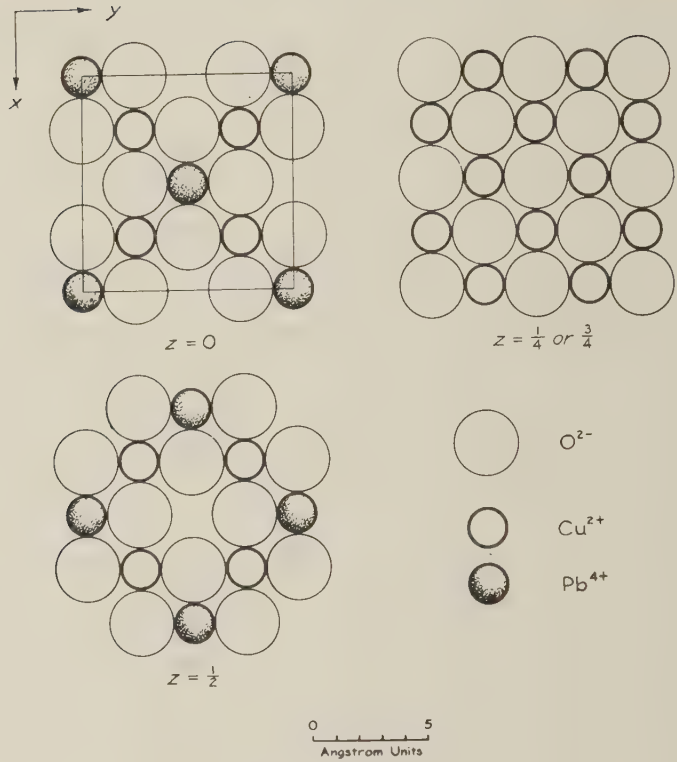

FIG. 2. Structure of murdochite, Cu_6PbO_8.

gm.), Fahey (1955) found 6.47. H. T. Evans Jr., (private communication) using the Berman balance and hand-picked crystal fragments, obtained the following results.

Sample	*A*	*B*	*C*
Sample wt., mg.	9.68	5.41	6.77
Density	6.4	6.1	5.9

These latter results indicated that the density of the mineral varied according to the sample. In order to test this conclusion further, more accurate determinations using a micropycnometer were carried out by Frank Cuttitta (private communication), with the following results:

Sample	*A*	*B*	*A*+*B*
Sample wt., mg.	90.6	64.9	155.5
Density	6.7	6.0	6.3

It seems likely from the densities obtained that solid solution occurs in the mineral, probably with Pb^{++} substituting for Cu^{++}. At this stage

of the investigation only about 90 mg. of the mineral remained in existence, and it was decided not to destroy this in attempting to determine the Pb^{++} content. Attempts to synthesize murdochite and related compounds are being carried out in the U. S. Geological Survey laboratories at the present time. If these attempts are successful the problem of solid solution and other questions of interest can be dealt with more effectively.

The lattice constant herein reported for murdochite is given with a fairly high degree of precision (9.210 ± 0.002 Å). For solid solution the lattice constant would be expected to vary as a function of chemical composition, hence the above figure applies only to the sample studied.

A second mineral of the murdochite type has been found at the Higgins mine, at Bisbee, Ariz. The mineral was first collected by a miner, from whom it was obtained by Mr. Arthur L. Flagg, a mining engineer of Phoenix, Ariz. Mr. Flagg then collected the material of interest remaining in the mine and submitted several specimens to the U. S. National Museum. The total quantity of this mineral available for study is quite limited.

The x-ray diffraction powder pattern of the mineral shows that it is of the same structural type as murdochite with $a_0 = 9.224 \pm 0.002$ Å. Spectrographic examination (K. J. Murata, private communication) shows, however, that it has a greater lead than copper content. This fact lends support to the hypothesis that lead and copper may occur in varying ratios to give the same murdochite structure type.

This second mineral is now under further investigation and will be described more completely in a future paper.

Acknowledgments

Various colleagues in the U.S. Geological Survey helped in many ways: Fred A. Hildebrand took the first x-ray diffraction powder pattern of murdochite and found that it could not be identified with any known mineral; Joseph M. Axelrod drew our attention to the mineral from Bisbee; Howard T. Evans, Jr., and Frank Cuttitta made density measurements on murdochite; K. J. Murata made the spectrographic analyses. Drs. W. F. Foshag and George Switzer, of the U. S. National Museum furnished us with the mineral from Bisbee. We are greatly indebted to all of these persons.

References

Bertaut, E. F. (1953), Contribution à l'étude des structures lacunaires: la pyrrhotine: *Acta Cryst.*, **6**, 557.

Bradley, A. J., and Jay, A. H. (1932), A method for deducing accurate values of the

lattice spacing from x-ray powder photographs taken by the Debye-Scherrer method: *Proc. Phys. Soc.*, **44,** 563.

Byström, A., and Westgren, A. (1943), The crystal structure of Pb_3O_4 and $SnPb_2O_4$: *Arkiv. for Kemi, Min. och Geol.*, **16 B,** 1.

Christ, C. L., and Clark, Joan R. (1954), Crystal structure of murdochite (abstract): *Am. Mineral.*, **39,** 321.

Christ, C. L., Clark, Joan R., and Fahey, J. J. (1953), Crystal structure of a new Cu-Pb-O mineral (abstract): *Am. Cryst. Assoc.* meeting, Ann Arbor, Mich., June 22–26 (1953).

Cochran, W. (1948), The correction of x-ray intensities for polarization and Lorentz factors: *J. Sci. Instr.*, **25,** 253.

Fahey, J. J. (1955), Murdochite, a new copper lead oxide: *Am. Mineral.*, **40,** 905–906.

International Tables for the Determination of Crystal Structures (1935). Berlin: Borntraeger.

Kasper, J. S., and Christ, C. L. (1953), A new structure type for metallic oxides of formula A_6BO_8: *J. Chem. Phys.*, **21,** 1897.

Kasper, J. S., and Prener, J. S., (1954), The crystal structure of Mg_6MnO_8: *Acta Cryst.*, **7,** 246.

Luzzati, V. (1952), Traitement statistique des erreurs dans la détermination des structures crystallines: *Acta Cryst.*, **5,** 802.

Tunell, G., Posnjak, E., and Ksanda, C. J. (1935), Geometrical and optical properties and crystal structure of tenorite: *Zeits. Krist.*, **90,** 120.

Wilson, A. J. C. (1942), Determination of absolute from relative intensity data: *Nature*, **150,** 152.

Manuscript received July 24, 1954.

NOTES AND NEWS

STUDIES OF URANIUM MINERALS (XXI): SYNTHETIC HYDROGEN-AUTUNITE

VIRGINIA ROSS

The amount of hydrogen occurring in autunite is apparently quite variable and dependent on the extent of base-exchange from acid solution. C. Frondel synthesized the pure, hydrogen end-member of the autunite series employing Bourgeois' method (1898) from solutions of ammonium dihydrogen phosphate and uranyl nitrate. Re-crystallization from a boiling solution of dilute hydrochloric acid yielded tiny, brilliant lemon-yellow crystals of hydrogen-autunite.

Chemical analysis† yielded the data of column 1, below.

	1	2
UO_3	65.08%	65.29%
P_2O_5	16.03	16.20
H_2O	19.33 (Penfield)	18.51
	100.44%	100.00%

indicating the composition: $HUO_2PO_4 \cdot 4H_2O$. Of the total water of hydration, 9.28% is lost at 110° C. The calculated weight percentages for this formula are given in column 2.

Harris and Scott (1949) synthesized uranyl-hydrogen-phosphate-tetrahydrate crystals from solutions of uranyl nitrate and concentrated phosphoric acid. From their description, this phase appears to be identical with hydrogen-autunite. The density of their material, determined by pycnometer measurement was 3.399 g./cc. at 25° C.

Optical Data

The hydrogen-autunite synthesized by Frondel consisted of microscopic, square and octagonal plates exhibiting parallel extinction with no perceptible biaxial character. The refraction data are as follows:

Uniaxial negative
$n\mathrm{E}=1.568$
$n\mathrm{O}=1.579$ $\pm .001$

Harris and Scott reported the following values:

$n\mathrm{E}=1.577$
$n\mathrm{O}=1.588$

X-Ray Data

The x-ray powder diffraction analysis of synthetic hydrogen-autunite reveals that it is the tetragonal meta-phase with probable space group:

† Analysis by H. J. Hallowell, 1951.

TABLE 1

X-Ray Powder Diffraction Data: Hydrogen-Autunite, $HUO_2PO_4 \cdot 4H_2O$, synthetic. Tetragonal, $c_0 = 9.043$ Å, $a_0 = 7.020 \pm .005$ Å, $c/a = 1.288$. Space Group, probably, $P4/nmm$. CuK radiation. Ni filter. Corrected for shrinkage

I	$d_{meas.}$	hkl	$d_{calc.}$	I	$d_{meas.}$	hkl	$d_{calc.}$
10	9.032	001	9.043	2	1.755	400	1.755
5	5.556	011	5.546			105	1.751
4	4.971	110	4.964	2	1.722	401	1.723
½	4.542	002	4.522	3	1.697	115	1.699
3	4.360	111	4.352	3	1.633	402	1.636
9	3.799	102	3.801			323	1.635
7	3.511	200	3.510	VB-D	1.61–1.57	314, etc.	1.854, etc.
8	3.270	021	3.272	1	1.546	421	1.547
6	2.964	121	2.966	1	1.477	324	1.475
7	2.765	022	2.773			106	1.474
		103	2.770	1	1.439	116	1.442
3	2.576	122	2.579	2	1.401	315	1.402
		113	2.576	1	1.383	206	1.385
3	2.488	220	2.482			511	1.361
4	2.397	221	2.393	1	1.359	414	1.360
2	2.267	301	2.265			216	1.359
		004	2.261	½	1.338	334	1.335
3	2.216	310	2.220	½	1.288	424	1.289
B-5	2.163	311	2.156			226	1.288
		104	2.152	1	1.270	107	1.270
B-4	2.075	302	2.078			306	1.267
2	1.902	321	1.905	B-2	1.249	316	1.246
		204	1.901	½	1.221	335	1.221
B-3	1.844	303	1.848	3	1.194	531	1.194
3	1.789	322	1.789			504	1.193
		313	1.788			326	1.192

I—Relative Intensity. hkl—interplanar spacing. B—broad line, VB—very broad line, D—Diffuse.

$P4/nmm$. The cell dimensions are $c_0 = 9.043$ Å and $a_0 = 7.020 \pm .005$ Å The spacings were refined by the method of least squares. The calculated cell contents are $2(HUO_2PO_4 \cdot 4H_2O)$ and the density is 3.28 g./cc. The x-ray d-spacings are tabulated below. Hydrogen-autunite is closely similar to or isostructural with meta-autunite.

Acknowledgment

This work was done on behalf of the Division of Raw Materials of the U. S. Atomic Energy Commission.

References

Bourgeois, L. (1898), *Bull. Soc. Min.*, **21**, 32.

Harris, W. W., Scott, Roberta H. (1949), Optical properties of three uranium phosphates; *AEC Report 2746*. (Sept., 1949). Carbide and Carbon Chemicals Corp., Oak Ridge, Tenn.

MANGANESE CONTENT OF GARNETS FROM THE FRANCISCAN SCHISTS

A. Pabst, *University of California, Berkeley 4, California.*

Introduction

Some years ago the writer (Pabst, 1931) described the garnets found in the Franciscan schists of California and reported that their composition could be expressed in terms of end members as being roughly 50 mole % almandite, usually with substantial proportions of pyrope, grossularite and andradite, but with only a very little spessartite. In summarizing the range of spessartite content was given as "0–1%."

Several years ago, at the suggestion of Dr. Max D. Crittenden, Jr., some of these garnets were reexamined and it was found that the manganese content previously reported was far too low. Additional analyses and spectrographic examination now permit a revised statement of the composition range of these garnets.

About two years ago, in response to an inquiry, the writer informed Dr. H. M. E. Schürmann of the Hague of the old error in a letter closing with the words "Reexamination of garnet *A* has shown that it contains about 2% MnO, equivalent to about 4½ mol % spessaritite." This was acknowledged by Dr. Schürmann in a letter dated 31 December, 1952, in these words: "Many thanks for your letter of November 25th with your information on literature on glaucophane and on chemical analysis of spessartite." In view of this correspondence it is surprising that Dr. Schürmann (1953) nearly a year later cited my old erroneous figures (his Tabelle 7 and Tabelle 8) without comment.

Dr. Max D. Crittenden, Jr., and Dr. Iris P. Borg have kindly permitted the use of unpublished data which makes possible the corrected statement of the composition of garnets from the Franciscan schists given below.

New Data

A new analysis of garnet from eclogite associated with glaucophane schist ¼ mile north of the Junction School near Healdsburg, California, has recently been reported by Mrs. Borg (1954, II, p. 57) in an unpublished thesis. The locality is but a few hundred yards from the source of

the garnet designated "*C*" by Pabst (1931). Table 1 contains the report of this analysis and its interpretation in terms of end members given by Mrs. Borg. It may be noted that the $RO:R_2O_3:SiO_2$ ratios depart from the ideal relation 3:1:3 in the fashion that is usual in garnets and that was commented upon earlier (Pabst, 1931).

Crittenden in an unpublished thesis (1951, p. 109) has recorded the corrected manganese content for the garnet from Hilton Gulch, Santa

Table 1. Analysis of Garnet from Eclogite, ¼ Mile N of Junction School, Near Healdsburg, Sonoma County, California

Quoted from Borg (1954, II, p. 57)

		Molecular Quotients			
SiO_2	37.36	0.620	0.620	$RO:R_2O_3:SiO_2$	
Al_2O_3	20.12	0.197		2.78:1:2.82	
TiO_2	0.54	0.007	0.220		
Fe_2O_3	2.60	0.016		End-member Mole Per Cent:	
				almandite	57.4%
FeO	25.18	0.351		pyrope	11.7
MnO	0.92	0.013	0.612		
MgO	2.96	0.073		spessartite	2.0
CaO	9.83	0.175		andradite	9.8
H_2O −105° C.	0.04			grossularite	19.1
H_2O +105° C.	0.09				
	99.54				100.0%

W. Herdsman, *analyst.*

Clara County, California, designated "*A*" by Pabst (1931). In the same place he has reported a garnet of even higher manganese content in Franciscan schists but a few miles distant. Unfortunately in the published account of his work Crittenden (1951*a*) did not include these mineralogical details.

In Table 2 are given the MnO content and some physical properties of several garnets from Franciscan rocks. The specific gravity of garnet "*A*" has been newly determined by Berman balance and supersedes the value, 3.884, previously reported. The lattice constants have been newly determined for each garnet from a back-reflection powder pattern obtained with a focussing camera. The wave length for Co-Kα_1 radiation being taken as 1.78890, the results are properly given in Å units. The previously reported value of the lattice constant for garnet "*A*," "11.60 Å ± 0.03 Å," is to be considered as having been in kX units. Upon conversion this agrees within the limits of error with the newly determined value.

Table 2. Manganese Content and Physical Properties of Three Garnets from the Franciscan Rocks of California

Locality and reference	MnO (wt. %)	S. G.	N_{Na}	a_0§
¼ mile N. of Junction School, near Healdsburg, California, Borg (1954)	0.92*	4.08±0.02‡	1.795±0.003‡	11.62±0.01 Å
South of Calaveras Valley, San Jose Quadrangle, Calif., Crittenden (1951)	4.63†	4.00±0.03‡	1.795±0.002‡	11.61±0.01‖
Hilton Gulch, San Jose Quadrangle, Calif. "*A*" of Pabst (1931)	2.03†	3.95±0.04§	1.795±0.002‡	11.62±0.01

* From Table 1.

† Determinations by Abbot A. Hanks, Inc., San Francisco.

‡ Quoted from references cited.

§ New determinations, see text.

‖ A low "shoulder" on the low angle side of the diffraction lines indicates that a small part of this garnet has a lattice constant as high as 11.65 Å. The other two garnets showed very sharp simple peaks indicating little or no variation in lattice constant.

Table 3. Results of Spectrographic Examination of Garnets from Franciscan Rocks in California

	MnO %	TiO_2 %	Si	Al	Fe	Ca
From eclogite, ¼ mile N. of Junction School, near Healdsburg, Calif. Borg (1954)	(0.92) 0.9	(0.54) 1.1	PC	PC	PC	10%
S. of Calaveras Valley, San Jose Quad., Calif. Crittenden (1951)	(4.63) 5.0	0.6	PC	PC	PC	10
Hilton Gulch, San Jose Quad., Calif. "*A*" of Pabst (1931)	(2.03) 1.4	2.1	PC	PC	PC	10
Near Reed Station, Marin County, Calif. "*B*" of Pabst (1931)	2.2	2.0	PC	PC	PC	10
Near mouth of Russian River, Sonoma Co., Calif. "*I*" of Pabst (1931)	0.9	1.4	PC	PC	PC	10

Figures in parentheses quoted from Tables 1 and 2. Spectrographic results from report by Mr. George M. Gordon, dated July 17, 1954. PC means principal constituent.

Descriptions of the rocks in which these garnets occur may be found in the references cited.

As previously noted (Pabst, 1931, p. 332), the composition of garnets in the range of interest here cannot be closely estimated from physical properties. Similarity of physical properties of other garnets from the Franciscan schists then suggests similarity of composition but allows no conclusion as to manganese content. In order to check the garnets whose composition had been previously reported, five samples were subjected to spectrographic examination by Mr. George M. Gordon of the Division of Mineral Technology with the results given in Table 3. There is reasonable agreement between spectrographic and direct chemical determination of manganese. The manganese content of garnets "*B*" and "*I*," previously (Pabst, 1931, Tables I and II) reported to be very low, is seen to lie in the range found for the other garnets by chemical analysis. All of the garnets are shown spectrographically to have Fe as a principal constituent and to contain about 10% of Ca in agreement with their first description (Pabst, 1931). However, the spectrographic results indicate that the TiO_2 content is in all cases higher than the "trace" previously reported.

Conclusions

The range of composition of "garnets in glaucophane rocks" given in Table III by Pabst (1931) should be revised to read:

Grossularite	8–30%
Andradite	4–24
Almandite	48–56
Pyrope	16–20
Spessartite	1–10

Their spessartite content, though less than that of the other end members, may exceed the limits 0–3% or 1–2% given for eclogite garnets by Heritisch (1926) and by Eskola (1921) respectively. The TiO_2 content of garnets in the Franciscan schists may attain one or two per cent as indicated by spectrographic examination. Since these rocks generally contain sphene and rutile this result is not surprising.

References

Borg, Iris Parnell (1954), Studies in metamorphism: II. Glaucophane and related schists near Healdsburg, California: unpublished Ph.D. thesis, University of California, Berkeley.

Crittenden, Max D. Jr. (1951), Geology of the San Jose-Mount Hamilton quadrangles, California: unpublished Ph.D. thesis, University of California, Berkeley.

—— (1951*a*), Geology of the San Jose-Mount Hamilton area, California; *Bull.* **157**, *California State Division of Mines*, 74 pp.

Eskola, Pentti (1920), The mineral facies of rocks; *Norsk Geologisk Tidsskrift*, **6**, 143–194.

Hertisch, Franz (1926), Studien über den Chemismus der Granaten: *Jb. Min., Beil. Bd.* **A 55,** 60–91.

Pabst, Adolf (1931), The garnets in the glaucophane schists of California: *Am. Mineral.*, **16,** 327–333.

Schürmann, H. M. E. (1953), Beiträge zur Glaukophanfrage (2): *Jb. Min., Abh.* **85,** 303–394.

LAUMONTITE AND LEONHARDITE CEMENT IN MIOCENE SANDSTONE FROM A WELL IN SAN JOAQUIN VALLEY, CALIFORNIA

M. E. Kaley and R. F. Hanson, *California Research Corporation, La Habra, California.*

The occurrence of a zeolite cement was noted in a feldspathic sandstone at a depth of approximately 11,000 feet in the Standard Oil Company of California Well C.C.M.O. 4, No. 35, Tejon Field, 30 miles southeast of Bakersfield, California. The zeolite mineral was identified by microscopic and x-ray powder diffraction methods as laumontite and its alteration product, leonhardite.

The occurrence of zeolites in rocks of igneous origin is a matter of common knowledge but their occurrence in rocks of sedimentary origin is less well known. Zeolites, nearly always secondary minerals formed by hydration of aluminum silicates of Ca, Na, etc., are derived chiefly from lime-bearing plagioclase feldspars.

Laumontite and leonhardite were found as an important alteration product in graywackes of New Zealand by Hutton (1949) and by Coombs (1952); laumontite as a cement in Cretaceous (?) sandstones from Anchor Bay, Mendocino County, California, is reported by Gilbert (1951). Hutton states that laumonitite and leonhardite probably have a much wider distribution than supposed; that in graywackes and similar rocks which have been subjected to low grade dynamothermal metamorphism the feldspars may be completely altered to laumontite and leonhardite instead of to albite.

The chemical composition of laumontite is given by Coombs (1952, p. 812) as:

$$Ca_x(Na, K)_yAl_{2x+y}Si_{24-(2x+y)}O_{48} \cdot 16H_2O$$

where $x+y/2$ does not exceed 4

and $x+y$ is not less than 4.

On exposure to the atmosphere or gentle heating laumontite loses approximately $\frac{1}{8}$ of its water to form leonhardite. This process is readily reversible and is accompanied by changes in the refractive index, optic angle, and extinction angle.

Optical properties as reported in the literature are listed in Table 1.

TABLE 1. OPTICAL PROPERTIES OF LAUMONTITE AND LEONHARDITE ACCORDING TO SEVERAL AUTHORITIES

	Larson	Gilbert	Coombs	Shannon	McClellan	Hutton
Laumontite	$(-)2V = 25°$ ca	$45° \pm 5°$	33°–37°	Med.		
	$\alpha = 1.513$	1.515	1.510 to 1.514	1.505	1.505	
	$\beta = 1.524$		1.518 to 1.522	1.515		
	$\gamma = 1.525$	1.525	1.521 to 1.525	1.517	1.513	
	$\gamma - \alpha = .012$	.010		.012		
	$Z/\wedge c = 20°–30°$	10°	8°–11°	large	50°	
	$Z'/\wedge c$		11°–14°			
Leonhardite	$(-)2V =$	30°–35°	26°–44°			21°
	$\alpha = 1.506$	1.506	1.502 to 1.507			1.505
	$\beta = 1.512$		1.512 to 1.516			1.514
	$\gamma = 1.517$	1.517	1.514 to 1.518			1.515
	$\gamma - \alpha = .011$	.011				.009
	$Z/\wedge c = 44°$	32°–34°	8°–35°			
	$Z'/\wedge c =$	39°–41°	11°–47°			

TABLE 2. ZEOLITE *X*-RAY POWDER DIFFRACTION DATA; STANDARD OIL COMPANY OF CALIFORNIA WELL C.C.M.O. 4, NO. 35

Intensity	*d/n* in Å	Intensity	*d/n* in Å
vs	9.42	vw	1.97
s	6.81	vw	1.94
w	6.20		
w	5.04	vvw	1.86?
vvw	4.73	mw	1.808
w	4.46	vvw	1.748
vs	4.16	vvw	1.657
vw	3.67	w	1.618
s	3.49	mw	1.536
vs	3.32	w	1.51
vvw (b)	3.20	vvw (b)	1.49?
m	3.02	vw (b)	1.46
w+	2.87	mw (b)	1.37
w+	2.77	vvw	1.32?
vvw	2.56	vvw	1.31?
vvw	2.52	vvw	1.296
m	2.42	vvw	1.27?
w	2.34	vvw	1.25
w	2.27	vw	1.22
m (b)	2.15	vw	1.21
vvw	2.06	vvw	1.176
		vw	1.157

s = strong, m = medium, v = very, w = weak, b = broad.

The crystals are prismatic with perfect 010 and 110 cleavages. The optic plane is 010 (Winchel, 1951).

The zeolite mineral in the sandstone core sample from the Standard Oil Company of California Well C.C.M.O. 4, No. 35, San Joaquin Valley, was isolated from the rock by hand picking under a stereoscopic microscope.

Optical properties of the mineral are as follows: crystals are prismatic with two good cleavages; $(-)2V$ = moderate; $\alpha = 1.508 \pm .002$, $\gamma = 1.516 \pm .002$; $\gamma - \alpha = .008$; Ext. to $c = 40° - 45°$.

X-ray diffraction data were obtained with a G. E. powder camera of 7.1744 cm. radius. The powder sample, mounted with Duco cement on a rotating glass filament, was exposed to Cu K_α radiations for 6 hours. Intensities of the lines were estimated visually.

These *x*-ray data agree closely with the data reported by Coombs (1952) for laumontite and leonhardite.

References

Coombs, D. S. (1952), Cell size, optical properties and chemical composition of laumontite and leonhardite. With a note on regional occurrences in New Zealand: *Am. Mineral.*, **37,** 812–830.

Gilbert, C. M. (1951), Laumontite from Anchor Bay, Mendocino County, California: *Geol. Soc. Am. Buli.*, **62,** 1517.

Hutton, C. O. (1949), Occurrence of leonhardite: *Geol. Soc. Am. Bull.*, **60,** 1939–1940.

Larson, E. S., and Berman, H. (1934), The microscopic determination of nonopaque minerals: *U. S. Geol. Survey Bull.* **849.**

McClellan, H. W. (1926), Laumontite from Southern Oregon: *Am. Mineral.*, **11,** 287.

Shannon, E. V. (1921), Massive laumontite from Montana: *Am. Mineral.*, **6,** 6–7.

UNIT CELL DIMENSIONS OF URANINITE

Eleanor R. Berman, *Department of Mineralogy, Harvard University Cambridge, Massachusetts.*

It appears that, in general, samples of pitchblende from hydrothermal veins have a smaller cell size than uraninites from pegmatites (Table 1). The values of a_0 of uraninites from different sources reported in the literature (1) support this observation.

The relatively small cell size of pitchblende is due to the following factors: (*a*) Relatively high oxidation, due to the fine-grain or fine fibrous permeable nature of the material and the resulting large surface area. The oxidation involves the conversion of U^{IV} to U^{VI} with valence compensation effected by the entrance of oxygen into the vacant 8-fold

position of the fluorite-type structure; the U^{VI} ion being relatively smaller than the U^{IV} ion, greater oxidation tends to decrease the unit cell size. (*b*) Relative freedom from larger thorium and rare earth ions, ($U^{IV} = 1.05$ Å; $Th^{IV} = 1.10$ Å; $Ce^{IV} = 1.02$ Å) (2), which are ordinarily present in relatively large amounts in uraninite from pegmatite. Pitchblende and relatively highly oxidized uraninite in general give diffuse and faint diffraction effects. This is due both to line broadening from small particle size, and also, as Brooker and Nuffield (1*b*) have pointed out, to variation

TABLE 1. UNIT CELL DIMENSIONS OF SOME UNTREATED SAMPLES OF URANINITE

Locality	*Description*	*Film Character*	*Analysis Reference**	a_o *in Angstroms*
Himmelfahrt Mine, Freiberg, Saxony	Pitchblende Vein	Poor pattern		5.39 ±0.01
Shinarump I*b* Mine, Seven Mile Canyon, near Moab, Utah	Pseudomorph after wood Hydrothermal	Faint broad lines		5.406±0.003
Happy Jack Mine, White Canyon, Utah	Black friable mass Hydrothermal	Sharp lines		5.411±0.003
Near Schmeideberg, Silesia, Germany	Pitchblende Vein	Broad lines	4	5.413±0.002
Monument #2 Mine, Apache County, Arizona	Sandstone Hydrothermal	Broad lines		5.415±0.003
Ranwick claims, Theano Point area, Algoma district, Ontario	Pitchblende Vein	Poor pattern		5.42 ±0.02
Joachimsthal, Bohemia	Pitchblende Vein	Broad lines	4	5.430±0.001
Marienberg, Saxony	Pitchblende Vein	Broad lines		5.435±0.001
Palermo, North Groton, New Hampshire	Hard black crystal Pegmatite	Broad lines		5.439±0.006
Mansfeld, Germany	Vein in "kupferschiefer" Hydrothermal	Broad diffuse lines		5.440±0.004
Newry, Maine	Altered crystal Pegmatite	Broad lines		5.447±0.001
Ruggles Mine, Center Grafton, New Hampshire	Hard black crystal Pegmatite	Broad lines	5	5.447±0.004
Beryl Mountain, near Acworth, New Hampshire	Hard black crystal Pegmatite	Broad lines		5.457±0.004
Beryl Mountain, near Acworth, New Hampshire	Hard black crystal Pegmatite	Broad lines		5.465±0.001
Pied des Monts, Saguenay District, Quebec	Hard black crystal Pegmatite	Sharp lines	6	5.480±0.003
Strickland Quarry, Portland, Connecticut	Glossy black crystal Pegmatite	Sharp clear lines	7	5.484±0.003
Wilberforce, Ontario	Hard black crystal Pegmatite	Sharp clear lines	8	5.487±0.001
Karelia, U.S.S.R.	Glossy black crystal Pegmatite	Sharp clear pattern	9	5.489±0.002
Gordonia, South Africa	Hard black crystal Pegmatite	Broad lines	10	5.490±0.001

* The analysis referred to was made on the *x*-rayed material in the case of the Gordonia and Wilberforce samples, and on samples from the same locality in all other cases.

in degree of oxidation within the sample, with accompanying variation in cell size.

The cell size also should vary with the amount of radiogenic lead present ($Pb^{IV} = 0.84$ Å; $U^{IV} = 1.05$ Å) (2). As Wasserstein (1*d*) has pointed out this offers a means of age determination by measurement of cell size. For the ideal application of this method, allowance must be made for the effect on a_0 of secondary oxidation, the presence of thorium and other elements in solid solution, and radiation damage.

All of the present samples were run on the Philips *x*-ray diffractometer and paper recorder. An internal standard of ThO_2 was employed. The Mansfeld and Palermo specimens also were photographed on film in 114 mm. cameras. None of the samples had been heated or otherwise treated. The ThO_2 value was 5.59543 Å ± 0.00005 Å, earlier obtained from a precision back-reflection camera. The value of a_0 for the synthetic UO_2 (Synthetic "C. P. Brown UO_2" prepared by the Shattuck Company, Denver), thus obtained was 5.468 Å ± 0.002 Å. The best value available for this substance is 5.4682 Å at 20° C. (3).

References

1. (*a*) Arnott, R. J., *Am. Mineral.*, **35,** 386 (1950).
   (*b*) Brooker, E. J., and Nuffield, E. W., *Am. Mineral.*, **37,** 363 (1952).
   (*c*) Kerr, P. F., Priv. Comm. (1950).
   (*d*) Wasserstein, B., *Nature,* **168,** 380 (1951).
2. Rankama, K., and Sahama, T. G., *Geochemistry;* Chicago (1950).
3. Swanson, H. E., and Fuyat, R. K., *Natl. Bureau of Stds., Circular,* **535,** 53 (1953).
4. Hecht, F., and Kroupa, E., *Zeit Analyt. Chemie,* **106,** 82 (1936).
5. Shaub, B. M., *Am. Mineral.*, **23,** 334 (1938).
6. Ellsworth, H. V., *Am. Mineral.*, **19,** 421 (1934).
7. Foye, W. G., *Am. Jour. Sci.*, Series 5, **28,** 127 (1934).
8. Baxter, G. P., and Bliss, A. D., *Jour. Am. Chem. Soc.*, **52,** 4852 (1930).
9. Labuntzov, A. N.; Pegmatites of the U.S.S.R., Vol. II (Pegmatites of North Karelia and their minerals); Moscow and Leningrad (*Acad. Sci. U.S.S.R.*) (1939).
10. Holmes, A., *Am. Jour. Sci.*, Series 5, **27,** 343 (1934).

REMOVAL OF MINERAL GRAINS FROM THIN SECTIONS*

Stewart R. Wallace†

A simple method by which individual mineral grains may be removed from a thin section and isolated for study by oil immersion, *x*-ray, or microchemical techniques has been used by the writer with considerable success. The basic concept of removing material from a thin section is

* Publication authorized by the Director, U. S. Geological Survey.

† Geologist, U. S. Geological Survey.

undoubtedly not a new one. However, during the past 5 years the writer has talked with several workers in mineralogy who were not familiar with this technique and it may serve some purpose to present it here. An example is given to illustrate the usefulness of the method.

Method

The basic method of grain removal is to make a series of perforations around a selected grain, and then pick the freed grain from the section. Any uncovered section may be used, but the writer found that best results were obtained if a second section were made especially for the purpose. This has several advantages: (1) the original section is not damaged and may be kept for reference, (2) the second section can be made thicker, preferably 0.06 to 0.09 mm. thick; the grains are more apt to break up in a section of standard thickness and more material is obtained from thicker sections—this is especially important if an x-ray is required, (3) the process of grain removal is less difficult if there is no balsam on the upper surface of the rock slice.

After the grain to be removed has been selected, a series of pricks are made along the periphery of the grain with a small fine-pointed needle; the point can be kept sharp by dressing with fine sand paper.

The operation is observed under the microscope and the space required for manipulation necessitates the use of a long focal length objective. The needle cannot be held exactly vertical; to prevent the grain from shattering, the needle should be in such a position that the horizontal component of the perforation is parallel with the edge of the grain. The holes should be spaced about 2 to 3 diameters apart and when the grain has been completely encircled these will appear as a dark band surrounding the grain (Fig. 1).

Next, a small drop of acetone, ether, or some other suitable solvent is applied to the spot. For this purpose the writer found that a thin stirring rod drawn out to a long fine point and then fire burnished was more effective than a micro-pipette. A small drop of solvent on the end of the rod can be held just over the grain until it has nearly evaporated and then applied to the proper spot. The solvent spreads rapidly on the surface of the slide, and this method prevents "flooding" the slide with a single large drop; several applications may be needed to soften the balsam.

The solvent attacks the balsam through the perforations and after several drops have been placed on the spot, the dark band around the grain will disappear and the perforations appear as holes in the slide. These holes are enlarged using the needle with a drawing motion and by chipping until a channel has been cut all the way around the grain. During this process it is sometimes necessary to apply more solvent and

if the rock material surrounding the grain is especially hard and cohesive it may be necessary to prick additional holes. When the grain has been freed from the rock, and the balsam beneath the grain is soft enough so that the grain may be moved, the point of the needle is placed under one edge of the grain, the grain pried up and removed from the slide.

Commonly the grain (especially if it is large), will break up during the process of removal but the larger pieces can usually be salvaged; grain boundaries are natural lines of weakness and it is not unusual to remove

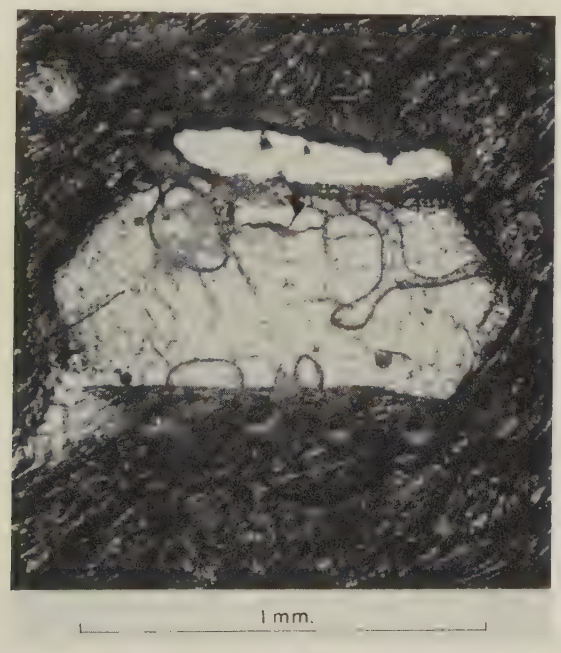

FIG. 1. Photomicrograph of pseudomorphic aggregate of natrolite after sanidine from tinguaite, showing two steps in the method of grain removal from thin section. Small "craters" along bottom margin of grain are needle perforations; elongate white space along top of grain is channel made by enlarging and connecting needle holes. Irregular spots are bubbles beneath grain.

a grain intact. Some grains will fracture when the perforations are being made along the grain boundaries. No harm is done unless the grain is poorly bonded to the mounting medium and fragments of the grain chip loose and fly off. Loss of material in this manner can generally be prevented by adding a small drop of acetone to the slide after the first hole has been made. This makes the balsam beneath the grain tacky and holds the fragments in place.

When the grain is removed from the section it is transferred to a glass

slide and cleaned by adding a drop of solvent and agitating the grain, and the process repeated until it is free of balsam. It is then ready for testing—by oil immersion, micro-chemical, or *x*-ray methods. An amount equal to 3 to 4 thick grains 1 mm. in diameter was found sufficient for an *x*-ray determination. In determining the indices of anisotropic minerals, grains of suitable orientation must be selected from the section, as the grains will generally have the same orientation when tested by immersion methods.

Example

In a thin section of a tinguaite from the Judith Mountains, Montana, several small euhedral grains of an isotropic, low-index substance occurred as micro-phenocrysts in an extremely fine-grained groundmass. The grains were 5, 6, and 7 sided to roughly circular in outline, and the shape together with the optical data and the geologic occurrence suggested that they were either sodalite, haüyne, analcime, leucite, or basal or near basal sections of nepheline. In order to identify the mineral it had to be isolated for further study.

The euhedral grains were a minor constituent of the rock, and the section also contained anhedral masses of a similar appearing substance, patches of partially devitrified glass, and zeolites. Because of the probable similarity in specific gravity and indices of these various substances with the euhedral mineral, and because of the scarcity of the euhedral grains and their small size (less than 1 mm), the use of heavy liquids seemed to be a difficult, if not impossible, solution to the problem of separation.

In an attempt to solve this problem, several grains were picked from the thin section and the refractive index determined as 1.487. This eliminated all except two possibilities—analcime or sodalite. A micro-chemical test for the chloride ion was then made with nitric acid and silver nitrate. The test was positive, suggesting sodalite, but more material was removed from the section and examined with *x*-ray; the powder pattern identified the mineral as analcime. Several additional thin sections of the rock specimen were then made at different orientations and all gradations in outline from hexagons to stubby rectangles were noted. These facts suggest that original nepheline crystals were in part replaced by sodalite, and later, the remaining nepheline and most of the sodalite were replaced by analcime.

Conclusions

The method will probably find limited application and will supplement other methods of separation. For determinations in which only small amounts of material are required, this method is less time consuming

than a heavy liquid separation; with ideal conditions enough material for an x-ray analysis may be obtained in less than an hour. For rocks in which unknown minerals occur as isolated masses greater than $\frac{1}{4}$ to $\frac{1}{3}$ mm. in diameter, a pure sample (barring inclusions) may be removed, tested, and identified and can be positively referred to the mineral observed in the thin section. This is especially useful when the unknown mineral is present in minor amounts and is associated with minerals having similar properties.

A SIMPLE COLLECTOR FOR CONCENTRATING A MINERAL PHASE FOR ANALYSIS

V. D. Frechette*

It is not uncommon to encounter the necessity for concentrating a mineral phase from a granular specimen for analysis by x-ray diffraction, spectroscopy, or other means. This may be done conveniently by a simple apparatus which is used in conjunction with the microscope.

The apparatus consists of an 8 mm. sample vial into which the specimen is to be collected and a two-hole stopper from one opening of which a tube extends to fit a length of rubber tubing whose free end is held in the mouth. From the other opening a glass tube drawn to a fine tip extends in an inverted L-shape. The vial may be manipulated by hand or preferably may be supported mechanically with the glass tip just above the grains at the center of the microscope object stage. Gentle suction will induct a mineral grain from beneath the tip and deposit it in the sample vial.

With care in sprinkling the sample over the object slide, not too great a suction, and the use of a tip of appropriate bore, a single grain may be collected at a time without drawing in neighboring unwanted grains. If too many other grains are collected it may occasionally be necessary to repeat the process on the collected sample. The time required for the process depends very much on the size of the particles and these should be as large as possible. In many cases it is feasible to eliminate the fines by sieving prior to the collecting process.

A small pamphlet of 45 pages with 7 maps entitled "Maine Mines and Mineral Locations" has been prepared by Philip Morrill. It can be purchased through John Dillingham, Naples, Maine. Price $1.00.

At the annual meeting of Die Deutsche Gesellschaft für Edelsteinkunde, held on May 7,

* The State University of New York College of Ceramics at Alfred University, Alfred, N. Y.

1955, Dr. Edward H. Kraus, professor emeritus of crystallography and mineralogy at the University of Michigan, was elected to honorary membership in recognition of his numerous publications and services in the field of gemology.

The University of New Mexico Publications in Geology has issued Number Five—Regional Tectonics of the Colorado Plateau and Relationship to the Origin and Distribution of Uranium, by Vincent C. Kelley. The principal objective of this bulletin has been to determine the relationship between regional structure and regional concentration of uranium deposits. Bulletin Five can be obtained from The University of New Mexico Press, Albuquerque, New Mexico. Price $2.00. This publication contains a tectonic map of the Colorado Plateau showing uranium deposits, which is sold separately for $1.00.

The Editor, *The American Mineralogist:*

Dear Sir:

I must apologize for the omission (noted by your reviewer, *Am. Mineral.*, **39,** p. 845) of the details for the specimens of phlogopite used in preparing the conoscopic figures in Figure 1 of my book "Manual of the Polarizing Microscope." The specimens were two very similar sheets in the Wiggins Collection of Micas, which was presented to the Museum of Practical Geology, London, by Mr. Harold Wiggins. There is no detail of the locality, but one specimen is noted as "Ceylon"; this, however, may be conjectural as in very many cases the fine Wiggins material had come through trade sources with some doubt as to the original locality. The thickness was just sufficient to permit the insertion of the mica between the support and a high power objective, say about half a millimeter.

This kind of mica has been an object of interest since the houppes were described by D. Brewster in *Phil. Trans. Roy. Soc.*, **109,** 24, 1819. Sketches of the houppes were given by T. Crook (*Min. Mag.*, **16,** 1–29, 1911) with several references, and there are brief accounts in textbooks such as Rosenbusch-Wülfing, 1924, 200. In a brief search I have not found any certain description or locality for this mineral. The numbers in the Wiggins Collection are 36, 120, 211. In the British Museum (Natural History) there is a small square plate mounted in card and this is labelled as given by Mr. T. Crook; from Canada.

I have felt a great interest in these specimens since Mr. Harold Wiggins first pointed out to me a remarkable uniaxial band which traverses them. They are beautifully pleochroic with great contrast between β and γ. In each sheet the material is in twin orientation with about 60° difference of extinction on either side of the band. The band, which is about 3/16 inch in width, is intermediate in depth of colour between the β and γ waves for the neighbouring material, and is clearly uniaxial. This I have always felt to be inconsistent with the customary explanation that the uniaxial appearance was due to the overlapping of the neighbouring twin members, since that would still give a biaxial symmetry. The band seems rather to be due to the local loss of the power for biaxial orientation in the neighbourhood of the composition surface, the material being then arranged equally in any of the three directions at 120°.

The biaxial twinned material has the axial plane 010 and is probably of the usual phlogopite structure as described by Levinson and Heinrich (*Am. Mineral.*, 1954, **39,** 939).

A. F. Hallimond,
75 Corringham Road, London, N.W.11.

MINERALOGICAL SOCIETY (LONDON)

A meeting of the Society was held on Thursday, June 9th, 1955, at 5 P.M., in the apartments of the Geological Society of London, Burlington House, Piccadilly, W.1 (by kind permission.

The following papers were read:

(1) *Okenite and nekoite (a new mineral).*

By J. A. Gard and H. F. W. Taylor

The unit-cell of okenite ($CaO \cdot 2SiO_2 \cdot 2H_2O$) has been determined for a specimen from Bombay, India, using a combination of *x*-ray, electron-microscope, and electron-diffraction methods. It is triclinic with *a* 9.84, *b* 7.20, *c* 21.33 Å, α 90.0°, β 103.9°, γ 111.5°, elongation *b*, Z=9. These data are compatible with the goniometric results of Böggild (1922) and allow the latter to be interpreted.

A specimen from Crestmore, California, which Eakle (1917) had described as okenite, was also examined. It was found to be a new species, having the same composition as okenite but distinguishable from it by its optical properties, *x*-ray powder data, and unit-cell. The latter is triclinic with *a* 7.60, *b* 7.32, *c* 9.86 Å, α 111°48′, β 91°30′, γ 103°54′, elongation *b*, Z=3. Because of the relation to okenite, the name "nekoite" is suggested.

(2) *X-ray study of raspite (monoclinic $PbWO_4$)*

By Rosemary Shaw and G. F. Claringbull

The monoclinic form of $PbWO_4$, raspite, has been studied by chemical and *x*-ray methods and its relation to stolzite, the tetragonal form of $PbWO_4$, investigated. Raspite (Broken Hill, N.S.W.) crystallizes in the space group $P2_1/c$ and has cell dimensions *a* 5.58, *b* 5.00, *c* 13.64 Å, β 107.7°. It has so far been reported from only three localities; and has not yet been prepared synthetically. Natural raspite transforms irreversibly to stolzite at about 400° C.

The Pb and W atoms were located from F_0-syntheses computed from *h*0*l*, *h*1*l* and *h*2*l* reflections but the O atoms could not be detected. Possible positions for the oxygens were found by considering limitations on W—O and O –O bond lengths. These limitations are quite stringent and the proposed oxygen positions are probably near the correct ones. A structure closely related to stolzite has been derived which has reasonable values of bond lengths and angles and which accounts in detail for the observed cleavage and twin laws.

(3) *Ceruléite ($CuAl_4(AsO_4)_2(OH)_8 \cdot 4H_2O$) from Wheal Gorland, Gwennap, Cornwall*

By Arthur Russell and G. F. Claringbull

Sky blue botryoidal aggregates and spheres, 1–1½ mm. in diameter, occurring on liroconite and associated with clinoclase and olivenite or chrysocolla are shown to be ceruléite. This is the second known occurrence of the mineral.

(4) *The convergent lead ages of the earth's oldest monazites and uraninites (Rhodesia, Manitoba, Madagascar and Klerksdorp, Transvaal).*

By L. H. Ahrens

The lead age distribution

$$\left(\frac{206}{238}, \frac{207}{235}, \frac{208}{232} \text{ and } \frac{207}{206}\right)$$

of three specimens of Rhodesia monazite form a regular pattern. Such an array, produced

evidently by varying lead loss, may be used for a precision estimate of age—the *convergent* age. The convergent age of each Rhodesian monazite is estimated at 2680×10^6 years. The lead age distributions of monazite from Antsirabe, Madagascar, and uraninite from the Huron Claim, south-eastern Manitoba, fit an extension of the Rhodesia age pattern closely ($\pm10\times10^6$ years) and hence their convergent ages are estimated also at 2680×10^6 years; uraninite from Klerksdorp, Transvaal, may have a similar age. The convergent ages of these most primitive specimens are somewhat greater ($50-700\times10^6$ years) than previously recommended estimates.

The formation of a well-ordered age array suggests that physical causes, rather than chemical, have controlled lead loss. There is a possibility, however, that other causes—natural fission, for example—could bring about the age array.

The following paper was taken as read:

(1) *Twentieth list of new mineral names*

By L. J. Spencer

(*Titles and abstracts kindly submitted by G. F. Claringbull, General Secretary.*)

Dr. Charles P. Berkey, professor emeritus of geology at Columbia University, and one of the nation's foremost geologists in the application of geology to various engineering projects, died on Aug. 23, 1955, after a prolonged illness. He was 88 years old.

The Sixth International Colloquium on Spectroscopy will be held from May 14–19, 1956, at Amsterdam, Holland. As usual the colloquium will cover both emission and absorption spectroscopy, with special stress on their practical applications in analysis. More detailed information may be obtained from the secretary, Mr. F. Freese, Laboratory for Analytical Chemistry, 125 Nieuwe Achtergracht, Amsterdam-C4, Netherlands.

The following are the officers of the Society of Exploration Geophysicists for 1955–1956.
President: R. C. Dunlap, Jr., Dallas, vice-president of Geophysical Service Inc.
Vice-President: Dave P. Carlton, Houston, chief geophysicist of Humble Oil & Refining Co.
Secretary-Treasurer: George A. Grimm, Midland, Texas, district geophysicist for Tide Water Associated Oil Co.
Editor: Norman Ricker, Tulsa, senior research physicist for The Carter Oil Co.

The 1955 annual meeting of the Society for Experimental Stress Analysis will be held on November 16, 17, 18, 1955, at the Hotel Sheraton, Chicago, Illinois. Further information may be obtained by writing to Dr. W. M. Murray, secretary-treasurer, P.O. Box 168, Cambridge 39, Mass.

BOOK REVIEWS

FESTBAND BRUNO SANDER: Tschermaks Mineralogische und Petrographische Mitteilungen, Dritte Folge, Band IV, Heft 1–4, 463 pp., Springer-Verlag, Vienna (1954).

Friends and former students of Professor Bruno Sander have dedicated this attractive Festschrift to him on the occasion of his seventieth birthday. The volume was put out with Dr. Josef Ladurner, Innsbruck, as cooperating guest editor.

It is appropriately introduced by a six page article written by Prof. R. von Klebelsberg and with a portrait of Prof. Sander, entitled "Prof. Dr. Bruno Sander und die Universität Innsbruck." There follow 46 technical papers by 51 authors. The subject matter ranges from descriptive mineralogy and stratigraphy through structural, economic, igneous, and metamorphic geology to petrofabrics and structural petrology. Twenty-six of the papers are in the last two categories, to the development of which Prof. Sander has contributed so largely from his pioneering paper, Über Zusammenhänge zwischen Teilbewegung und Gefüge in Gesteinen (1911), in which many of the important concepts in this field were presented.

There are in this volume more original articles concerning *Gefügekunde der Gesteine* than have ever appeared together in a single book or journal. It is recommended to all who would like to keep abreast of what is happening in this important and interesting field.

Earl Ingerson,
U. S. Geological Survey, Washington 25, D. C.

GEOLOGIE, MINERALOGIE UND LAGERSTÄTTENLEHRE, by Paul Kukuk; 2nd edition, xvi+334 pages; 406 figures. Springer-Verlag, Berlin, 1955. Price, DM 28.50.

The second edition follows exactly the outline of the first one (see *Am. Mineral.*, **37,** 350–351, 1952, for scope and discussion of the earlier edition.) No new topics or headings have been added but some sections have been revised and brought up to date, so that both text and illustrations have been increased by approximately ten per cent.

The bibliography has been much more drastically revised than any other part of the book. In the first edition it contained only 30 references, two of which were later than 1949. In the new edition 51 references with dates 1950–54 and 25 older ones have been added. The index has been enlarged by about 25 per cent.

All of the remarks made in the review of the first edition still apply, including those concerning a half dozen shortcomings and inadequacies of the book.

Earl Ingerson,
U. S. Geological Survey, Washington 25, D. C.

GEOLOGY AND MINERAL DEPOSITS OF BARSTOW QUADRANGLE, SAN BERNARDINO COUNTY, CALIFORNIA, by Oliver E. Bowen, Jr., with a report on Thermal Properties of Ceramic Materials from Barstow Quadrangle, California, by Joseph A. Pask and Oliver E. Bowen, Jr. *Division of Mines, Bull.* **165,** 208 pages, geologic map, structure sections; San Francisco, 1954, price $3.00.

This bulletin gives a rather thorough account of the geology and geologic history (118 pages), metallic (22 pages), and non-metallic (40 pages) mineral deposits, and brief notes about water and petroleum possibilities in almost a thousand square miles of the structurally complicated and interesting Mojave Desert area of Southern California.

It has a colored topographic-geologic map of the region and larger scale geologic maps of some of the more important and interesting areas. The report is well illustrated with numerous photographs and a few line drawings.

The short section (14 pp.) on thermal properties of ceramic materials includes 23 differential thermal analysis curves of ceramic (clay) materials and individual minerals.

The whole bulletin will be very useful to everyone interested in the geology and minerals of the Barstow area and surrounding parts of the Mojave Desert.

EARL INGERSON,
U. S. Geological Survey, Washington 25, D. C.

CATALOGUE OF METEORITES, with special reference to those represented in the Collections of the British Museum (Natural History) by G. T. PRIOR and revised and enlarged by MAX. H. HEY. Printed by order of the Trustees of the British Museum, 432 pages, published 1953, £ 3; 10; 0.

The general arrangement is essentially that of Prior's 1923 catalogue. The alphabetical listing of the known meteorites in the 1923 catalogue required 195 pages but in the 1953 catalogue 416 pages were required. The introduction contains a classification of meteorites; list of "paired" falls; a history of the British Museum's Collection; two tables in which the numbers of the meteorites "seen to fall" and "found" are given for the world and for those in the British Museum's collection. Another table gives a geographic distribution of the meteorites for the world.

The author should be complimented for these tables because they contain useful data. However, it would be less confusing if some minor editorial changes had been made. Also the totals given are not in every case the summation of the figures listed, e.g. the total known meteorites including "paired" falls is given as 1702 while the figures total 1734.

Although the information in the tables is useful, this reviewer believes that the catalogue would have been improved if the author, in place of listing the numbers of certain types of meteorites, had given the names of these meteorites. It surely would be more helpful to have the names of the 17 eucrites than merely to learn that there are 17.

The main part of this catalogue is the alphabetical listing of the meteorites. Here the synonyms, date of fall or find, type, known weight, distribution of the important specimens, references and weights of the specimens in the British Museum are given. Following that are 8 pages of the "reasonably authenticated" meteoritic craters and a list of the casts of meteorites and thin sections of meteoritic stones in their collection.

This book is a catalogue of meteorites in the British Museum and is not a text on meteorites. However, this volume will serve as a source book of information for those interested in meteorites because it is more than a listing of the specimens in the British Museum. If the name of a meteorite is known, it is possible to get considerable information about it from this book, so all persons interested in meteorites will need this book in their library.

The author has listed many "paired" falls in the introduction but these possibly related meteorites are not always associated as paired falls in the text. Ex. Accalana, Artracoona, Carraweena are "paired" falls but in the text under Accalana it says "possibly from the same fall as Carraweena, which is five miles away" but no mention is made that it may be related to Artracoona. However, under the latter name the reader finds it is related to Accalana and Carraweena. The LaLande is also listed as a "paired" fall but in the text the author says, "the B.M.'s specimens of the LaLande and Melrose appear to be distinct."

This reviewer did not make a point of searching for mistakes but a few are given. Some of these are listed with mental reservations because many readers of this review probably will think it is not proper to cite errors which were copied from the literature, especially since, in some cases, the British Museum's collections did not have a sample of the meteorite for Dr. Hey to confirm the information, and also a catalogue may not be the place to make corrections to published records. Actually this reviewer carefully went through this cata-

logue to compare it with his records and more corrections were found in my records than are cited as errors to be corrected in Hey's new catalogue.

This volume is one of the most frequently used books in the reviewer's library. Only one who has tried to keep this type of data up-to-date can appreciate the time and labor that must go into the preparation of such a catalogue. Since the literature relating to meteorites is replete with inaccurate statements, it is easy to innocently perpetuate old mistakes.

Corrections

1. Arcadia, Neb., is a chondrite and not an achondrite.
2. Aurora, New Mex. is a chondrite and not an achondrite.
3. Bogoslovka, Russia, is a stone, chondrite, found Aug. 5, 1948, weight 2.21 kgs. was omitted. (Prioroda No. 10, Oct. 1949, p. 43).
4. Bennett County, South Dakota, is a hexahedrite not a octahedrite.
5. Boelus, Howard Co., Nebraska, was found in 1941, stone chondrite, weight 730 gms. (Listed in *U. S. Nat. Museum Annual Report*, **1942**, p. 56).
6. Drum Mountains, Utah, iron was 529 kgs. not 52 kgs.
7. El Simbolar, Argentine, iron, coarse octahedrite, was omitted. (*Pub. Museo Mineral. Geol. Facultad de Sci. Ex. Fix. Nat. 3–13*, **1940**).
8. Haven. Reon Co., Kansas. Stone chondrite, weight 2948 gms. was omitted. (*Earth Science Digest*, **6**, No. 2, pp. 331–334, 1952).
9. Kunashak, Russia, stone, fell June 11, 1949, was omitted. (*Priroda*, Aug. 1950, p. 26–33, *Meteoritica Acad. Sci.*, **1952**, No. 10, pp. 42–56).
10. Mikmoto Jima, Japan. Iron was omitted. (*Sci. Rept. Yohohama Nat. Univ.*, Sec. 2, No. 1, **1952**).
11. Minnesota Iron, also Minnesota Stone—were omitted. (*Nininger Collection of Meteorites*, **1950**).
12. Newton, Conn. Iron is a pseudometeorite (*private communication*).
13. Palchatchie, Miss. The town is spelled Pelahatchie so the meteorite should have the same spelling.
14. South Strafford, Vermont. A pseudometeorite. Tested and found to be cast-iron.
15. Williamette, Oregon. Listed as a medium octahedrite but all samples of this iron are granulated and none show a Widmanstätten pattern.

E. P. Henderson,
U. S. National Museum, Washington, D. C.

CLAYS AND CLAY TECHNOLOGY, edited by Joseph A. Pask and Mort D. Turner, *Division of Mines, Bull.* **169**, 326 pp. California Dept. of Natural Resources, San Francisco, July [March] 1955, $4.50. (*Proc. First Nat. Conference on Clays and Clay Technology, Berkeley, July 21–25, 1952.*)

This cloth-bound volume contains an introduction and seven parts, namely: (I) Geology and mineralogy of clays, (II) Properties of clays, (III) Methods of identifying clays and the interpretation of results, (IV) Clay technology in soil science, (V) Clay technology in soil mechanics, (VI) Clay technology in ceramics, and (VII) Clay technology in the petroleum industry. Twenty-five papers were contributed by 26 different authors, the asterisk (indicating an author) belonging with the name, C. G. Dodd, apparently having been inadvertently omitted. An additional 37 "contributing authors" are listed because of participation in the discussions.

Although certain papers, such as "Physical-chemical properties and engineering per-

formance of clays" by R. C. Mielenz and M. E. King, are closely related to mineralogy and geology, only those included in parts I to III will be considered here.

In the introductory remarks, R. E. Grim discusses the reasons for interest of the various areas of knowledge in clay minerals. P. F. Kerr discusses "Formation and occurrence of clay minerals" and G. F. Brindley considers "Structural mineralogy of clays" in part I. These authors have contributed numerous papers on these subjects in other places.

Four papers make up part II, namely: (1) "Electrochemical properties of clays" by L. E. Davis, (2) "Ion exchange reactions of clays" by D. R. Lewis, (3) "Adsorption and swelling properties of clay-water system" by I. Barshad, and (4) "Interlamellar sorption by clay minerals" by D. M. C. MacEwan.

Part III contains nine papers, on particle size distribution, interpretation of chemical analyses, petrographic study, identification by dye adsorption, infrared spectroscopy, x-ray diffraction, electron microscopy and differential thermal analysis. Although some of the authors' names are familiar to most mineralogists in connection with the topics discussed, particularly those of R. E. Grim, G. W. Brindley, T. F. Bates and R. A. Rowland, a few are either persons who have specialized extensively during a brief period or persons who are discussing topics outside their areas of special interest. W. P. Kelley, for example, is an authority on soil science, and it is somewhat surprising that he is so versatile as to be able to contribute to the fundamental concepts of isomorphism and crystal chemistry.

In connection with the latter paper and one or two others, the editors have omitted much critical discussion that had a straightforward bearing on the subjects presented. Another matter of editorial policy involves the submittal of oral statements to contributors for correction prior to printing—something that was not done in this instance, although it is being done in connection with the proceedings of the second conference (Columbia, Mo., 1953).

The proceedings are of great value, bringing together many diverse viewpoints of pure and applied scientists. The elapse of nearly three years prior to their appearance is unfortunate, but probably arises from the gigantic task performed by the editors.

Duncan McConnell,
Ohio State University, Columbus, Ohio

MINERALIEN UND LAGERSTÄTTEN IN OSTBAYERN, by Hugo Strunz. Gustav Bosse Verlag, Regensburg, 128 pages, 77 illustrations, Regensburg, Germany 1953. Price bound DM 9.80.

With the introduction and rapid spread of the new physical and chemical techniques in mineralogy, there has been a natural tendency to neglect the preparation of general papers on regional mineralogy. The book under review, written by one of the leading scholars in systematic mineralogy, is therefore an appropriate reminder of the need for more books of this type.

The book opens with a general synopsis of the descriptive and historical geology of the area. The region is divided into two zones—the Moldanubic and the Saxothuringic. The deposits of minerals and rocks within each zone are then succinctly described. This is done in the framework of the geologic setting. Pertinent chemical, mineralogical, and petrological data are cleverly integrated with some historical facts. Each description is illustrated and includes a useful collection of references. Illustrations consist of sketch maps, geologic maps, stratigraphic columns and cross sections, photographs of rocks, and paragenetic charts.

Under the Moldanubic zone are included: Bayerischer Wald und Oberpfälzer Wald als Teile des Moldanubikums; Der Graphit von Passau; Schwefelkies und Magnetkies im Ostbayerischen Grundgebirge. Bodenmais und Lam; Die Ostbayerischen Pegmatite; Der Pfahl; Die Flusspatgänge bei Donaustauf und Wolsendorf.

Under the Saxothuringic zone are included; Nördlicher Oberpfälzer Wald und Fichtelgebirge als Teile des Saxothuringikums; Speckstein, Talkschiefer und Serpentin aus dem Fichtelgebirge; Der Speckstein von Göpfersgrun-Thiersheim; Serpentin und Talkschiefer von Wurlitz; Schwefelkies und Magnetkies im Ostbayerischen Grundgebirge; Die Golderze von Brandholz im Fichtelgebirge; Die Blei-Zinkerze von Erbendorf; Die Juraformation bei Regensburg; Die Danubische Kreideformation; Das Ostbayerische Bruchschollenland; Die Eisenerze von Sulzbach-Auerbach-Amberg; Die Kaoline von Hirschau and Schnaittenbach; Die Bleierze von Freihung; Die tertiären Tone und Braunkohlen der Oberpfalz; Die Ostbayerischen Basalte.

Professor Strunz has written a very interesting and useful book. It should appeal to those working in topographical mineralogy. The museum curator and the advanced collector will find the five-page index of the localities and minerals of Eastern Bavaria of particular value.

George T. Faust

DIE OXYDATIONSZONE SULFIDISCHER LAGERSTÄTTEN. S. S. Smirnow. Akademie-Verlag, Berlin, 312 pp. (1954), 17.50 DM.

The preface to this volume states that Smirnow published the first Russian edition in 1936 and that after his death in 1947 a second Russian edition was prepared in 1951 by his co-workers; the present volume is a translation into German of the 1951 edition.

The book is divided into three parts. Part I, pp. 12–66, is on the general properties of the zone of oxidation and the processes that occur in it. Part II, pp. 69–283, is on the geochemical behavior of individual elements in the oxidation zone of sulfide deposits. Part III, pp. 287–304, is on the significance of the oxidation zone in the evaluation, mining, and prospecting for sulfide deposits.

The scope of Part II is perhaps best shown by the contents of the section on one element. Under Copper, there are sections on Hypogene Mineralogy (p. 113), The Oxidation of Copper Sulfides (pp. 113–120), The Migration and Precipitation of Copper in the Zone of Oxidation (pp. 121–124), Mineralogy of Copper under the Conditions of the Zone of Oxidation of Sulfide Deposits (pp. 124–138), Comments on the Zone of Secondary Sulfide Enrichment (pp. 124–138), The Lower Zone of Leaching in the Zone of Oxidation of Copper Ore Deposits (pp. 140–142), The Limonite of the Zone of Oxidation of Copper Ore Deposits (pp. 142–146).

The book is well organized and the treatment is clear and comprehensive. The literature coverage was world-wide; more than 70% of the 133 references are to works published in the United States and Canada. Nevertheless, the book was a great disappointment to the reviewer, who had hoped that it would summarize the very large amount of work in this field that has been published in recent years in Russian. It is evident, regrettably, that the 1951 revision must have been very superficial; the latest reference cited is to work published in 1935, and there is no indication of the incorporation into the text of more recent data. As a necessary consequence, discredited minerals are included, new ones are omitted, and many incorrect formulas are given.

A minor irritation, which could have been avoided by more careful editing, is mistaken transliteration, perhaps inevitable when English goes to German through Russian. Examples are biverite for beaverite, janevixite for chenevixite, and hildite for guildite. There are a good many misprints. The lack of any subject index is a serious inconvenience. The book is nicely printed on good paper.

In summary, the book is an excellent account of the subject as of 1935.

Michael Fleischer,
U. S. Geological Survey, Washington, D. C.

THE PRINCIPLES OF CHEMICAL WEATHERING, by W. D. Keller. Size 8½ by 11, 88 pp. including appendix and index, 21 figs. Lucas Brothers Publishers, Columbia, Missouri (1955). Price $2.75.

This short treatment of chemical weathering evolved from classroom materials at the University of Missouri, and from visiting lectures by Professor Keller at the California Institute of Technology and at the University of Texas. Largely because of this inheritance, the text embodies a strange (to the geological literature) admixture of technical theoretical treatment, and the more philosophical significance of weathering on society and man. This intent is clearly stated in the *Foreward:* "The subject matter that has been incorporated herein has not been restricted to a narrow view of chemical weathering for its own sake. Instead, chemical weathering has been related naturally and freely to other fields of science and into areas of the humanities."

Its success in accomplishing these objectives will doubtlessly vary with the scientific and philosophic experience of its readers. Most mineralogists and geologists will be favorably impressed with the fresh and modern treatment of chemical weathering based upon bonding energies and energy changes of chemical weathering reactions which form the common tone underscoring the discussion of processes and mechanisms. This is the outstanding contribution of the text in that it summarizes modern research and thought from both field and laboratory investigations. It augments, rather than replaces, Reiche's classical treatment of weathering processes and products. The humanistic significance of chemical weathering, while a specific objective of the text, is interesting but not overly impressive as to its appropriateness in the scientific literature. Perhaps the reviewer is so inured by past experience as to expect only the scientific significance of our scientific progress, that it is best for the reader to form his own opinion in this respect.

The following phases are covered in the treatment of chemical weathering: introduction and definitions (Ch. 1–4), processes, agents, and mechanisms (Ch. 5–9), products of weathering (Ch. 10–12), and sociological importance of weathering (Ch. 13–15). It is supplemented with a modern (but not comprehensive) list of references, an appendix of minerals and formulas mentioned in the text, and an index.

Misspelled words are not frequent but more care should have been exercised in checking and integrating references in the text with the "References" at the end of the pamphlet. A few instances will illustrate this point. The date of the reference to Jackson, et al., cited on page 47, is given as 1946, but recorded as 1948 in "References"; the date is ommitted in the same reference on page 48. This is confusing as there are two references to Jackson *et. al.* in the "References." The date on page 54 for the Grim article should be 1953, not 1053; the reference to Keller, Westcott and Bledsoe is variously referred to as 1954 and 1955, although 1955 is given in the "References." There are other inconsistencies in bibliographic form and completeness in the "References," which however should not prevent the serious minded student from finding the article referred to.

The Principles of Chemical Weathering is to be recommended to advanced undergraduate students and graduate students as a reference work for classes in petrology, sedimentation, and geomorphology. Teachers will find it equally useful, especially in supplementing the standard texts in these fields.

L. I. Briggs,
University of Michigan, Ann Arbor, Michigan

NEW MINERAL NAMES

Kurgantaite

YA. YA. YARZHEMSKII, Kurgantaite—a new borate mineral. *Mineralog. Sbornik, Lvovskoe geol. Obschestvo* No. **6**, 169–174 (1952) (in Russian).

The mineral occurs in nodules up to 4 cm. in diameter, but usually much smaller, in gypsum-anhydrite beds in the western Kurgan-Tau (western Kazakhstan). It is extremely fine-grained. Analysis by T. V. Mandr'ikin gave B_2O_3 36.08, CaO 17.64, SrO 32.66, SO_3 6.07, loss when heated 7.5; sum 99.95%. The SO_3 is deducted as gypsum and anhydrite in the ratio 3:1, and the remainder gives nearly $(Sr, Ca)_2(BO_2)_4 \cdot H_2O$ with Sr slightly greater than Ca. The mineral is hard (scratches glass). It is optically biaxial with a very small optic angle, nearly uniaxial positive. Measurements by the immersion method gave $\alpha = 1.641$, $\gamma = 1.682$. Elongation positive. The specific gravity is variable, about 3 in one sample (sank slowly in bromoform with D. = 2.89), but is less in other samples. A differential thermal analysis showed several endothermic reactions; those below 350° C. are attributed to gypsum. A large effect at 500° C. is attributed to loss of water of crystallization, and one beginning at 900° C. is attributed to the fusion of the borate, which is complete at 1040° C. It is stated that *x*-ray data indicate that the mineral differs from other borates; the data will be published later.

The name is for the locality.

DISCUSSION: Differs in many ways from veatchite, the only other known strontium borate.

MICHAEL FLEISCHER

Suanite

TAKEO WATANABE, Suanite, a new magnesium borate from Hol Kol, Suan, North Korea. *Mineralogical Journal* (*Mineralog. Soc. Japan*) **1**, No. 1, 54–62 (1953).

A preliminary report on this mineral was abstracted in *Am. Mineral.*, **39**, 692 (1954). Suanite is white, luster silky to pearly, hardness $5\frac{1}{2}$, G. = 2.91. Optically biaxial, negative, $\alpha = 1.596$, $\beta = 1.639$, $\gamma = 1.670$, $2V_\alpha$ 70°, $X = b$ (parallel to fibers), dispersion $r > v$, weak. *X*-ray data are given in the previous abstract.

Analyses (1) by K. Isono, (2) and (3) by N. Saito and N. Kokubu gave (1 and 2 contained a little calcite, 3 contained a little szaibelyite): B_2O_3 38.20, 40.08, 42.28; MgO 46.48, 46.63, 50.64; CaO 3.70, 5.06, 1.52; $Al_2O_3 + Fe_2O_3$ 1.30, 0.95, 0.63; SiO_2 0.70, 0.60, 0.80; Na_2O 0.90, —, —; CO_2 5.70, 5.01, —; H_2O^+ 3.50 (inc. H_2O^-), 0.90, 3.87; H_2O^- —, 0.23, 0.19; sum 100.48, 99.46, 99.93%. Difficulty soluble in cold dilute HCl, difficult to fuse. *D.T.A.* study shows an endothermal break at 630°; this is probably due to transformation to the triclinic dimorph of $Mg_2B_2O_5$. The mineral occurs at the Hol Kol gold copper mine, Suan County, Korea, in kotoite marble associated with calcite, szaibelyite, kotoite, spinel, and clinohumite.

The name is for the locality.

M. F.

Severginite

G. P. BARSANOV, The isomorphous series of axinite, and the new mineral species severginite. *Trudy Mineralog. Muzeia, Akad Nauk S.S.S.R. No. 3*, 10–18 (1951) (In Russian) (from an abstract kindly prepared by Dr. Wilhelm Eitel).

The mineral occurs in quartz veins in the metamorphosed manganese silicate deposit of Tungatorovo-Uralinsk, southern Urals. It occurs as bright-yellow compact aggregates. Analysis gave SiO_2 42.84, TiO_2 none, Al_2O_3 16.50, Fe_2O_3 2.82, FeO none, MgO 0.66, MnO 14.79, CaO 16.96, alkalies none, H_2O^+ 0.69, B_2O_3 4.13, F none; sum 99.39%, formula (Ca,

$Mn)_2Mn(Al, Fe^{III})BH(SiO_4)_4$; this is considered to be the Mn end-member of the axinite series.

The mineral is optically positive, α 1.687, γ 1.698, 2V variable, 75–85°, dispersion $v>r$, γ: (011) = 10°. Pleochroism weak, colorless to yellowish. Anomalous dispersion was noted with deep-blue and reddish-brown colors.

X-ray powder data are given; they are practically identical with those for axinite. No data on hardness or sp. gr. are given. The data are compared with those for analyzed axinites; the indices of refraction increase with increasing Mn content and the optic sign changes from negative to positive.

The name is for Vasiliy Michailovich Severgin, 1765–1826, Russian mineralogist.

Discussion: The name seems to be unnecessary; the composition is far from that of a hypothetical manganese end member. Tinzenite (*cf* Milton, Hildebrand, and Sherwood, *Am. Mineral.* **38,** 1148–1158 (1953)) is an axinite with 21.19% MnO. Tinzenite is optically negative, showing that the relation between optic sign and MnO content is not as simple as Barsanov indicates.

M. F.

Likasite

A. Schoep, W. Borchert and K. Kohler, La likasite, $Cu_{12}(OH)_{14}(NO_3)_4(PO_4)_2$, nouveau minéral. *Bull. soc. franc. minéral. et crist.*, **78,** 84–88 (1955).

The mineral, discovered by Madam R. Stradiot-Duvieusart, occurs at the Likasi copper mine, Belgian Congo, as crystals implanted on cuprite or as blue masses in cuprite, surrounded by a crust of malachite and by malachite pseudomorphs after likasite. Associated minerals are native Cu, native Ag, buttgenbachite, and brochantite. Likasite is orthorhombic; the crystals are tabular with *c* (001) predominant; other forms measured include *r* (101), *k* (105), *g* (108), *b* (010), *d* (012), *e* (014), *f* (018). Rotation and Weissenberg diagrams give: $a=5.79$, $b=6.72$, $c=21.65$ Å, $a:b:c=0.862:1:3.222$. Probable space group D^9_{2h}—*Pcma*. Cleavage perfect and easy on (001), giving sky-blue lamellae.

Analysis gave Cu 55.54, NO_3 15.06, PO_4 14.56 (these on a 38 mg. sample), OH 16.50% (on a 24.1 mg. sample). (This gives a sum of 101.66% M.F.). [The formula $Cu_{12}(NO_3)_4(PO_4)_2(OH)_{14}$ requires Cu 53.0, NO_3 17.2, PO_4 13.2, OH 16.5%. M.F.] Sp. gr. = 2.96–2.98, by suspension in a mixture of methylene iodide and benzol. The unit cell contains 1 formula weight. Likasite dissolves readily in dilute acids; it gives H_2O when heated in a closed tube.

Indices of refraction measured were 1.61 (=*a*, blue, slightly greenish), 1.69 (=*b*, blue, somewhat violet). The optic axial plane is parallel to (001).

Discussion: According to an editorial note, the Committee on Nomenclature of the French Society suggested that it would be of interest to make an *x*-ray comparison of likasite with gerhardtite (whose formula may be written for comparison $Cu_{12}(NO_3)_6(OH)_{18}$), but material was lacking for this comparison.

M. F.

Vésigniéite

Claude Guillemin, Une nouvelle espèce minérale: la vésigniéite $Cu_3Ba(VO_4)_2(OH)_2$. *Compt. rend.*, **240,** 2331–2333 (1955).

Samples from Friedrichsroda, Thuringia, labelled "calciovolborthite," from Perm, Urals, labelled "volborthite," and from Agalik, Uzbekistan, labelled "kolovratite" were found to be a new mineral. It occurs as lamellar aggregates and as polysynthetic twins with pseudohexagonal outline up to more than 0.5 mm. in diameter. The color varies from yellow-green to dark olive-green, luster vitreous. There is a good cleavage parallel to the base.

The *x*-ray powder pattern differs from those of volborthite, tangeite, and mottramite, but is similar to that of monoclinic bayldonite, $Cu_3Pb(AsO_4)_2(OH)_2$. The strongest lines have spacings 3.20, 2.71, and 2.29 Å. Vésigniéite is optically biaxial, negative with *n*s $\alpha=2.04$, $\beta=2.07$, $\gamma=2.08$, $2V$ about 60°, extinction 10° from the twin plane. The acute

bisectrix is perpendicular to the plane of cleavage; Z is parallel to the elongation. G. 4.05 $\pm$0.03, hardness 3 to 4.

Microchemical analysis on a 14 mg. sample from Friedrichsroda gave CuO 37.6, BaO 23.9, V_2O_5 31.2, H_2O^+ 3.5, insol. 3.3; sum 99.5%. Analysis of synthetic material gave CuO 39.8, BaO 26.4, V_2O_5 30.8, H_2O^+ 3.1; sum 100.1%. These correspond to $Cu_3Ba(VO_4)_2(OH)_2$. The mineral loses water between 445° and 530°.

Vésigniéite was synthesized (*a*) by heating volborthite with barium acetate solution at 180°; (*b*) by heating barium metavanadate with copper nitrate solution; (*c*) by heating malachite, witherite, and vanadic acid at 180° in a sealed tube.

The mineral occurs at Friedrichsroda with barite and calcite in geodes in manganese ores, including vanadium-bearing psilomelane, and at Agalik and Perm on quartzite. It is suggested that the unnamed copper barium vanadate of Hillebrand and Merwin (*Am. J. Sci.*, **8**, 201 (1924)) from Paradox Valley, Colorado, was vésigniéite.

The name is for Colonel Louis Vésignié, 1870–1954, mineral collector, president of the Mineralogical Society of France in 1932.

M. F.

Chalconatronite

Clifford Frondel and Rutherford J. Gettens, Chalconatronite, a new mineral from Egypt. *Science*, **122**, No. 3158, 75–76 (1955).

The material was found as a fine-grained, greenish-blue crust, associated with cuprite and atacamite, as a corrosion product of three ancient bronze objects. Analysis gave Na_2O 20.0, CuO 26.8, CO_2 29.5, H_2O 20.4, PbO 2.8, SiO_2 0.5, R_2O_3 0.6; total 100.6%, corresponding to $Na_2Cu(CO_3)_2 \cdot 3H_2O$. The artificial compound was first prepared by Deville in 1952; it can be made by grinding copper acetate with a saturated solution of Na_2CO_3. The material is partly decomposed by water, completely soluble in cold acid with effervescence. The crystals are small laths or pseudohexagonal plates, probably monoclinic. $\alpha = 1.483$, $\beta = 1.530$, $\gamma = 1.576$, 2V large, probably positive; Z is perpendicular to flattening of the crystals, Y is parallel to the elongation of the laths; $Z \wedge c$ apparently very small. Strongly pleochroic, X nearly colorless, Y pale blue, Z blue. Hardness low, G. 2.27 $\pm$ .03. The five strongest lines of the *x*-ray powder pattern have spacings 6.92, 4.17, 3.68, 2.87, and 2.42 Å, in order of decreasing intensity. The material was probably formed by reaction of solutions containing alkali carbonates with the bronze objects. The name is from the Greek words for copper and sodium.

Discussion: There is considerable difference of opinion as to whether mineral names should be given to materials like this. Compare the lead oxychlorides from Laurium, Greece, also calclacite (*Am. Mineral.*, **32**, 254 (1947)).

M. F.

Coffinite

L. R. Stieff, T. W. Stern, and A. M. Sherwood, Preliminary description of coffinite—a new uranium mineral. *Science*, **121**, 608–609 (1955).

See *Am. Mineral.*, **39**, 1037 (1954) for preliminary data. The following additional data are given. Formula probably $U(SiO_4)_{1-x}(OH)_{4x}$. Infrared absorption spectra indicate the presence of bonded OH groups. G. 5.1. Tetragonal with a_0 6.94, c_0 6.31 Å. Found at more than 15 uranium mines on the Colorado Plateau, also in Fremont Co., Wyo., near Globe, Ariz., and "several foreign localities." The name is for Reuben Clare Coffin, a pioneer in the study of the uranium deposits of the Colorado Plateaus.

M. F.

NEW DATA

Ianthinite

Claude Bignand, Sur les proprietés et les synthèses de quelques minéraux uranifères. *Bull. soc. franc. minéral. et crist.*, **78**, 1–26 (1955).

Ianthinite from the type locality, Chinkolobwe, Katanga, was re-examined. A semi-microchemical analysis gave UO_3 71.6, UO_2 10.9, CaO 6.8, H_2O 7.2, CO_2 3.6, Fe traces; sum 100.1%, corresponding to $3CaO \cdot UO_2 \cdot 6UO_3 \cdot 2CO_2 \cdot 10H_2O$ or $3CaO \cdot 7UO_{2.83} \cdot 2CO_2 \cdot 10H_2O$. The formula had previously been supposed to be $2UO_2 \cdot 7H_2O$. Rotation measurements gave $a = 11.25 \pm 0.03$, $b = 7.08 \pm 0.02$, $c = 20.98 \pm .05$ Å. $Z = 2$. G. $= 4.94 \pm .03$. Optical and dehydration data are given. The water is lost between 80° and 260°, the CO_2 at 650°. *X*-ray powder data are given.

A violet hydrate, closely resembling ianthinite, was synthesized. Three analyses gave $UO_{2.84} \cdot xH_2O$. The *x*-ray powder pattern differs from that of ianthinite, but agrees closely with that of "ianthinite" from Puy-de-Dome, France, described by Branche, Chervet and Guillemin, *Bull. soc. franc. minéral et crist.*, **74,** 457 (1951). Its oxidation product gave the formula $4UO_3 \cdot 5H_2O$ and gave an *x*-ray powder pattern close to that of the oxidation product of the French material. Pending further study, no name is given to this material.

M. F.

Griffithite (=Ferroan Saponite)

G. T. Faust. Thermal analysis and *x*-ray studies of griffithite. *J. Wash. Acad. Sci.*, **45,** 66–70 (1955).

Griffithite (Larsen and Steiger, 1917) has generally been classed with the chlorites or vermiculites. New *x*-ray and *D.T.A.* data show it to be a member of the montmorillonite group, an iron-rich saponite.

M. F.

DISCREDITED MINERALS

Lehnerite = Ludlamite

Ljudevit Barić, Zur Identiät des Lehnerits und des Ludlamits: *Neues Jahrb. Mineral., Monatsh.* **1955,** No. 3, 49–53.

Crystallographic and optical study of "lehnerite" from the North Hagendorf pegmatite confirm its identity with ludlamite (*c.f.* Berman, *Am. Mineral.*, **10,** 428–429 (1925), Wolfe, *Am. Mineral.*, **34,** 94–97 (1949).

M. F.

Wisaksonite (=uranoan thorite)

C. O. Hutton, *Am. Mineral.*, **39,** 825–829 (1954).

M. F.

Koĭvinite (=Florencite)

V. A. Frank-Kamenetsky, A. I. Komkov, and V. V. Nardov, *X*-ray data on florencite and koĭvinite. *Zapiski Vses. Mineral. Obshch.* (*Mém. soc. russe minérale*) **82,** 297–301 (1953).

Labuntsov (*Trudy Mineral. Muzeya*, 1950, 135–136) described crystals of florencite from Ural placers. Kukharenko (*Zapiski Vses. Mineral. Obshch.*, **80,** 238 (1951)) stated that these differed optically from florencite and also differed chemically, analyses (not given) leading to the formula $(Ce, etc.)_2Al_5(PO_4)_4(OH)_2 \cdot 2H_2O$ whereas florencite is

$$Ce_2Al_6(PO_4)_4(OH)_{12}.$$

Optical, goniometric, and *x*-ray data by Frank Kamenetsky *et. al.* now show that koĭvinite is identical with florencite. The optical data show some variation, perhaps indicating a range of composition.

M. F.

Lembergite (=iron-rich Saponite)

Toshio Sudo, Iron-rich saponite found from Tertiary iron sand beds of Japan. (Re-examination of "Lembergiet"). *J. Geol. Soc. Japan,* **60,** 18–27 (1954).

X-ray study and differential thermal analysis of "lembergite" (see *Am. Mineral.*, **32,** 483 (1947)) shows it to be a saponite. Analysis by Joyo Ossaka gave SiO_2 39.68, TiO_2 0.37, Al_2O_3 3.93, Fe_2O_3 19.82, FeO 1.12, MnO 0.19, CaO 2.37, MgO 11.21, H_2O^- 15.11, H_2O^+ 6.16; sum 99.96%. This is higher in Fe than any saponite previously recorded.

M. F.